A Thesis

entitled

ACOUSTICAL PROPERTIES OF LIQUID FOAMS

submitted for the

Degree of Doctor of Philosophy

in the

University of London

by

Bridget Hay, M.Sc., B.Sc., A.R.C.S.

1967

ABSTRACT

In this thesis, a review is given of the development of the theory and experimental work on acoustic wave propagation in water containing air bubbles. Then, the various processes of attenuation of sound for distributions of air bubbles in a liquid, which are regarded as simulating the properties of foams, are considered theoretically by the author.

The measurements of the attenuation of sound in air-liquid foams, whose parent liquids have viscosities in the range 1-10 centipoise, show an order of magnitude agreement with a theory which suggests that the attenuation is due to viscous dissipation in the bubble walls. The possibility of energy loss due to pressure relaxation in an atmosphere of saturated vapour is rather discounted by the smallness of the calculated value as compared with the overall measured attenuation.

The measured values of the velocity of sound in air-liquid foams, for those with very large volume air concentrations, lie in the neighbourhood of the computed adiabatic values. This contrasts with the measurements of Karplus[14] in water containing air bubbles, of lower volume air concentrations, which agreed well with computed values for the isothermal velocity of sound.

ACKNOWLEDGEMENTS

The author wishes to thank Dr. R.W.B. Stephens of the Acoustic Group, Imperial College, for his constant guidance and encouragement throughout the project, and to Professor C.C. Butler for the laboratory facilities provided. She acknowledges help with mathematical theory from Dr. D.W. Moore of the Mathematics Department, Mr. D. Salt of the Acoustics Group, and Mr. J. Davis and Dr. D.E. Roberts of the Spectroscopy Group.

She is grateful to the members of the Acoustics Group, in particular Dr. A.E. Brown, and Messrs. B. Ray, E. Neppiras, A. Fry, and Dr. G. Curtis for technical advice. She wishes to thank the technical staff of the Physics Department, in particular Messrs. A. Sutherland, O. Millbank, B. Weekly, W.H. Page, R. Goddard, J. Last, F.W. Martin and the workshop staff under Mr. W. Shand for much assistance. Thanks are due to Dr. B.A. Scott and Mr. P. Hall of Unilever Research Laboratory, Isleworth for the use of laboratory facilities. Finally she wishes to thank Mr. M. Wallace for help with cinephotography and Miss M. Wright for painstakingly typing the manuscript. Above all, she is most grateful to her parents, whose financial support and encouragement made this thesis possible.

CONTENTS

		Page No.
Abstract		2
Acknowledgements		3
List of contents		4
List of principal symbols		10
Chapter 1. Introduction		14
	Theory	
Section 1.1	Attenuation of sound due to an isolated single bubble in a liquid.	15
Section 1.2	Attenuation of sound due to a multiple system of bubbles in a liquid.	18
Section 1.3	Velocity of sound in a multiple system of bubbles in a liquid.	21
	Experiment	
Section 1.4	Review of previous work on measurement of attenuation in bubble systems.	23
Section 1.5	Review of previous work on measurement of sound velocity in bubble systems.	29

Chapter 2. Acoustic wave propagation in air-liquid media 35

Attenuation

Section 2.1 Viscous damping in a foam. 36

Section 2.2. Pressure relaxation due to the presence of saturated vapour. 45

Section 2.3 Scattering of sound. 57

Velocity

Section 2.4 Velocity of sound in air-liquid media. 65

(i) Adiabatic velocity. 67

(ii) Isothermal velocity. 69

Chapter 3. Review of work on the stability of foams 70

Section 3.1 Classification of "foams". 70

Section 3.2 The role of surface rheology. 70

Section 3.3 Mixed foams. 74

Section 3.4 Rheology of the foam. 76

Section 3.5 Diffusion of gas. 77

Section 3.6 Mechanism of rupture. 77

Section 3.7 Foam destruction by acoustic waves. 78

(i) Acoustic pressure effect. 78

(ii) Unidirectional radiation pressure. 79

(iii) Induced resonant vibrations. 79

(iv) Sonic wind. 80

Chapter 4. Experimental apparatus and method 82

The Original Experimental System 82

Section 4.1.0 Foam generation system.

Section 4.1.1 Air system. 85

Section 4.2.0 Acoustic measurement system. 86

Section 4.2.1 Mechanical system. 87

Section 4.2.4 Electrical instrumentation. 87

Section 4.3.0 Measurement of foam density. 89

The Modified Experimental System 91

Section 4.4.0 The modified foam generation system. 91

Section 4.4.1 Modified jet tube. 96

Section 4.4.2 Solution level control circuit 96

Section 4.4.3 Air pressure control system 101

Section 4.4.4 Compressor control circuit. 101

Section 4.5.0 The overall modified acoustic measurement system. 104

Section 4.5.1 Acoustic measurement tube. 104

Section 4.5.2 Sound source. 106

Section 4.5.3 Probe tube. 106

Experimental Procedure 109

Section 4.6.0 The modified mechanical instrumentation. 109

Section 4.6.1 Axial positioning of the probe. 113

Section 4.6.2 The modified electrical instrumentation. 113

Measurement of Foam Parameters 116

Section 4.7.0 Foam density. 116

Section 4.7.1 Bubble size and distribution. 117

Section 4.7.2 Foam viscosity. 120

Section 4.7.3 Liquid density. 121

Section 4.7.4 Liquid surface tension. 121

Section 4.7.5 Liquid viscosity 121

Chapter 5. Experimental results and discussion on the acoustical properties of liquid foams 122

Section 5.1 Introduction 122

Section 5.2 Computation of attenuation results. 122

Section 5.3 Attenuation in air-liquid foams of constant bubble size. 126

Section 5.4 Discussion of the limited frequency range. 132

Section 5.5 Computation of phase velocity results. 133

Section 5.6 Phase velocity in air-liquid foams of constant bubble size. 136

Section 5.7 Conclusions from phase velocity and attenuation measurements. 137

Suggestions for further work. 138

Appendices

A1 Resonance frequency for an isolated bubble in a liquid. 143

A2 Scattering of sound from air bubbles in water. 145

A3 Calculation of foam density. 150

A4	Glossary of terms for surface-active agents.	152
A5	Calculation of sound intensity level for foam breakdown.	153
A6	Electrical instrumentation.	154
A7	The most probable shape of a bubble in foam. Measurement of bubble size.	155
A8	Foam viscosity measurements.	161
A9	Velocity of sound in terms of the volume concentration of bubbles.	162
A10	Sound propagation in a tube.	168
A11	The method of least squares.	170
A12	Attenuation and phase velocity in air-liquid foams of varying bubble size.	173
	Definitions.	178
	References	181

LIST OF PRINCIPAL SYMBOLS

Subscripts

G,L,T referring to Gas, Liquid and Total mixture respectively

F referring to Foam

A,I Adiabatic, Isothermal values

o equilibrium values

i,s referring to incident and scattered waves respectively

s,a,t referring to scattered, absorbed and total cross sections

---

a bubble radius

a_m maximum radius

A area of liquid surface, amplitude of velocity potential

B radiation resistance load

B_s surface compressional modulus

c velocity of sound

$\overline{c^2}$ mean square velocity

D radius of sphere containing bubble scatterers

E expansion factor, acoustic energy density

f applied frequency

f_o resonance frequency

f_r resonance frequency

$g(a,\omega)$ function of the applied frequency ω and bubble radius a

$G(\underline{r})$ average density of the bubble scatterers at $\underline{r}$

$\sqrt{1-4\pi G(\underline{r})}$ index of refraction

G_s surface shear modulus

IL	Intensity Level
I	Intensity
j	$(-1)^{\frac{1}{2}}$
k	wave number
K	compressibility
$K(\underline{r}/\underline{r}_o)$	Green's function
M	mass
m	integer
n	density of vapour molecules at time t
n_o	equilibrium density of vapour molecules
$n(\underline{r},a)$	density function
N	total number of vapour molecules at time t, total number of bubbles
p	excess pressure
$\hat{p}$	peak pressure
p_{RMS}	Root Mean Square pressure
p_v	partial pressure of vapour molecules
p_{ve}	equilibrium vapour pressure
p_a	partial pressure of air molecules
P	instantaneous total pressure
P_r	radiation pressure
q	polytropic factor
Q	cross section of bubble
r	radial direction
$\underline{r}$	location of a bubble with respect to the centre of the sphere
$\underline{r}_n$	location of the nth bubble with respect to the centre of the sphere

R_e	Real part
$S(\underline{r})$	total scattering cross section of bubbles per unit volume at the point specified by vector $\underline{r}$
s	stiffness of the gas in the bubble
t	time
T	surface tension
u	velocity component in r direction, molecular average velocity
U	velocity component in x direction
v	phase velocity of sound, change in volume from equilibrium volume
v_r	radial velocity
V	instantaneous volume, voltage, velocity component in y direction
V_o	equilibrium volume
w	velocity component in z direction
x	volume concentration of gas in the mixture, co – ordinate direction
y	co – ordinate direction
α	attenuation constant
β	phase constant
γ	ratio of the principal specific heats
Γ	periodic time
δ	liquid wall half – thickness
$\delta(\omega,a)$	function of the applied frequency ω and bubble radius a
η	(Newtonian) shear viscosity coefficient
η_v	coefficient of volume viscosity

λ	wavelength
μ	surface shear viscosity coefficient
ρ	density
σ	root mean square deviation
τ	relaxation time
ϕ	phase angle
ψ	velocity potential
$\underline{\Phi}$	dissipation function
ω	applied angular frequency
ω_o	resonance angular frequency
$\underline{\nabla}$	differential operator (vector)

CHAPTER 1

INTRODUCTION

In this chapter, a historical review is given of the development of the theory and experimental work on acoustic wave propagation in water containing air bubbles.

The passage of plane acoustic waves through a non-dispersive medium can be adequately described in terms of two parameters, viz., the phase velocity c and the attenuation constant α.

THEORY

Section 1.1 Attenuation of sound due to an isolated single bubble in a liquid.

Mallock[1] (1910) derived an expression for the efficiency of the bubbles in damping vibrations for the case of a pulsating spherical bubble of air surrounded by a sphere of viscous but incompressible liquid. He suggested that the damping was due to the increased distortion of the liquid resulting from the sound pressure acting effectively on the air, with little impression on the relatively incompressible liquid. Mallock[1] concluded that damping increased as the diameter of the bubbles decreased and as their distance of separation decreased. This derivation assumed that each bubble would execute spherical pulsations uninfluenced by its neighbours.

Sewell[2] (1910) considered the absorption and scattering by a fixed rigid sphere in a viscous fluid without considering thermal conductivity, but allowed for viscosity in considering the equation of motion of a shell of fluid surrounding the sphere. The absorption coefficient of a dilute suspension of particles in a viscous fluid will consist of two terms, one accounting for viscous losses, the other for scattering losses.

The latter are dominant when the particles are of the same order as the wavelength, for smaller particles viscous losses are important. A restriction in the theory is that the volume occupied by the obstacles should be small compared with the total volume.

Sewell[2] assumed the particles to be immobile spheres, but when the particle is very small and the wavelength large, the liquid and spheres will tend to move together and hence diminish the effect of viscosity; in an appendix to his paper he made a correction for such mobility.

Later a model closer to the actual conditions was analysed by Epstein[3] (1941). He considered theoretically the absorption of sound by a suspension of free non-rigid particles in a viscous fluid, where the effects of thermal conductivity were again ignored. The particles considered were (a) spheres of viscous fluid, and (b) spheres of elastic solid. The effect of the oscillatory motion of the particles in the medium was taken into account. Epstein[3] considered that viscous energy losses were due to partial conversion of the incident longitudinal sound wave into a transverse wave on interaction with the spherical obstacle. This transverse wave is completely absorbed in the fluid after a very short path.

Epstein and Carhart[4] (1953) continued the analysis for the frequency range 1000 - 8000 c/s, taking into account the effect of heat conduction between the viscous fluid spheres and the surrounding viscous medium. Whenever a compressional acoustic wave falls on a surface of discontinuity these authors state that in addition to the reflected and transmitted waves, waves of two other kinds are produced, spreading from the surface to both sides; one a highly damped longitudinal wave and the other a highly damped transverse wave. These additional waves suffer practically complete absorption in very thin layers of the two media. The additional transverse waves, due to the viscosity of the media were considered by Epstein[3], and are termed viscous waves. The additional longitudinal waves, considered by Epstein and Carhart[4] as due to heat conduction are known as thermal waves.

Chow[5] (1964) in studying the attenuation of acoustic waves by a suspension of fluid spheres in a fluid medium, took into account the effect of surface tension. He also formulated the basic equation with respect to a moving co-ordinate system fixed in the fluid sphere, so that the restriction of small amplitude oscillations inherent in previous work was removed. For a suspension of air bubbles in water thermal attenuation is far more important than viscous attenuation, and the effect of surface tension is

to considerably increase this thermal attenuation, especially for small bubbles.

In all the above cases, scattering was ignored since the bubbles considered were small compared with the wavelength and due to the low volume concentration there was no interaction between the bubbles.

Section 1.2. Attenuation of sound due to a multiple system of bubbles in a liquid.

Hsieh and Plesset[6] (1961) investigated the propagation of sound in a liquid containing a homogeneous and isotropic distribution of gas bubbles, and assumed the bubbles were sufficiently small and numerous for the mixture to be considered as a uniform medium. Their analysis was confined to mixtures in which the proportion of gas by volume is large enough for the gas compressibility of the mixture to play the dominant role in the overall compressibility, but at the same time is not so large that the mass of gas becomes comparable with the mass of liquid in the mixture. The calculated attenuation due to thermal conduction was very small, in most cases being much smaller than the thermal attenuation in the pure gas; viscosity effects were ignored.

Murray[7] (1963) has extended the analysis of Hsieh and Plesset[6] to take account of attenuation in the mixture

arising from volume viscosity. He showed this mechanism to be by far the most important for small concentrations of gas. An incompressible fluid possesses only one coefficient of viscosity because, by definition, no changes in volume can occur. If such a fluid contains air bubbles it becomes compressible, and any changes in volume involves a contraction or expansion of the bubbles which is resisted by the ordinary viscosity of the surrounding fluid. The resulting coefficient of volume viscosity η_V has been calculated by Taylor and Davies[8] (1954) to be $\eta_V = 4\eta_L/3x$, where η_L is the shear viscosity of the incompressible fluid and x is the volume concentration of gas in the mixture, which is necessarily small to satisfy the theoretical assumptions.

Spitzer[9] (1943) extended Mallock's[1] analysis to the case of a homogeneous air-water mixture containing numerous spherical bubbles of uniform radius a ($a > 0.015$cm and much smaller than the wavelength of sound). He derived a formula for the attenuation α at all frequencies if the volume concentration x of air in the mixture is small ($x < 0.03$).

Vignaux[10] (1961) and Connor[11] (1962) investigated the viscous attenuation of plane acoustic waves in air-water foams containing bubbles of one size. They considered

the foam as a homogeneous fluid, and assumed that the attenuation could be expressed [52] by the classical viscous attenuation coefficient :

$$\frac{\alpha}{f^2} = \frac{8}{3}\left(\frac{\eta_F}{\rho_F}\right)\frac{\pi^2}{c^3} = \text{const.} \qquad (1.0.1)$$

In this equation, f was the frequency and η_F, ρ_F, c_F were the shear coefficient of viscosity, density and adiabatic velocity, respectively, in the foam.

It should be noted that Vignaux[10] and Connor[11] ignored the effect of foam structure.

Section 1.3 Velocity of sound in a multiple system of bubbles in a liquid

Mallock[1] (1910), Wood[13] (1930), Karplus[14] (1958), and Hsieh and Plesset[6] (1961) derived an equation for the velocity of sound in a liquid containing a homogeneous and isotropic distribution of air bubbles, at applied frequencies well below resonance. The bubble size must be small compared with the wavelength of the incident sound wave. The formula is derived on the assumption that the bubbles pulsate isothermally, because of the enormous heat capacity of the water. Wood's[13] formula shows that the average velocity c of the sound in the mixture is determined by the product of the average compressibility K_T and average density ρ_T

$$c = (\rho_T K_T)^{-\frac{1}{2}}$$

Murray[7] (1963) evaluated the speed of sound in a similar air-water mixture to Wood[13] for all values of air concentration, by making use of the equations of motion for the propagation of an infinitesimal disturbance. In the range where the mixture was distinctly that of a liquid with a distribution of bubbles (rather than a foam), the speed of sound was effectively

the isothermal value. However, as the gas/liquid volume ratio $V_G/V_L \rightarrow \infty$ the speed of sound approaches the strictly adiabatic value.

From these investigations, the question arises whether the compression of an air bubble in a foam is isothermal or adiabatic, i.e., does the gas transfer its heat of compression to the surrounding liquid film in a time long or short compared with the period of the acoustic pressure fluctuation. These limiting cases are discussed by the author in chapter 2.

EXPERIMENT

Section 1.4 Review of previous work on measurement of attenuation in bubble systems.

Sewell[2] (1910) applied his theory (discussed in section 1.1.0) for the absorption of sound in a suspension of small particles to the propagation of sound in fogs and clouds. His condition that the particles did not oscillate in the sound field was satisfied for water droplets in air at audio-frequencies. However, this condition is by no means satisfied for aqueous suspensions of small particles at ultrasonic frequencies, for the particles under both these conditions ~~do~~ partake to a considerable extent of the motion of the fluid. This is a probable explanation for the failure of Sewell's theory when applied by Hartmann and Focke[15] (1940) to the absorption produced by lycopodium spores in water at megacycle frequencies.

The theory of Epstein and Carhart[4] (1953) (discussed in section 1.1.0) ~~does~~ takes into account the effect of the oscillations of the suspended particles. Quantitative

agreement (see fig. 1) in the low frequency region (1000 - 2000 c/s) is found between their theory for the absorption of sound in a suspension of water droplets in air and the attenuation measurements of Knudsen[16] (1940) in water fog (see fig. 1).

Silberman[17] (1957) made measurements of the attenuation constant in a mixture of air bubbles in water, using a standing-wave tube at applied frequencies from 600 - 20,000 c/s. An experimental difficulty was the maintenance of bubbles of a single uniform size, but the limits of control were not given. The measurements show (see fig. 2) that theory gives at least a good estimate of attenuation constant for bubbly mixtures containing large bubbles (radii of the order of 0.03cm or greater) and small concentrations (a few percent or less).

Macaulay[18] (1961) carried out some work on the acoustic properties of soap foams using an impedance tube, which covered a density range from about 0.1 to 0.9 gm cm^{-3} and a frequency range of 100 - 1400 c/s. This work has not yet been published.

Vignaux[10] (1961) investigated the variation of attenuation with frequency in the range 1000 - 6000 c/s

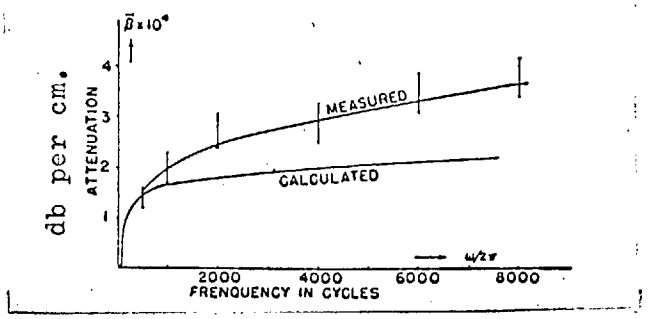

Fig. 1. Comparison of theoretical and experimental attenuations. (Epstein and Carhart, and Knudsen.)

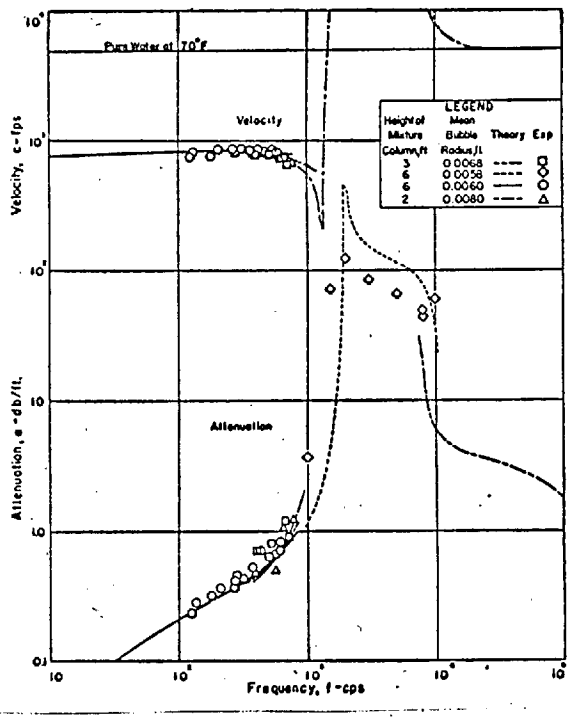

Fig. 2. Phase velocity and attenuation constant. vol. conc. of air x = 0.0022, r= 0.007 ft.(0.2 cm.) (Silberman)

in air-water foams stabilised by detergent, using a short measurement tube. Bubble sizes in the foams were in the range 0.08 to 0.14 cm diameter, and the density range was 0.003 to 0.5 gm cm^{-3}. The bubble volumes remained constant to within $\pm$ 10 percent, but no reliable estimate could be placed on the density servo-control system. Vignaux's[10] analysis involved the recognition of the presence of different modes from peaks occurring in his attenuation - frequency graphs (see fig. 3). Interference effects between such modes make this an uncertain procedure and it is suggested that to obtain reliable information about a particular mode it is necessary to use sound sources which ensure the propagation of one mode at a time.

Connor[11] (1962) avoided this difficulty by modifying the source and using longer tapered acoustic measurement tubes, to reduce standing wave effects. He worked in the frequency range 200 - 3000 c/s with the rather limited foam density range 0.010 to 0.025 gm cm^{-3}; no measurements of bubble size were recorded.

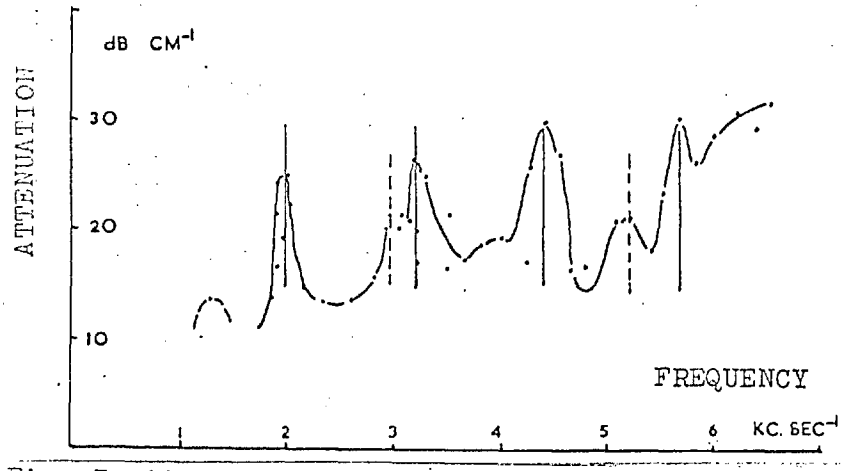

Fig. 3. Attenuation vs. frequency. (Vignaux).

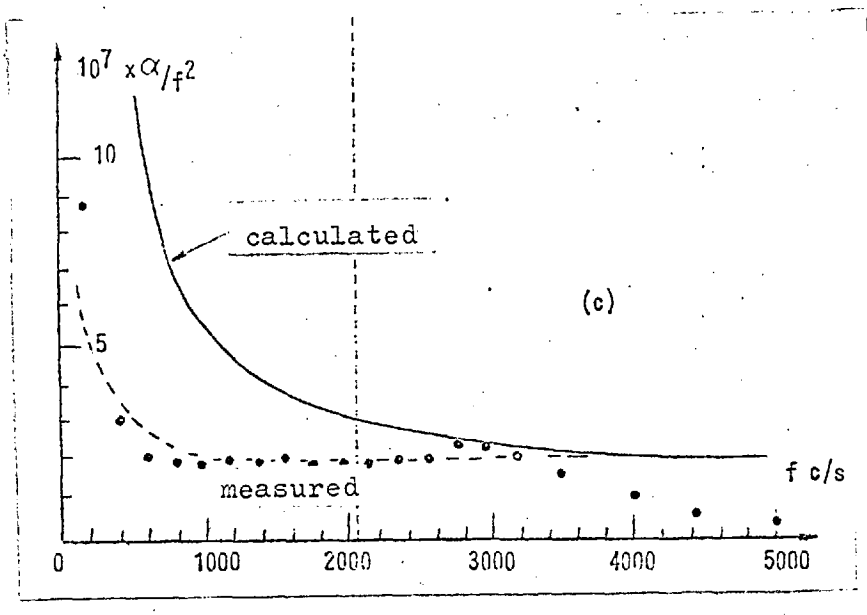

Fig. 4. Comparison of theoretical and experimental attenuations.
f_c = 2050 c/s. (Connor)

Connor[11] found that at high frequencies (see fig. 4) the ratio of the attenuation coefficient to the square of the frequency, α/f^2, was approximately constant (see equation 1.0.1).

The above experiments pointed to the need of measuring the attenuation constants of air-liquid foams, for liquids of higher viscosity than water and in the range 1-10 centipoise. The order of magnitude of the attenuation constants are compared with the predictions of three possible dissipation mechanisms. These are viscous dissipation; pressure relaxation due to the presence of saturated vapour; and multiple scattering.

Section 1.5 Review of previous work on measurement of sound velocity in bubble systems.

Silberman[17] (1957) has verified by experiment that Wood's expression (see section 1.3.) for the isothermal velocity of sound in bubble-water mixtures is valid for frequencies up to one half of the resonance frequency of the bubbles (see fig. 2).

Karplus[14] (1958) measured the velocity of sound in water containing air bubbles, of diameter 0.01 cm, as a function of frequency and volume concentration of air in the mixture (see fig. 5). These bubbles have a resonance frequency of about 55,000 c/s (see appendix A1), which was well above the applied frequency range (250 - 1,500 c/s). The measurements of Karplus agree well with computed values based on Wood's theory (see section 1.3.) for the isothermal velocity of sound. Karplus found that the velocity of sound in water containing air bubbles was very low. In pure water at 20°C, sound travels with a speed of 1500 m/s; this velocity decreased to 100 m/s in water containing one percent by volume of air (see fig. 5). The minimum occurred at 50 percent volume concentration, at which a velocity of 20 m/s was observed.

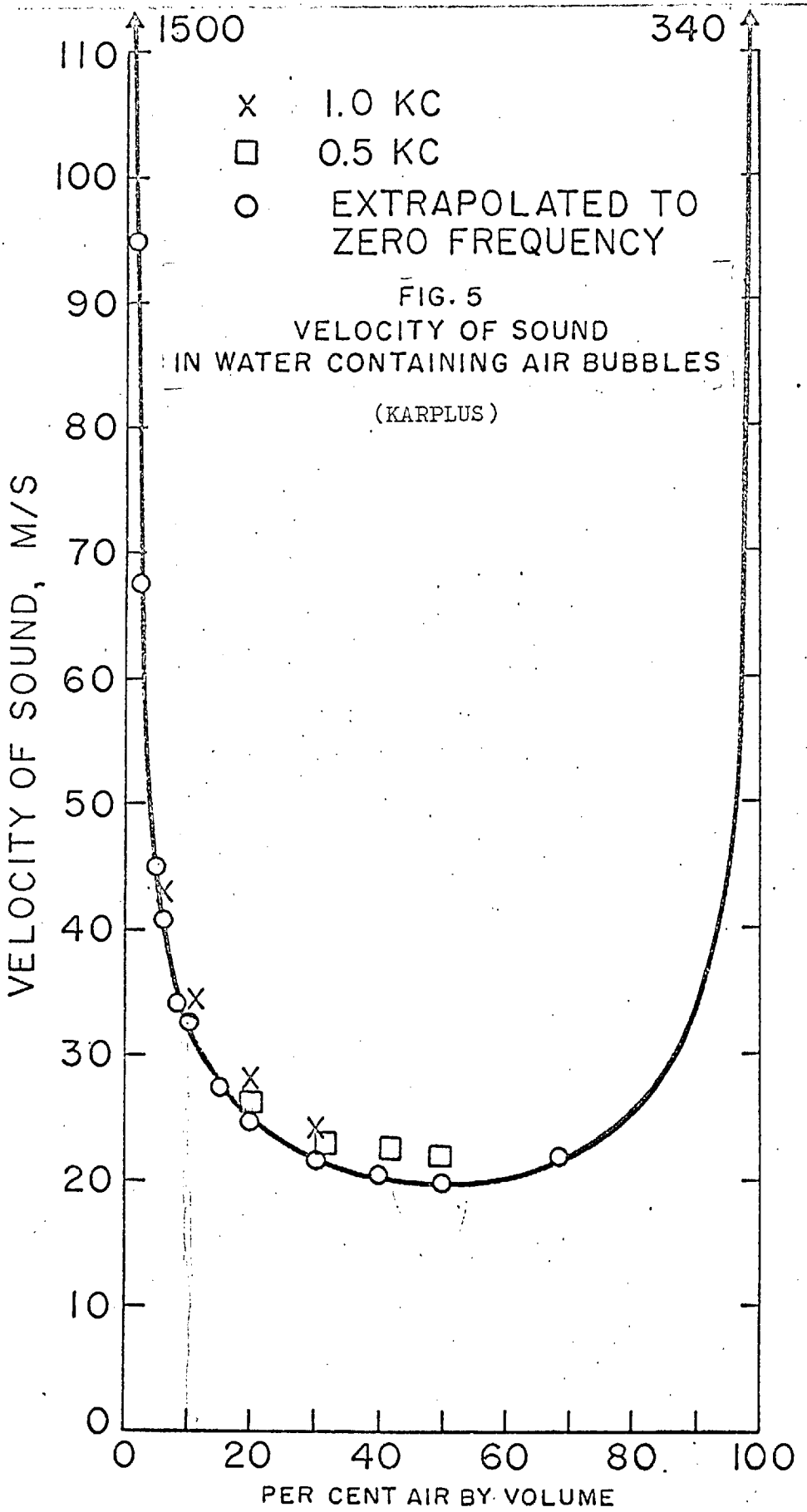

FIG. 5
VELOCITY OF SOUND
IN WATER CONTAINING AIR BUBBLES

(KARPLUS)

Vignaux[10] (1961) measured the velocity of sound in air-water foams over a frequency range of 1000 to 6000 c/s. The observed phase velocities in general increased with increasing frequency but in a discontinuous fashion. However, substantial differences were reported between predicted isothermal values and extrapolated zero frequency values (see fig. 6). This led Vignaux to propose a theory of propagation based on the existence of a foam shear modulus and corresponding shear waves. In the author's opinion this technique is uncertain due to the possible presence of mode interference effects.

Following Vignaux[10], Connor[11] (1962) carried out measurements in the frequency range 200 - 3000 c/s which did not reveal any substantial variation of the velocity of sound in the foams as the frequency was varied, provided observations were limited to frequencies below those at which higher mode propagation begins (f_c) (see fig. 7).

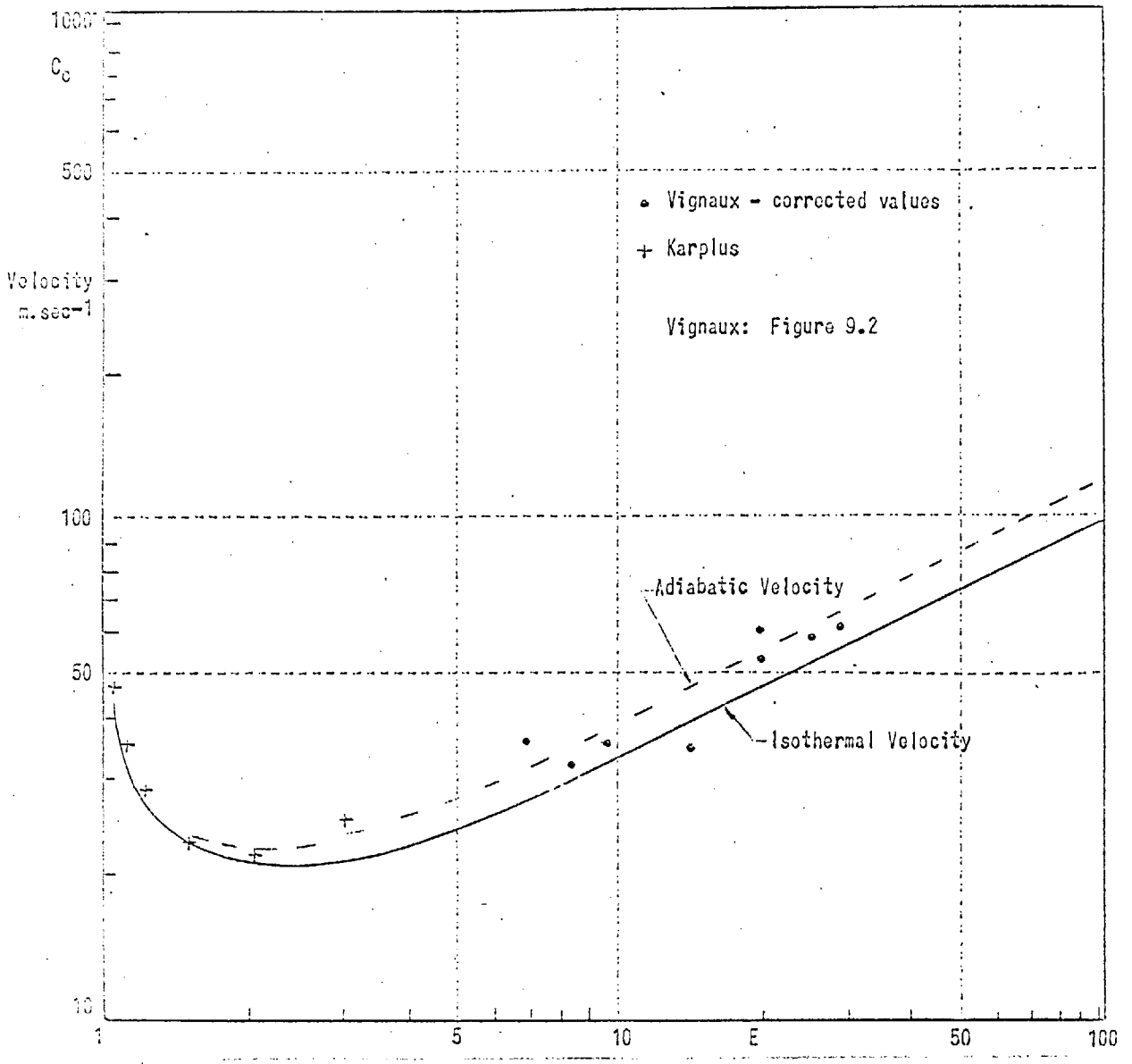

Fig. 6. Measured phase velocity as a function of expansion ratio E (= density of liquid / density of foam)
(Vignaux)

Fig. 7. Velocity vs. frequency. Graphs (a), (b), & (c) are for foams of approx. the same bubble size and expansion ratio.

(Connor)

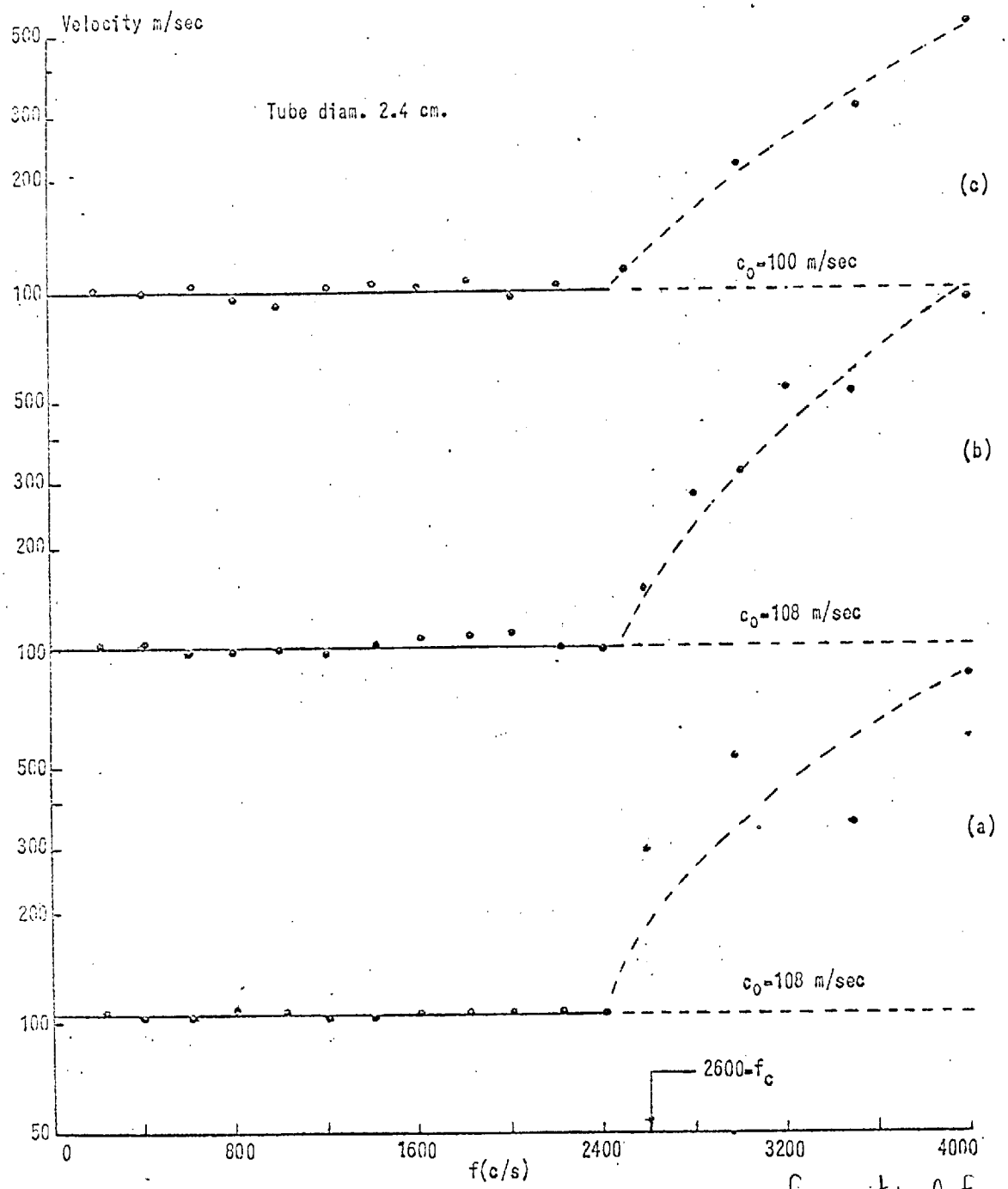

f_c = critical frequency

The present experiments were planned to measure the velocity of sound in air-liquid foams in the frequency range 200-2000 c/s, whose parent liquids had viscosities in the range 1-10 centipoise. The results were compared with computed values for the isothermal and adiabatic velocity of sound (see chapter 2).

CHAPTER 2

ACOUSTIC WAVE PROPAGATION IN AIR-LIQUID MEDIA

ATTENUATION

In this chapter the various processes of attenuation of sound in air-liquid media are considered. Distributions of air bubbles in a liquid are regarded as simulating the properties of foams. The chapter is divided into three parts, each of which refers to a different mechanism of sound attenuation. These are

Section 2.1 Viscous damping in a foam

Section 2.2 Pressure relaxation due to the presence of saturated vapour

Section 2.3 Scattering of sound

Section 2.1 Viscous damping in a foam

If a foam is confined in a cylindrical tube, then a sound wave will cause shearing of the solution in the bubble walls, as the bubbles expand and contract, by a "squishing mechanism" (see fig. 8a).

Therefore, in this section an order of magnitude result is worked out for the viscous dissipation due to the motion of an incompressible solution between two stress free parallel surfaces. It is assumed that the surfaces behave as ideal liquid surfaces on the grounds that the period of the sound wave is short compared with the time it takes for surface energy to change if the surface is stretched.

Liquid motion between moving parallel planes

It is assumed that the movement of the planes is small compared with the thickness of the liquid layer so that the motion may be regarded as taking place about a fixed plane. If the distribution of velocities exhibit axial symmetry with velocity components (u,w) in the directions (r,z) respectively and further that the velocity w varies linearly across the liquid plate half-thickness δ then

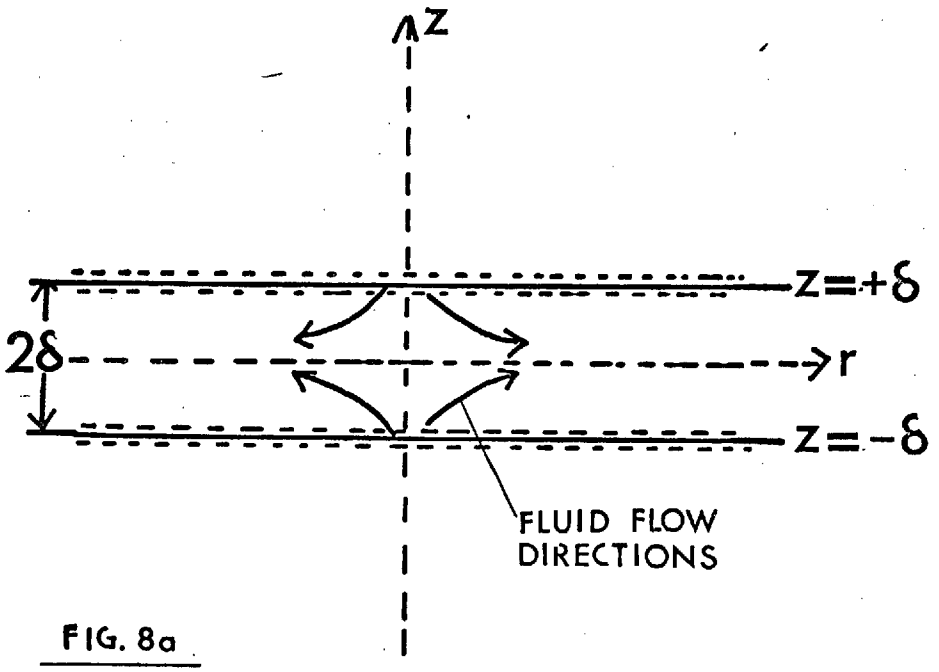
z
z=+δ
2δ
r
z=-δ
FLUID FLOW
DIRECTIONS

FIG. 8a

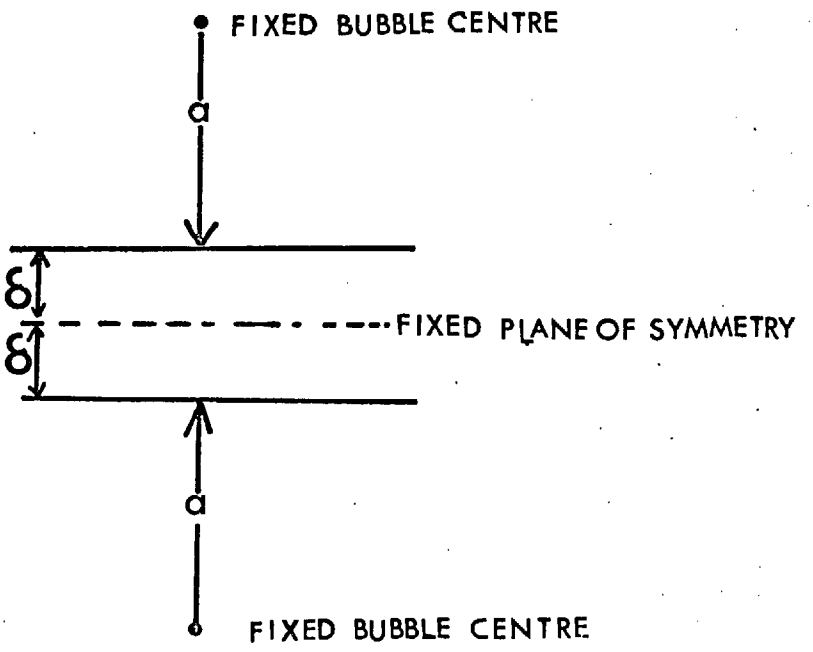
FIXED BUBBLE CENTRE
a
δ
δ
FIXED PLANE OF SYMMETRY
a
FIXED BUBBLE CENTRE

FIG. 8b

$$w = \frac{\dot{\delta}}{\delta} z \qquad (2.1.1)$$

where $\dot{\delta}$ equals the rate at which the surface is moving.

Hence $$\frac{\partial w}{\partial z} = \frac{\dot{\delta}}{\delta}$$

The equation of continuity for an incompressible liquid in cylindrical co-ordinates[52] is given by

$$\frac{1}{r} \frac{\partial}{\partial r} (ru) + \frac{\partial w}{\partial z} = 0 \qquad (2.1.2)$$

Integrating equation (2.1.2) with respect to r

$$ru = - \frac{r^2}{2} \frac{\partial w}{\partial z} + c \qquad (2.1.3)$$

In equation (2.1.3), when $r = 0$, $c = 0$. Substituting for $\partial w / \partial z$ from equation (2.1.1) into (2.1.3)

$$u = - \frac{r}{2} \frac{\dot{\delta}}{\delta} \qquad (2.1.4)$$

From equation (2.1.4),

$$\frac{\partial u}{\partial z} = 0 \quad \text{at} \quad z = \pm \delta \qquad (2.1.5)$$

hence the condition for a stress-free boundary is satisfied.

Summarising, the velocity fields are given by

$$u = -\frac{1}{2}\frac{\dot{\delta}}{\delta} r \qquad (2.1.4)$$

$$w = \frac{\dot{\delta}}{\delta} z \qquad (2.1.5)$$

Transforming the velocity fields to cartesian co-ordinates, related to cylindrical co-ordinates by $U = u \cos \phi$, $V = u \sin \phi$, the velocity fields are

$$\begin{aligned} U &= -\tfrac{1}{2}\frac{\dot{\delta}}{\delta} x \\ V &= -\tfrac{1}{2}\frac{\dot{\delta}}{\delta} y \\ w &= \frac{\dot{\delta}}{\delta} z \end{aligned} \qquad (2.1.6)$$

For an incompressible liquid, the rate of dissipation of mechanical energy due to viscosity is given by the dissipation function[53]

$$\dot{\Phi}_{mech} = \eta_L \int\!\!\int\!\!\int \left[2\left(\frac{\partial U}{\partial x}\right)^2 + 2\left(\frac{\partial V}{\partial y}\right)^2 + 2\left(\frac{\partial w}{\partial z}\right)^2 + \left(\frac{\partial w}{\partial y} + \frac{\partial V}{\partial z}\right)^2 + \left(\frac{\partial U}{\partial z} + \frac{\partial w}{\partial x}\right)^2 + \left(\frac{\partial V}{\partial x} + \frac{\partial U}{\partial y}\right)^2 \right] dV \qquad (2.1.7)$$

where η_L is the shear coefficient of viscosity of the liquid. Because of the nature of the shearing mechanism, the last three terms of equation (2.1.7) are equal to zero. Hence, substituting from equation (2.1.6) into (2.1.7), the rate of dissipation of mechanical energy due to viscosity is given by:

$$\dot{\Phi}_{mech} = 3\eta_L \frac{\dot{\delta}^2}{\delta^2} V \qquad (2.1.8)$$

Pressure relations in a foam

It is assumed that a foam is made up of spherical bubbles of radius a surrounded by spherical liquid shells of uniform thickness δ.

Assuming an adiabatic law for the pressure p inside a spherical bubble, then

$$pa^{3\gamma} = \text{const.} \qquad (2.1.9)$$

Differentiating equation (2.1.9):

$$\frac{\partial a}{a} = \frac{-\partial p}{3\gamma p} \qquad (2.1.10)$$

Writing $\dot{a} = \partial a / \partial t$, $\dot{p} = \partial p / \partial t$,

$$\frac{\dot{a}}{a} = \frac{-\dot{p}}{3\gamma p} \qquad (2.1.11)$$

When the bubble expands, the radius a increases but the liquid wall thickness δ decreases, and to a first approximation (see fig. 8b) the rate at which the bubble surface is moving, $\dot{\delta}$ is taken as

$$\dot{\delta} = -\dot{a} \text{ approx.} \qquad (2.1.12)$$

Substituting from equation (2.1.12) into (2.1.11):

$$\dot{\delta} = \frac{a\,\dot{p}}{3\gamma p} \qquad (2.1.13)$$

Let the pressure p inside the bubble be represented by the sum of a constant term and a sinusoidally varying term:

$$\therefore p = P_o + \hat{p} \sin \omega t \qquad (2.1.14)$$

where P_o is the atmospheric pressure and $\hat{p}$ is the peak value of the pressure in the acoustic wave.

Differentiating with respect to t:

$$\frac{\dot{p}}{p} = \frac{\hat{p}\ \omega \cos \omega t}{P_o + \hat{p}\ \sin \omega t} = \frac{\hat{p}}{P_o}\ \omega \cos \omega t \qquad (2.1.15)$$

since $P_o >> \hat{p}$.

Substituting from equation (2.1.15) into (2.1.13):

$$\dot{\delta} = \frac{a\hat{p}}{3\gamma P_o}\ \omega \cos \omega t \qquad (2.1.16)$$

Assuming, to a first approximation, that the case of the spherical bubble can be reconciled with that of the parallel planes, then substituting from equation (2.1.16) for $\dot{\delta}$ into (2.1.8):

$$\dot{\Phi}_{mech} = \left[\eta_L \cdot \frac{a^2}{\delta^2} \cdot \frac{\hat{p}^2}{3\gamma^2 P_o^2} \cdot \omega^2 \cos^2 \omega t \right] V \qquad (2.1.17)$$

Hence the mean value of the energy dissipation due to viscosity over a cycle is given by

$$\dot{\Phi}_{mech} = \left[\eta_L \cdot \frac{a^2}{\delta^2} \cdot \frac{\hat{p}^2}{6\gamma^2 P_o^2} \cdot \omega^2 \right] V \qquad (2.1.18)$$

The dimensions of $|\dot{\Phi}|$ in this equation are energy per unit time.

If the volume V is put equal to the volume of liquid in 1 cc of foam, then for spherical bubbles,

$$V = \frac{3\delta}{a} \qquad (2.1.19)$$

Substituting from equation (2.1.19) into (2.1.18),

$$\left|\dot{\Phi}_{\text{mech}}\right| = \eta_L \cdot \frac{a}{\delta} \cdot \frac{\hat{p}^2}{2\gamma^2 p_o^2} \cdot \omega^2 \qquad (2.1.20)$$

The dimensions of $\dot{\Phi}$ in this equation are energy per unit volume per unit time.

Attenuation in an acoustic wave

When an acoustic wave is propagated through a foam, its intensity decreases with the distance x traversed. It is evident that this decrease will occur according to the law $e^{-2\alpha x}$, where the attenuation coefficient α is defined by Landau and Lifshitz[52] as

$$\alpha = \frac{|\dot{\Phi}|_{\text{mech}}}{2I} \qquad (2.1.21)$$

and $$I = \frac{p^2_{RMS}}{2\rho_F c_F} \qquad (2.1.22)$$

In these equations, I is the acoustic intensity defined in terms of the effective (i.e. R.M.S. for sine waves) sound pressure p_{RMS}, velocity c_F and density ρ_F of the foam medium.

This formula (2.1.21) is applicable so long as the attenuation coefficient determined by it is small: the amplitude must decrease relatively little over distances of the order of a wavelength (i.e. $\alpha c_F/\omega \ll 1$).

Substituting from equation (2.1.20) into equation (2.1.21), the following formula is found for the acoustic attenuation coefficient:

$$\alpha = \left[\eta_L \cdot \frac{a}{\delta} \cdot \frac{1}{\gamma^2 p_o^2} \cdot \rho_F c_F \right] \omega^2 \qquad (2.1.23)$$

It is pointed out that α is proportional to the square of the frequency ω of the sound.

Section 2.2 Pressure relaxation due to the presence of saturated vapour

If a small quantity of a liquid is put into a cylinder fitted with a piston, then there will be a mixture of inert gas and vapour molecules above the liquid (see fig. 8c). Let the partial pressures of the inert gas and vapour molecules be p_a and p_v respectively: then in a state of dynamic equilibrium between the vapour and liquid molecules $p_a + p_v = P_o$, where P_o is the external pressure.

Consider what happens, when as a result of a change in external pressure, the volume is suddenly decreased by a small amount. Clearly, the inert gas molecules and the vapour molecules, being confined in a smaller space will make more collisions with the walls, i.e. the partial pressures p_a and p_v will increase by amounts $(\delta p_a)_o$ and $(\delta p_v)_o$. Now, since p_v has increased, the number of vapour molecules striking the liquid surface will increase and the dynamic equilibrium mentioned above will be destroyed. Hence vapour molecules will decrease in concentration until the number of impacts once again balances the rate at which molecules leave the liquid. This condition will occur, under isothermal conditions, when the partial pressure

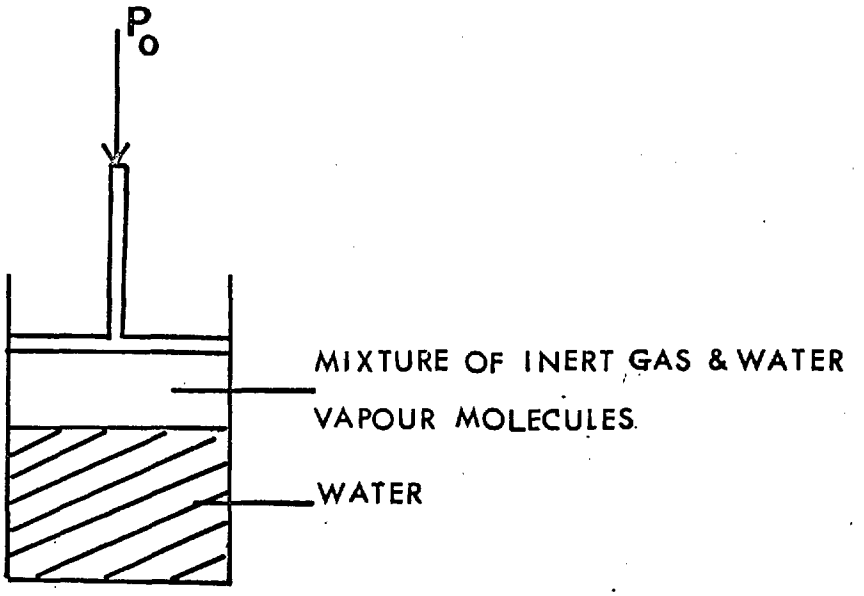

FIG. 8c

p_v has been restored to its initial value. Hence, if $(\delta p_v)_t$ is the excess of the vapour pressure over the equilibrium vapour pressure at time t at the given temperature, it is assumed that

$$(\delta p_v)_t = (\delta p_v)_o \; e^{-t/\tau} \qquad (2.2.1)$$

where τ is a relaxation time.

The number of impacts/cm^2/sec is $\frac{1}{4} n_o u$ where n_o is the equilibrium density of vapour molecules. Hence the rate at which vapour molecules are lost to the liquid is $\frac{1}{4} A n_o u$, where A is the area of the liquid surface.

In dynamic equilibrium, an equal number of liquid molecules enter the vapour state. Suppose that the concentration of vapour molecules is $n_o + \delta_n$ at time t. Then the number of molecules striking the liquid per unit time will be

$$\frac{1}{4} A(n_o + \delta_n)u$$

while the number leaving per unit time will be

$$\frac{1}{4} A n_o u$$

Hence the net number striking the liquid per unit time is

$$-\frac{dN}{dt} = \frac{A}{4}(\delta n)u \qquad (2.2.2)$$

where $N = nV$ is the total number of vapour molecules at time t, n is the density of vapour molecules at time t and V is the volume of the vapour at time t. Therefore equation (2.2.2) becomes

$$\frac{dn}{dt} = \frac{-A}{4V}(\delta n)u \qquad (2.2.3)$$

Integrating equation (2.2.3) with respect to t:

$$\delta n = (\delta n)_o e^{-t/\tau} \qquad (2.2.4)$$

where $$\tau = \frac{4V}{Au} \qquad (2.2.5)$$

Applying this theory to the case of a spherical bubble, it is assumed that for small volume changes, $V(t) \approx V_o$, where V_o is the equilibrium value. Hence for a bubble of radius a equal to 5.6×10^{-2} cm,

$$\frac{V_o}{A} = \frac{a}{3} = 1.9 \times 10^{-2} \text{ cm} \qquad (2.2.6)$$

and the molecular average velocity at N.T.P. for water vapour[54],

$$u = 5.65 \times 10^4 \text{ cm sec}^{-1} \qquad (2.2.7)$$

Hence the relaxation time τ is given approximately by

$$\tau \sim 1.3 \times 10^{-6} \text{ sec} \qquad (2.2.8)$$

and the relaxation frequency f_r is given by

$$f_r \sim 120 \text{ Kc/sec} \qquad (2.2.9)$$

Forced vibrations of the bubble

Following previous analysis, the density of vapour molecules at time t is given by

$$n(t) = \frac{N(t)}{V(t)} \qquad (2.2.10)$$

From equation (2.2.3),

$$\frac{d(nV)}{dt} = -\frac{A}{4}(\delta n)u \qquad (2.2.3)$$

Put $V = V_o + v$, where $v/V_o \ll 1$, (2.2.11)

$$\left[1 + \frac{v}{V_o}\right]\frac{dn}{dt} + \frac{n}{V_o}\frac{dv}{dt} = \frac{-A}{4V_o}(\delta n)u \qquad (2.2.12)$$

If $n = n_o + \delta n$, where $\delta n/n_o \ll 1$, and v/V_o is neglected in comparison with 1,

$$\frac{d(\delta n)}{dt} + \frac{n_o}{V_o}\frac{dv}{dt} = \frac{-A}{4V_o}(\delta n)u \qquad (2.2.13)$$

Put $v = v_o e^{j\omega t}$, so that $\delta n = (\delta n)_o \, e^{j\omega t}$ (2.2.14)

where ω is the angular frequency of the forcing agency i.e. a sound wave.

Hence $$(\delta n)_o = \frac{-j\omega v_o n_o}{V_o} \left[\frac{1}{(Au/4V_o) + j\omega}\right] \qquad (2.2.15)$$

Put $$\tau = \frac{4V_o}{A u} \qquad (2.2.5)$$

Then $$(\delta n)_o = \frac{n_o v_o}{V_o} \left[\frac{\omega^2 \tau^2 + j\omega\tau}{1 + \omega^2 \tau^2}\right] \qquad (2.2.16)$$

Now, the pressure exerted by the water vapour is given by

$$Pv = \frac{1}{3} m n \overline{c^2} \qquad (2.2.17)$$

where m is the mass of each molecule and $\overline{c^2}$ is the mean square velocity. Hence

$$\delta p_v = \frac{1}{3} m \overline{c^2} \delta n \qquad (2.2.18)$$

Put $\delta n = (\delta n)_o \, e^{j\omega t}$ (2.2.14)

and substitute for $(\delta n)_o$ from equation (2.2.16) into equation (2.2.18):

$$\delta p_v = \frac{m n_o \overline{c^2}}{3V_o} \left[\frac{\omega^2 \tau^2 + j\omega\tau}{1 + \omega^2 \tau^2} \right] v_o e^{j\omega t} \qquad (2.2.19)$$

Write the equilibrium vapour pressure as

$$p_{ve} = \frac{mn_o\overline{c^2}}{3} \qquad (2.2.20)$$

and $$\delta V = v_o e^{j\omega t} \qquad (2.2.21)$$

Hence from equation (2.2.19), (2.2.20) and (2.2.21)

$$\delta p_v = \frac{p_{ve}}{V_o} \left[\frac{\omega^2 \tau^2 + j\omega\tau}{1 + \omega^2 \tau^2} \right] \delta V \qquad (2.2.22)$$

Assuming the air, under the impact of a sound wave on the bubble, obeys the adiabatic law

$$p_a V^\gamma = \text{const.} \qquad (2.2.23)$$

then $$\delta p_a = \left(\frac{\gamma p_a}{V_o} \right) \delta V \qquad (2.2.24)$$

where p_a is the pressure of theair γ is the ratio of the principal specific heats for air, and V_o is the equilibrium volume.

The change in the total pressure is given by

$$\delta P = \delta p_a + \delta p_v \qquad (2.2.25)$$

Substituting from equations (2.2.24) and (2.2.22) into equation (2.2.25):

$$\delta P = \frac{\gamma p_a}{V_o} + \frac{p_{ve}}{V_o}\left[\frac{\omega^2 \tau^2}{1 + \omega^2 \tau^2}\right] + j\,\frac{p_{ve}}{V_o}\left[\frac{\omega \tau}{1 + \omega^2 \tau^2}\right]\delta V \qquad (2.2.26)$$

Put $$A = \frac{\gamma p_a}{V_o} + \frac{p_{ve}}{V_o}\left[\frac{\omega^2 \tau^2}{1 + \omega^2 \tau^2}\right] \qquad (2.2.27)$$

$$B = \frac{p_{ve}}{V_o}\left[\frac{\omega \tau}{1 + \omega^2 \tau^2}\right] \qquad (2.2.28)$$

$$\delta V = v_o (\cos \omega t + j \sin \omega t) \qquad (2.2.29)$$

Substituting from equations (2.2.27), (2.2.28) and (2.2.29) into equation (2.2.26)

$$\delta P = (A + j\ B) v_o (\cos \omega t + j \sin \omega t) \qquad (2.2.30)$$

Hence, from equation (2.2.30) the real part of the change in the total pressure.

$$R_e(\delta P) = v_o (A^2 + B^2)^{\frac{1}{2}} \cos (\omega t - \phi) \qquad (2.2.31)$$

where $$\phi = \tan^{-1} \frac{B}{A} \qquad (2.2.32)$$

Also, the real part of the change in the total volume,

$$R_e(\delta V) = v_o \cos \omega t \tag{2.2.33}$$

and $$\frac{R_e(\delta V)}{\delta t} = -\omega v_o \sin \omega t \tag{2.2.34}$$

The average rate at which the sound wave supplies energy to the bubble is given by

$$|\dot{\Phi}|_{\text{mech.}} = \frac{1}{T} \int_o^T P.\ \delta V \tag{2.2.35}$$

$$|\dot{\Phi}|_{\text{mech.}} = \frac{1}{T} \int_o^T \left[P_o + R_e(\delta P) \right] \frac{R_e(\delta V).}{\delta t}\ \delta t$$

where P_o is the equilibrium pressure of the air. Substituting from equation (2.2.31) and (2.2.34) into equation (2.2.36):

$$|\dot{\Phi}|_{\text{mech.}} = -\omega v_o^2 (A^2 + B^2)^{\frac{1}{2}} . \frac{1}{T} \int_o^T \cos(\omega t - \phi) \sin \omega t.\ \delta t \tag{2.2.37}$$

$$|\dot{\Phi}|_{\text{mech.}} = -\omega v_o^2 (A^2 + B^2)^{\frac{1}{2}} \frac{\sin \phi}{2} \tag{2.2.38}$$

Substituting from equation (2.2.32) for sin $\emptyset$:

$$|\dot{\Phi}|_{\text{mech.}} = - \frac{\omega v_o^2}{2} B \qquad (2.2.39)$$

By squaring equation (2.2.30):

$$v_o^2 = \frac{(\delta P)^2}{(A^2 + B^2)} \qquad (2.2.40)$$

Writing $(\delta P)^2 = p^2_{\text{RMS}}$ approx. (2.2.41)

where p_{RMS} is the root mean square sound pressure, equation (2.2.39) becomes

$$|\dot{\Phi}|_{\text{mech.}} = - \frac{\omega p^2_{\text{RMS}}}{2} \left(\frac{B}{A^2 + B^2} \right) \qquad (2.2.42)$$

From equation (2.2.27), (2.2.28) and (2.2.8) the following approximations are made in the audio frequency range,

$$B^2 \ll A^2 \qquad (2.2.43)$$

and $\omega^2 \tau^2 \ll 1$

Hence, substituting from equations (2.2.27) and (2.2.28) into equation (2.2.42), the average rate at which the second wave supplies energy to the bubble is given by

$$|\dot{\Phi}_{mech.}| = -\frac{p_{RMS}^2}{2\gamma^2} \cdot \frac{p_{vc}\, V_o}{p_a^2} \cdot \omega^2 \tau \qquad (2.2.44)$$

When a sound wave is propagated through a foam its intensity decreases with the distance x traversed. It is evident that this decrease will occur according to a law $e^{-2\alpha x}$, where the attenuation coefficient is defined by[52]

$$\alpha = \frac{|\dot{\Phi}_{mech.}|}{2I} \qquad (2.2.45)$$

$$\text{and} \quad I = \frac{p_{RMS}^2}{2\rho_F c_F} \qquad (2.2.46)$$

In equation (2.2.46) I is the acoustic intensity defined in terms of the effective (i.e. R.M.S. for sine waves) sound pressure $p_{R.M.S.}$, velocity c_F and density ρ_F of the foam medium.

Substituting from equation (2.2.44) and (2.2.46) into equation (2.2.45)

$$\alpha = \frac{p_{vc}\, V_o}{2\gamma^2\, p_a^2} (\rho_F\, c_F) \tau\, \omega^2 \qquad (2.2.47)$$

The parameters in equation (2.2.47) have the following approximate values:

Vapour pressure of water at 20°C, $p_{ve} = 2 \times 10^4$ dyn. cm^{-2}; pressure of the air, $p_a = 10^6$ dyn. cm^{-2}; ratio of principal specific heats for air, $\gamma = 1.4$; density of air-water foam, $\rho_F = 1 \times 10^{-2}$ gm cm^{-3}; velocity in air-water foam, for bubbles of radius 6×10^{-2} cm, $c_F = 1 \times 10^4$ cm sec^{-1}; pressure relaxation time due to presence of saturated vapour, $\tau = 10^{-6}$ sec; volume of a bubble of radius 6×10^{-2} cm, $V_o = 7 \times 10^{-4}$ cm^3.

$$\text{Hence} \quad \frac{\alpha}{f^2} = 2 \times 10^{-14} \text{ neper cm}^{-1} \text{ sec}^2 \qquad (2.2.48)$$

This theoretical value is 10^6 less than the experimental value for α/f^2 of 4×10^{-8} neper cm^{-1} sec^2 at a frequency of 1 kc/s, in an air-water foam.

Section 2.3 Scattering of sound from air bubbles in water

To illustrate the effects of multiple scattering[55], consider the case of the scattering of sound waves in water by a distribution os small air bubbles. Assume that the radius a of the bubbles is small compared to the wavelength λ, so that the scattering from individual bubbles is spherically symmetric.

First, consider the scattering from a single bubble:

2.3.1. Scattering from a single bubble

Since $a << \lambda$, the excess pressure p from the incident sound wave (over and above the average pressure P_o) is approximately uniform over the surface of the bubble. Let

$$p = \overset{A}{p}\, e^{-j\omega t} \qquad (2.3.1)$$

where $\overset{A}{p}$ is a constant. The relation between the excess sound pressure p and the change in bubble volume dV, for adiabatic expansion of the air in the bubble is

$$p = \frac{-\gamma P_o}{V_o}\, dV \qquad (2.3.2)$$

where P_o, V_o are the equilibrium pressure and volume and γ is the ratio of the principal specific heats for air.

The induced motion of the bubble surface sets up a radially out-going wave in the liquid (water). The velocity potential Ψ_s of the scattered wave is given approximately by

$$\Psi_s = \frac{A}{r} e^{j(kr - \omega t)}; \quad \omega = kc_L \tag{2.3.3}$$

where A is the amplitude of the velocity potential, and ρ_L, c_L are the density and sound velocity of the liquid, ρ_G, c_G the corresponding values for the gas, at equilibrium pressure P_o.

The boundary conditions are that the excess pressure of incident and scattered wave just outside the bubble must equal the excess pressure inside; also the radial velocity must match ar $r = a$. Finally, the velocity potential Ψ_s of the scattered wave is given by substituting from the amplitude A from equation (A2.14) in the appendix into equation (2.3.3):

$$\Psi_s \sim \frac{\frac{A}{a}p/j\omega\rho_L}{(\omega_o/\omega)^2 - 1 - j(B/\omega)} \quad \frac{e^{j(kr - \omega t)}}{r} \tag{2.3.4}$$

where $$\omega_o^2 = \frac{3\rho_G c_G^2}{\rho_L a^2} = \frac{3\gamma P_o}{\rho_L a^2} \tag{2.3.5}$$

is the resonance frequency of the air bubble

$$\text{and} \quad B = \frac{3\rho_G c_G^2}{a\rho_L c_L} \tag{2.3.6}$$

is the radiation resistance load on the spherical surface.

In practice there are other losses; viscosity effects, for example, also losses because the changes of pressure in small bubbles are not strictly adiabatic, and therefore not exactly reversible. Thus the last term in the denominator of equation (2.3.4) should be replaced by the somewhat larger $-j\delta(\omega)$, which depends on the frequency in a more complicated way than does $-j\,(B/\omega)$. Function δ is, in general, somewhat larger than unity at $\omega=\omega_o$.

Therefore, if the velocity potential at the bubble surface is

$$\Psi_i \, e^{-j\omega t} \tag{2.3.7}$$

the scattered velocity potential "produced" by the incident wave is given from equation (2.3.4) by

$$\Psi_s \sim \frac{a\Psi_i}{(\omega_o/\omega)^2 - 1 - j\delta(\omega)} \quad \frac{e^{j(kr-\omega t)}}{r} \tag{2.3.8}$$

The scattering cross section Q_s of the bubble is defined as the total power scattered per unit incident intensity. The absorption cross section Q_a is defined

as the total power absorbed per unit incident intensity. The total cross section Q_t is defined as the total power removed from the field space of the incident wave per unit incident wave intensity. Hence $Q_t = Q_s + Q_a$.

$$Q_s = \frac{4\pi a^2}{\left[(\omega_o/\omega)^2-1\right]^2 + \delta^2} \qquad (2.3.9)$$

$$Q_a = \frac{4\pi a^2(\delta/ka)}{\left[(\omega_o/\omega)^2-1\right]^2 + \delta^2} \qquad (2.3.10)$$

$$Q_t = \frac{4\pi a^2(1 + \delta/ka)}{\left[(\omega_o/\omega)^2-1\right]^2 + \delta^2} \qquad (2.3.11)$$

All exhibit resonance at $\omega = \omega_o$ between the stiffness of the air bubble and the effective mass of the liquid just outside the bubble. Both ω_o and $\delta(\omega)$ are functions of the bubble radius a.

2.3.2 Multiple scattering

The effect is now considered of a number of bubbles[55]. Suppose there are N bubbles inside a sphere of radius D. They vary in size and are randomly distributed with a density function $n(\underline{r},a)da$, which gives the average density, at the point specified by the vector $\underline{r}$, of bubbles having a radius between a and a + da.

Hence, the total number of bubbles is

$$N = \int_0^{a_m} da \iiint n(\underline{r},a)dV \qquad (2.3.12)$$

and $$n(\underline{r}) = \int_0^{a_m} n(\underline{r},a)da \qquad (2.3.13)$$

is defined as the average density of bubbles of all size at the point $\underline{r}$. In these equation, a_m is the maximum radius of the bubbles, and the volume integration, which is over the volume V, includes all the bubbles of any size. It is assumed that $\lambda_L >> 2\Pi a_m$, where λ_L is the wavelength of sound in free water.

Thus, the velocity potential at some point $\underline{r}$, $\Psi(\underline{r})$, can be written as the sum of the incident wave Ψ_i and the spherically symmetric scattered waves from N bubbles, the nth bubble being at $\underline{r}_n$;

$$\Psi(\underline{r}) = \Psi_i(\underline{r}) + \sum_{n=1}^{N} \frac{A_n}{r} e^{jkR_n} \qquad (2.3.14)$$

where $k = \omega/c_L$ and $R_n = |\underline{r} - \underline{r}_n|$.

The magnitude A_n (see equation A2.20 in the appendix) is related to the velocity potential at the position of the nth bubble. Here the effect on bubble n of the scattering from all the other bubbles has been included. Substituting for A_n into equation (2.3.14):

$$\Psi(\underline{r}) = \Psi_i(\underline{r}) + \sum_{n=1}^{N} \frac{g_n}{R_n} \Psi_n \, e^{jkR_n} \qquad (2.3.15)$$

where Ψ_n and g_n are given in equations A2.21, A2.27 and A2.23 in the appendix.

The fields for specific configurations of bubbles are not particularly interesting, even if they could be obtained. The more interesting is the average field, obtained by averaging over all configurations of bubbles inside the sphere of radius D. This average is indicated by the brackets $\langle\ \rangle$. Consequently, for N large,

$$\langle \Psi(\underline{r}) \rangle \sim \Psi_i(\underline{r}) + \iiint G(\underline{r}_n) \quad \langle \Psi(\underline{r}_n) \rangle \frac{e^{jkR_n}}{R_n} \, dV_n \qquad (2.3.16)$$

The quantity $G(\underline{r})$ is the average density of the bubble scatterers at $\underline{r}$. (See equation A2.25 in the appendix).

Equation (2.3.16) is an integral equation for $\langle \Psi(\underline{r}) \rangle$ equivalent to the partial differential equation

$$\underline{\nabla}^2 \langle \Psi \rangle + k^2 \langle \Psi \rangle = -4\pi G \langle \Psi \rangle \qquad (2.3.17)$$

or $$\underline{\nabla}^2 \langle \Psi \rangle + k_s^2 \ (r) \langle \Psi \rangle = 0 \qquad (2.3.18)$$

$$\text{where} \quad k_s(r) = k\left[1 + \frac{4\Pi G}{k^2}\right]^{\frac{1}{2}} \tag{2.3.19}$$

Substituting for G from equation A2.25 in the appendix,

$$k_s(r) \sim k + \frac{2\Pi}{k}\int_0^D \frac{n(r,a)\,da}{\left[\frac{\omega_o(a)}{\omega}\right]^2 - 1 - j\delta(\omega,a)} \tag{2.3.20}$$

Therefore, the configurational average of the velocity potential is a solution of the wave equation for an index of refraction $1 + (4\Pi G/k^2)$ which varies with the density of bubbles. Because of the $\delta(\omega,a)$ term, this index of refraction is complex, producing attenuation as the wave traverses the bubble filled region. The Green's function[56] for this wave equation is the solution of the equation

$$\underline{\nabla}_r^2 K(\underline{r}/\underline{r}_o) + k_s^2(r) K(\underline{r}/\underline{r}_o) = -4\Pi\delta(\underline{r} - \underline{r}_o) \tag{2.3.21}$$

which goes as R^{-1} when $|\underline{r} - \underline{r}_o| \to 0$, and represents an outgoing wave for large R.

A similar configurational average of $|\Psi(\underline{r})|^2$ can also be performed. The corresponding integral equation is

$$\langle|\Psi(\underline{r})|^2\rangle \sim |\langle\Psi(\underline{r})\rangle|^2 + \frac{1}{4}\iiint dV_o\, S(\underline{r}_o)\langle|\Psi(\underline{r}_o)|^2\rangle K(\underline{r}/\underline{r}_o)^2 \tag{2.3.2}$$

where

$$S(\underline{r}) = 4\Pi \int_0^{\mathbb{D}} n(\underline{r},a) \; |g(a)|^2 da = \int_0^{D} n(\underline{r},a) \; Q_s(a) da \qquad (2.3.23)$$

is the total scattering cross section of bubbles per unit volume at the point specified by vector $\underline{r}$. This equation shows that the coherent part of the scattered wave is given by the square of the configurational average of $\Psi(\underline{r})$, which is affected by the bubbles through their effect on the index of refraction $\sqrt{1 - 4\Pi G(\underline{r})}$.

In addition to the coherent wave $|\langle \Psi(\underline{r}) \rangle|^2$, there is also the incoherent scattering represented as being proportional to the density S of scattering cross section, with the radiation from each element of volume proportional to $\langle |\Psi(\underline{r})|^2 \rangle$ and attenuated in its passage through the bubbly region, according to the square of the Green's function $K(\underline{r}/\underline{r}_o)$.

The solution to the above equations to specific problems is extremely difficult. An example of the mathematical sophistication required for the solution to the above set of equations can be found in the work of Twersky[56].

VELOCITY

Section 2.4 Velocity of sound in air – liquid mixtures

Introduction

A sound wave propagated through a mixture of air and liquid may be considered to be transmitted with a velocity approximately determined by the average compressibility and density of the constituents. As a result, the medium should behave as a fluid having a high density like a liquid and a high compressibility like air.

Theory

Mallock[1] (1910), Wood[13] (1930), Karplus[14] (1958), Hsieh and Plesset[6] (1961) derived an equation for the

velocity of sound in a liquid containing a homogeneous and isotropic distribution of gas bubbles. This derivation assumes that (i) The natural frequency of vibration of the bubbles in their lowest modes is well above that of the sound frequency, i.e., the bubbles will vibrate in phase with the sound field, the amplitude of vibration being small. (See appendix A1). (ii) The medium is continuous, i.e., both the distance between bubbles and the bubble diameter are much less then the wavelength of the sound.

Let the suffixes G and L denote the gas and liquid components respectively, and x the volume concentration of the gas in the mixture as measured at room temperature and atmospheric pressure. Then the average density ρ_T and compressibility K_T of the mixture are

$$\rho_T = x\rho_G + (1 - x)\rho_L \; ; \quad K_T = xK_G + (1 - x)K_L \qquad (2.4.1)$$

The average velocity of sound c in the mixture for small amplitudes is given by

$$c = (\rho_T K_T)^{-\frac{1}{2}} \qquad (2.4.2)$$

Hence from (2.24) and (2.25)

$$c = \left\{ \left[x\rho_G + (1 - x)\rho_L \right] \left[xK_G + (1 - x)K_L \right] \right\}^{-\frac{1}{2}} \qquad (2.4.3)$$

The question now arises whether the compression of the gas bubbles is isothermal or adiabatic, i.e. does the gas transfer its heat of compression to the surrounding liquid in a time long or short compared with the period of the acoustic pressure fluctuation. These cases are calculated in appendix A9, but the results are given below.

(i) Adiabatic velocity

If the heat transfer between gas and liquid is negligible, then the propagation is adiabatic and the gas compressibility takes the value $K_{GA} = (\gamma P_o)^{-1}$ where γ is the ratio of the principal specific heats of the gas and P_o is the equilibrium gas pressure. Then the expression for the adiabatic sound velocity c_A in the air-liquid mixture becomes

$$c_A = \left[\frac{x^2}{c_G^2} + \frac{(1-x)^2}{c_L^2} + x(1-x) \left(\rho_G K_L + \frac{\rho_L}{\gamma P_o} \right) \right]^{\frac{1}{2}} \qquad (2.4.4)$$

for all values of gas concentration x in the mixture.

For an air-water foam ($x = 0.98 - 0.99$), at room temperature and atmospheric pressure, the following approximations apply (see appendix A9):

$$\rho_G K_L << \rho_L/(\gamma P_o)$$

and $(1 - x)^2/(c_L^2) << x(1 - x)\rho_L/(\gamma P_o)$

Hence equation (2.4.4) may be re-written to a good approximation as

$$c_A = \left[\frac{x^2}{c_G^2} + \frac{x(1-x)\rho_L}{\gamma P_o}\right]^{-\frac{1}{2}} \quad \text{for } 0.98 < x < 0.99 \qquad (2.4.5)$$

From equation (2.4.1) the average density of the foam ρ_F is given by

$$\rho_F = x\rho_G + (1 - x)\rho_L \qquad (2.4.1)$$

Substitution of equation (2.4.1) into equation (2.4.5) yields

$$c_A = \left[x^2\left(\frac{1}{c_G^2} - \frac{\rho_G}{\gamma P_o}\right) + \frac{x\rho_F}{\gamma P_o}\right]^{-\frac{1}{2}} \quad \text{for } 0.98 < x \leq 0.99 \qquad (2.4.6)$$

Since x remains constant to within 1 per cent for all the the liquid foams used, the following terms have these values, at room temperature and atmospheric pressure:

$$x^2\left(\frac{1}{c_G^2} - \frac{\rho_G}{\gamma P_o}\right) = 9.0 \times 10^{-12} \text{ cm}^{-2} \text{ sec}^2 = B_1 \qquad (2.4.7)$$

$$x/(\gamma P_o) = 7.0 \times 10^{-7} \text{ dyn.}^{-1} \text{ cm}^2 = B_2 \qquad (2.4.8)$$

Neglecting the term B_1 compared with $B_2 \rho_F$, (where ρ_F is in the range 0.01 to 0.02 gm cm^{-3}), equation (2.4.6) may be re - written as

$$c_A = \left(\frac{\gamma P_o}{x \rho_F} \right)^{\frac{1}{2}} \quad \text{for } 0.98 < x < 0.99 \qquad (2.4.9)$$

(ii) Isothermal velocity

If the heat transfer is so fast that the gas is in equilibrium with the constant - temperature liquid, then the process is isothermal and the compressibility takes the value $K_{GI} = (P_o)^{-1}$. Hence the expression for the isothermal sound velocity c_I in the air - water mixture becomes to a good approximation

$$c_I = \left[\frac{\gamma x^2}{c_G^2} + \frac{x(1 - x)\rho_L}{P_o} \right]^{-\frac{1}{2}} \qquad (2.4.10)$$

CHAPTER 3

REVIEW OF WORK ON THE STABILITY OF FOAMS

Section 3.1 Classification of foams

True foaming is dependent upon the presence of a property for which the general term "film elasticity" has been suggested. The essential requirement is that, when two bubbles of gas come together in a liquid (see fig. 9), the intervening liquid must thin down to a lamella, instead of rupturing at the point of closest approach. In persistent foams, the bubbles are eventually transformed into polyhedra separated by exceedingly thin, flat lamellae. (See fig. 10 due to Kitchener and Cooper[21], 1959). Thick lamellae are temporarily formed in transient foams, but they rupture after a period of drainage. Typical persistent foams are those of soaps, ionic and non-ionic detergents (see appendix A4), saponin and proteins. Typical transient foams are provided by solutions of sparingly soluble alcohols, undissociated fatty acids, pine oil, aniline and phenol.

Section 3.2 The role of surface rheology

The idea that foaming might be dependent on the viscosity or plasticity of the interfacial liquid layers

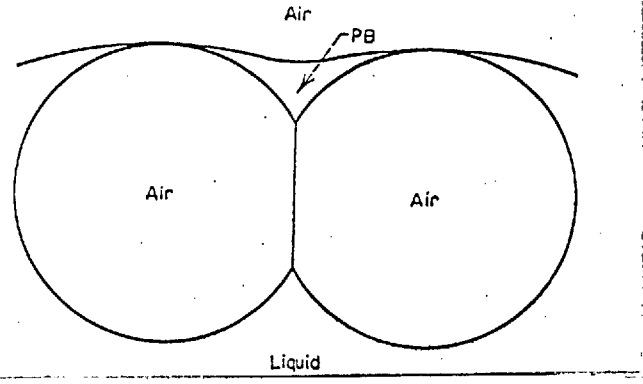

Fig. 9a. Mutual deformation of two foam bubbles in contact in the top layer of foam.
P.B. means Plateau's Border. The liquid in this space is under a lower pressure than the liquid in the walls of the bubbles.

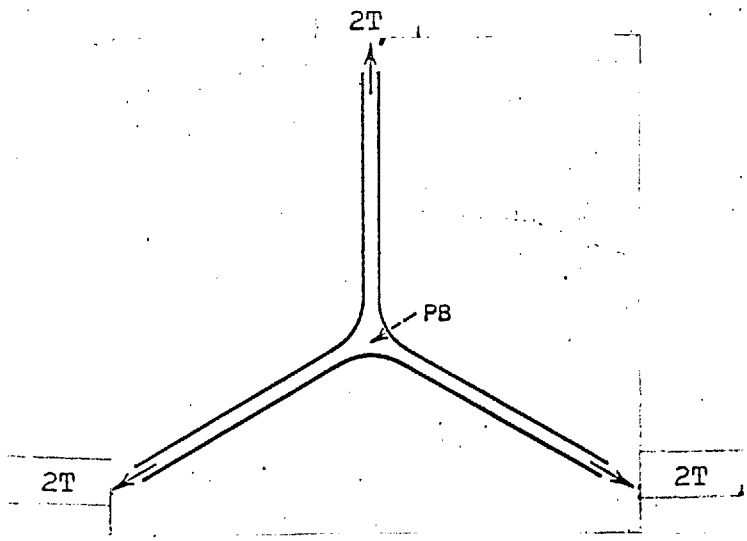

Fig. 9b. Three foam lamellae coming together in a Plateau Border (P.B.) and forming angles of 120 deg. with each other. (2T = surface tension force)

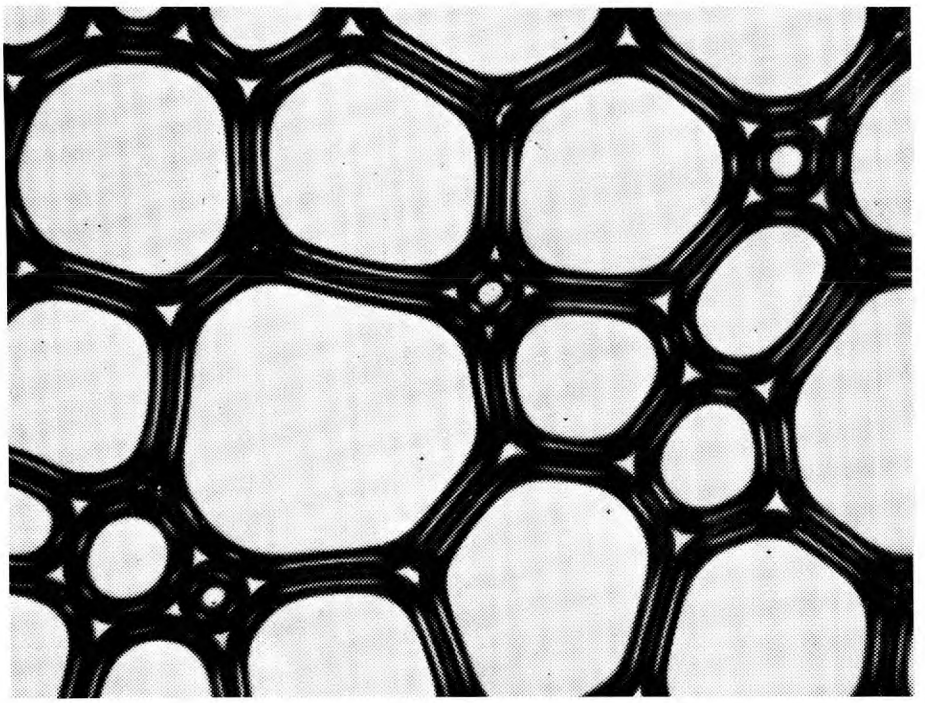

Fig.10a A partially-drained foam, showing distortion of bubbles.

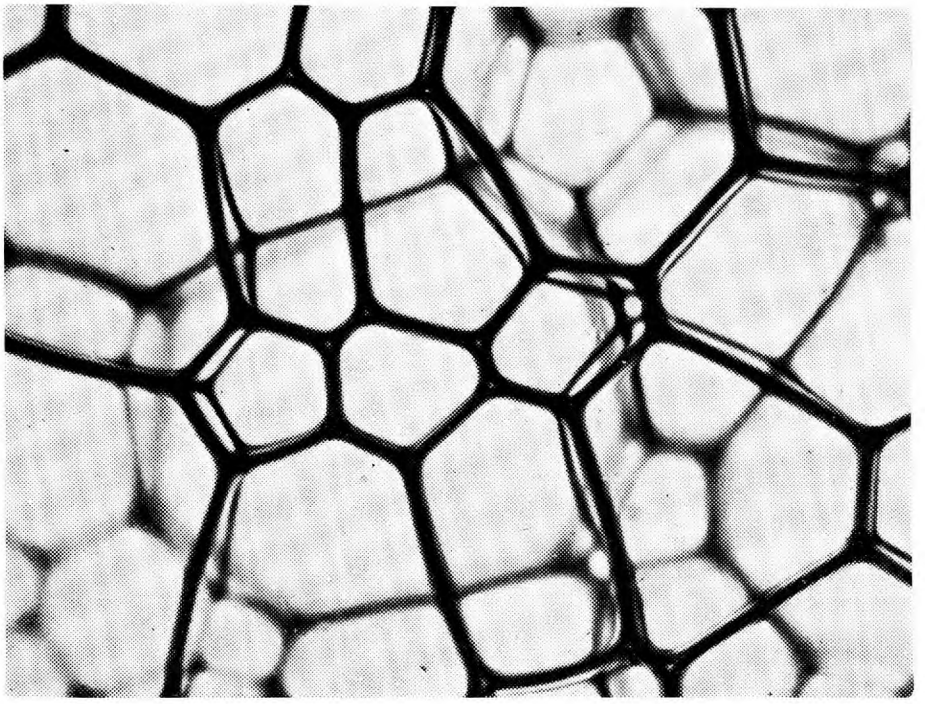

Fig.10b After further drainage: the lamellae and Plateau's borders continue to thin (Note curvature of some bubble walls, owing to unequal internal pressures)

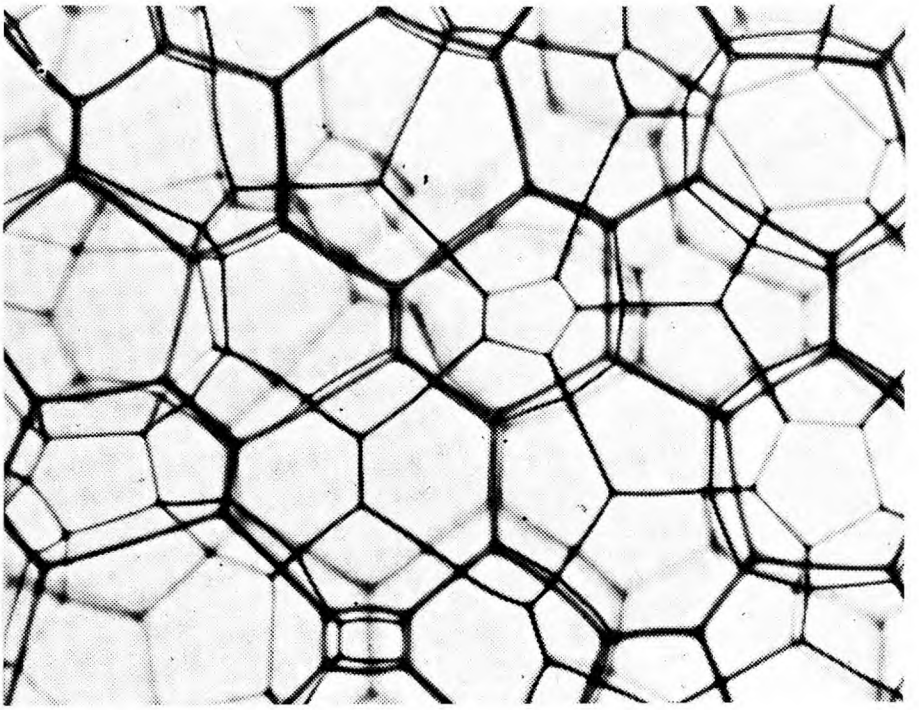

Fig.10c A well drained foam, showing polyhedral cells and very thin Plateau's borders. (In an ideal homo-disperse foam, the bubbles are pentagonal dodecahedra)

was first advocated as early as 1873 by Plateau[22]. The present point of view (Kitchener[23], 1964) is that surface viscosity alone could never lead to a film elasticity, viscosity being only a dissipation of momentum and not the generation of a net restoring force. The rheological properties of the surface layers undoubtedly ~~do~~ have however a great influence on the rate of relaxation of stresses in the lamellae, the most obvious effects of viscosity being the damping of any disturbances and the retardation of drainage of lamellae (Brown et al.,[24] 1953).

Investigations of Oldroyd[25] (1955) have shown that five parameters are required to characterize the linear behaviour of an interface completely. These are the two viscosity coefficients, i.e., the Newtonian shear viscosity at constant area and the surface dilational viscosity, and the two elasticity coefficients, a surface shear modulus and a surface dilational elastic modulus. The fifth parameter is the equilibrium surface tension. Only the surface shear viscosity has been the subject of many detailed investigations, which are reviewed by Joly[26] (1964).

Section 3.3 Mixed foams

High viscosity, either of the surface layers or of the bulk liquid, has the effect of retarding drainage

of liquid from foams. For example, transient foams of the amyl alcohol-water type have a considerably enhanced lifetime if a substantial proportion of glycerol is added to the solution. The best known example, however, is the effect of certain non-ionic additives (see appendix IV) on the persistence of synthetic detergent foams. Miles et al[27] (1945, 1950) distinguished between "fast draining" and "slow draining" detergent foams, and showed by studies of single films that the former correspond to freely mobile surfaces, while the latter have highly viscous or rigid mixed interfacial layers, the non-ionic components fitting between the ionized molecules to give a highly condensed film and low surface tension. Recently Kruglyakov and Taube (1965) studied the problems connected with the kinetics of collapsing foams caused by liquid drainage.

The patent literature on these "foam builders" is extensive. The best known examples are sodium dodecyl sulphate + dodecyl alcohol, and dodecylbenzene sulphonate + lauryl isopropanolamide. Davies[29] (1957) demonstrated the correlation between surface viscosity and foam life with sodium laurate + lauryl alcohol.

Kaertkemeyer[30] (1957), and Shick and Fowkes[31] (1957), noted the similarity between foam stabilization and the lowering of the critical micelle concentration (see appendix A4) by additives. The most effective additives for straight-chain detergents were found to be non-ionic compounds with a similar chain length, and a hydrophilic end group. Spitzer[32] (1960) described the drainage characteristics of various anionic + non-ionic mixtures (see appendix 18). Recently Pilpel[33] (1964) has reviewed the work on foam stabilizing agents used in synthetic detergents.

Section 3.4 Rheology of the foam

Foams in bulk behave as weak, plastic solids. At small stresses they undergo reversible elastic deformation, associated with distortion of the forms of the individual bubbles; at higher stresses they undergo plastic flow, with slip of bubbles. In a tube, the foam moves by "plug flow", shearing at the walls, an effect noticed by Eisner and Smith[34] (1956).

There appears to have been no fundamental work on the mechanical and rheological properties of foaming since the war-time studies on fire-fighting foams carried out by Penney and Blackmann[35] (1943) and Clark and Blackmann[35] (1947, 1948). Apparently the connection

between the rheology of lamellae and of bulk foam has not been studied systematically.

Section 3.5 Diffusion of gas

In ordinary, poly-disperse foams of persistent type, the first stage of ageing is drainage, with thinning of lamellae (see fig. 10); this is followed by migration of gas from the smaller bubbles into the larger by diffusion through the thin "windows" separating them, thus leading to the disappearance of small bubbles. The driving force is the difference of chemical potential arising from differences of internal pressure, the smaller bubbles having a higher Laplace capillary pressure[36], $2T/a$ (where T is the surface tension and a is the radius of the bubble). De Vries[37] (1958) made a study of gas diffusion in foams of oil-in-water emulsions and of rubber latex. He verified that the small bubbles shrank and the large ones grew.

Section 3.6 Mechanism of rupture

After drainage has taken place, the extruded liquid escaping down the interconnecting channels (called "Plateau borders"), the polyhedral foam begins to collapse by rupture of thin lamellae and union of bubbles (see fig. 9).

Foams in bulk are comparatively short-lived because, even if the foam is enclosed, there is always gas transfer by diffusion, which must ultimately cause all the gas to accumulate in a single bubble. In practice, the sudden rearrangements of packing of the polyhedral cells, necessitated from time to time because of gas diffusion, shatter the thin lamellae.

Section 3.7 Foam destruction by acoustic waves

Foam destruction by large amplitude sound waves was attributed by Boucher and Weiner[38] (1963) to (a) acoustic pressure; (b) unidirectional radiation pressure; (c) induced resonant vibrations in the bubbles; (d) turbulence produced by the "sonic wind".

(i) Acoustic pressure effect

Assume that the foam is constituted by a multitude of hollow tangent hemispheres. Because of surface tension forces, the pressure inside each hollow sphere is higher than the atmospheric pressure by approximately $2T/a$ The acoustic pressure is the major source of external pressure used to overcome the excess bubble pressure and so destroy the foam bubbles. The greater the wave amplitude, the larger the pressure gradient variation.

(ii) Unidirectional radiation pressure

High power sound waves can exert a radiation pressure against any obstacle upon which they impinge. It is assumed that this radiation pressure P_r can be derived as a first approximation from Rayleigh's general formula:

$$P_r = (\gamma + 1)E/2 \qquad (3.1)$$

where E is the acoustic energy density in front of the obstacle and γ is the principal specific heat ratio.

(iii) Induced resonant vibrations

Another key factor in bubbles destruction is the fact that each hollow liquid sphere responds favourably to a certain vibration frequency i.e. its natural resonance frequency. Most of the industrial foams are constituted by bubbles having a mean radius between 1.0 and 0.05 cm, and according to Boucher and Weiner[38] (1963) their resonance frequency lies in the very low audible range, viz. 325 - 650 c/s. This resonant frequency f_r was calculated using the formula due to Minnaert[19] (see appendix A1):

$$f_r = \frac{1}{2\Pi a_o}\left(\frac{3\gamma P_o}{\rho_L}\right)^{\frac{1}{2}}$$

where a_o is the equilibrium radius of the bubble, ρ_L is the liquid density, γ is the principal specific heat ratio, and P_o is the equilibrium pressure. For air and water at the usual temperature and pressure this reduces to

$$f_r = \frac{650}{2\,a_o}$$

(f_r in c/s and bubble radius in cm)

(iv) Sonic wind

The sonic wind which is observed in intense acoustic fields is a kind of hydrodynamic flow due to viscous losses in the medium of transmission. By creating a strong turbulence above the foam interface, the "sonic wind" helps to destroy the upper bubbles layer.

However, from the practical point of view, two types of acoustic defoaming mechanism are distinguished by Boucher and Weiner[38]: one at medium and high frequencies (above 2,000 c/s) and high intensity in which radiation pressure forces are predominant, and one at low frequency and high intensity in which acoustic pressure and natural resonance frequency phenomena play

the major role. Foam destruction can be accomplished with either an air jet whistle (11,000 c/s - 148 dB) or a membrane horn (700 c/s - 155 dB) which radiates downwards through the climbing foam. In the latter case, the foam is selectively destroyed in the minimum acoustic pressure regions (assuming for instance, standing wave conditions) where the bubbles explode in the rarefaction gaseous zone. On the contrary, with a high power air jet whistle the foam destruction corresponds to a downwards bubble squeezing mechanism whose intensity is an inverse function of the distance between sound source and foam level.

The author has recorded on cine-film the destruction of foam of mean bubble radius 0.05 cm. using a loud-speaker pressure unit (1,000 c/s - 115 dB) (see appendix 5).

CHAPTER 4

EXPERIMENTAL APPARATUS AND METHOD

THE ORIGINAL EXPERIMENTAL SYSTEM

Vignaux[10] (1961) and Connor[11] (1962) separately designed an apparatus to measure the absorption and velocity of wound in a detergent foam (see fig. 11). Foam produced by bubbling air into a detergent solution, was passed down an acoustic measurement tube, and sound was propagated into the foam from a loudspeaker at the base of the tube. A probe microphone was moved up the tube, the amplitude and phase relative to the input being noted. The absorption and velocity of sound were thus obtained.

The apparatus was composed of three major sections:

4.1.0. Foam generation system

4.2.0. Acoustic measurement system

4.3.0. Measurement of foam density

Each section will be criticised in detail.

Section 4.1.0 Foam generation system

A detergent solution was continually pumped from a reservoir to a constant head apparatus (see fig. 12a). From here the solution flowed down a connecting tube

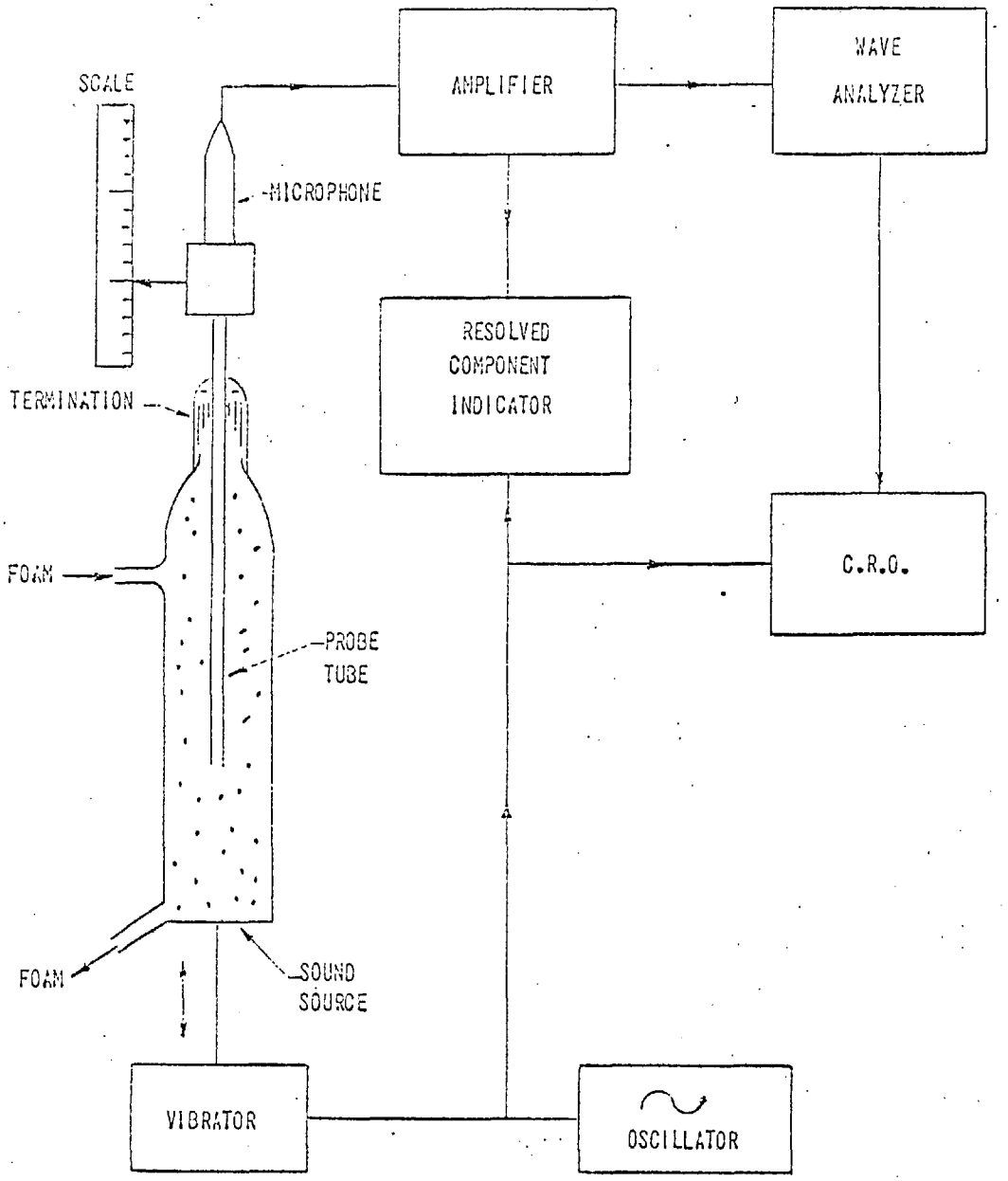

Fig. 11. Acoustic measurement system (Connor).

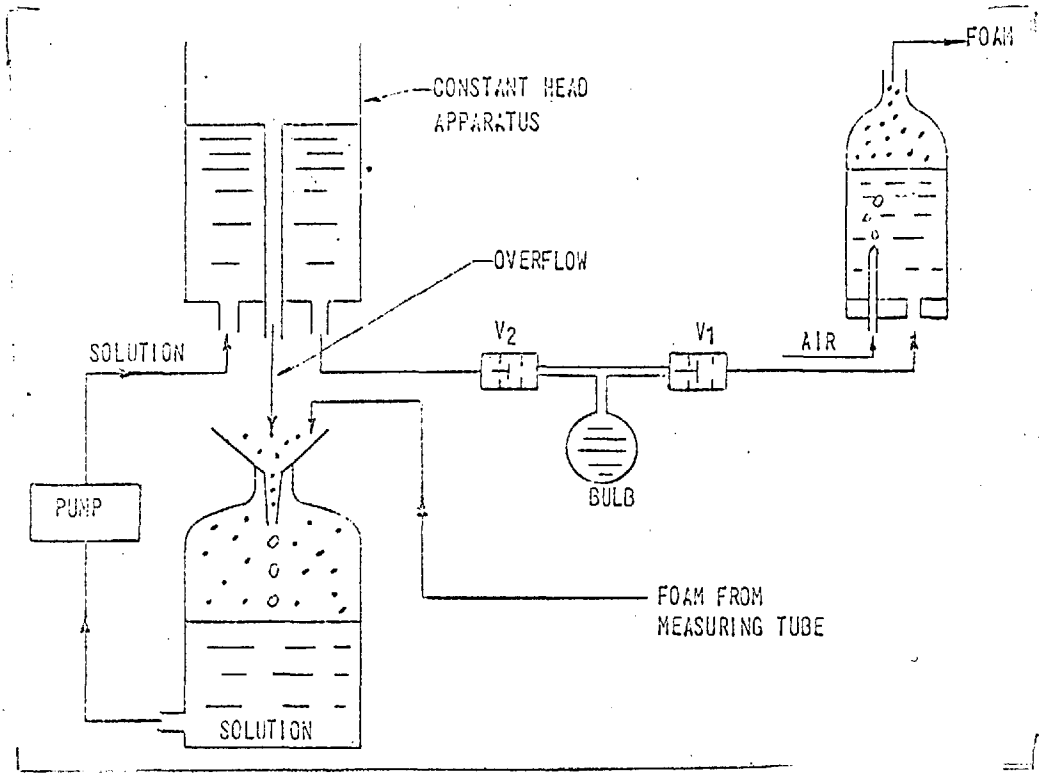

Fig. 12a. Foam generation system (Connor).

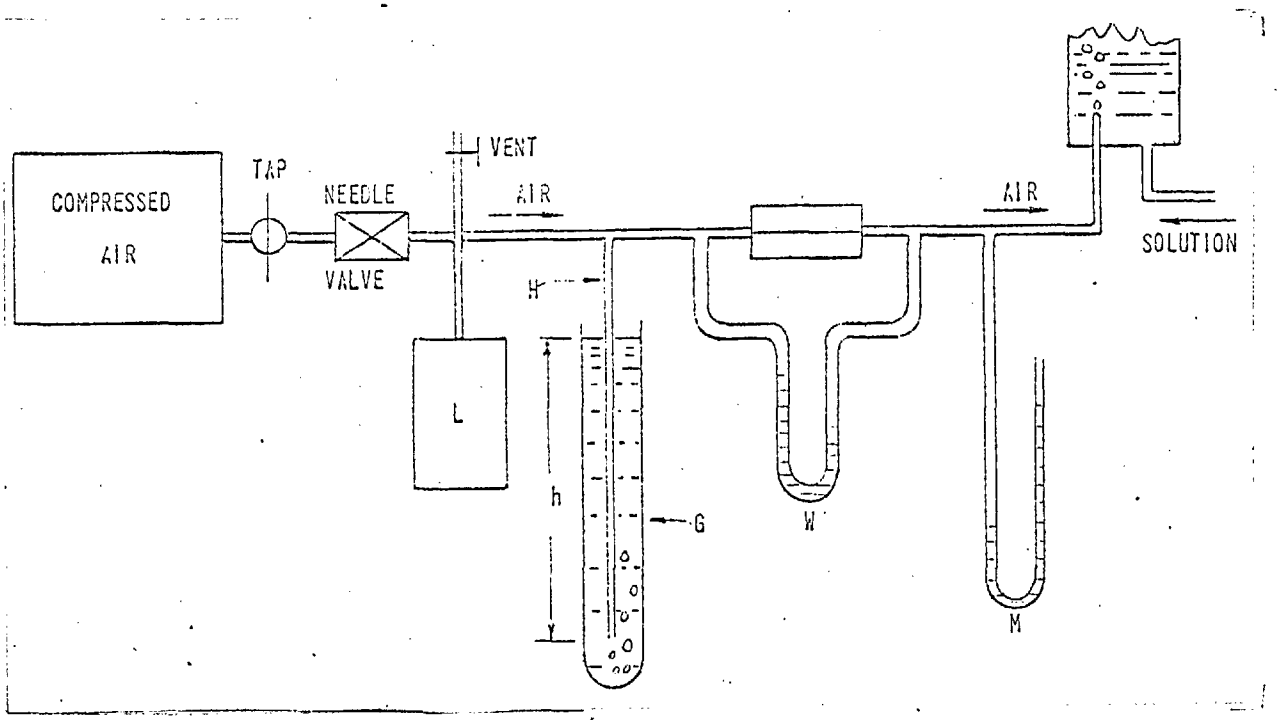

Fig. 12b. Air system (Connor).

into the foam-generator containing the air-jet. The connecting tube had two non-return valves V_1 and V_2 and a small bulb which was used as a force pump to adjust the level of the solution in the foam-generator. The foam produced then passed down the acoustic measurement tube and returned to the solution reservoir to be re-generated.

4.1.1 Air system

The air system is shown in figure (12b). Compressed air (5-10 lbs./sq.in) from the mains supply was passed through a needle valve to a 4 litre reservoir vessel L which served to smooth out fluctuations in pressure. This vessel was provided with a "blow-off" tube G as in standard practice. A mercury manometer M measured the air pressure with respect to atmospheric pressure. The air line then continued on to the jet tube.

Criticism

(i) The manual method of solution control meant that the solution level in the foam-generator could fall a considerable distance before corrective action could be taken. Thus it was difficult to produce a constant density foam and to take reproducible acoustic measurements.

(ii) The foam stabilizing agents may have evaporated from the foam returned to the solution reservoir. Thus Vignaux[10] Connor[11] re-generated foam from a solution depleted of its stabilizer.

(iii) The mains supply of compressed air was subject to large fluctuations in pressure, causing changes in the static pressure in the foam bubbles. This was another factor contributing to the difficulty of taking reproducible acoustic measurements.

(iv) The type of glass capillary jets used by Connor were subject to frequent blocking by sediment from the detergent solution. Replacements could not be guaranteed to be the exact hole size.

The modified foam generation system

The author has designed automatic systems for solution level control (see 4.4.2) and air pressure control (see 4.4.3). Glass jets with reproducible hole sizes can be made by the use of ruby watch jewels (see 4.4.1).

Section 4.2.0 Acoustic measurement system

The acoustic measurement system is shown in fig. 11. The component systems will be considered separately.

4.2.1. Mechanical system

The heavy probe microphone assembly was supported from a narrow horizontal bar attached to a travelling microscope carriage (see fig. 12c). This instrument had two major defects: (i) It was impossible to position the probe axially in the acoustic measurement tube, since the microscope base did not possess levelling screws. (ii) The instrument was unstable, due to the turning effect of the microphone assembly about a vertical axis through the microscope carriage.

Thus the author has to design a new vertically traversing instrument (see section 4.6.0).

4.2.2 Electrical instrumentation

After amplification by a Mullard power amplifier, the signal was fed into a Reslo-sound loudspeaker pressure unit, situated at the bottom of the foam tube (see fig. 11). The amplitude and phase relative to the input was measured using a probe tube fitted with a condenser microphone, mounted on a microscope movement. The output from the microphone was amplified and fed into a Resolved component indicator.

FIG.12c THE PROBE ASSEMBLY SUPPORTED FROM A NARROW HORIZONTAL BAR ATTACHED TO A TRAVELLING MICROSCOPE CARRIAGE (CONNOR)

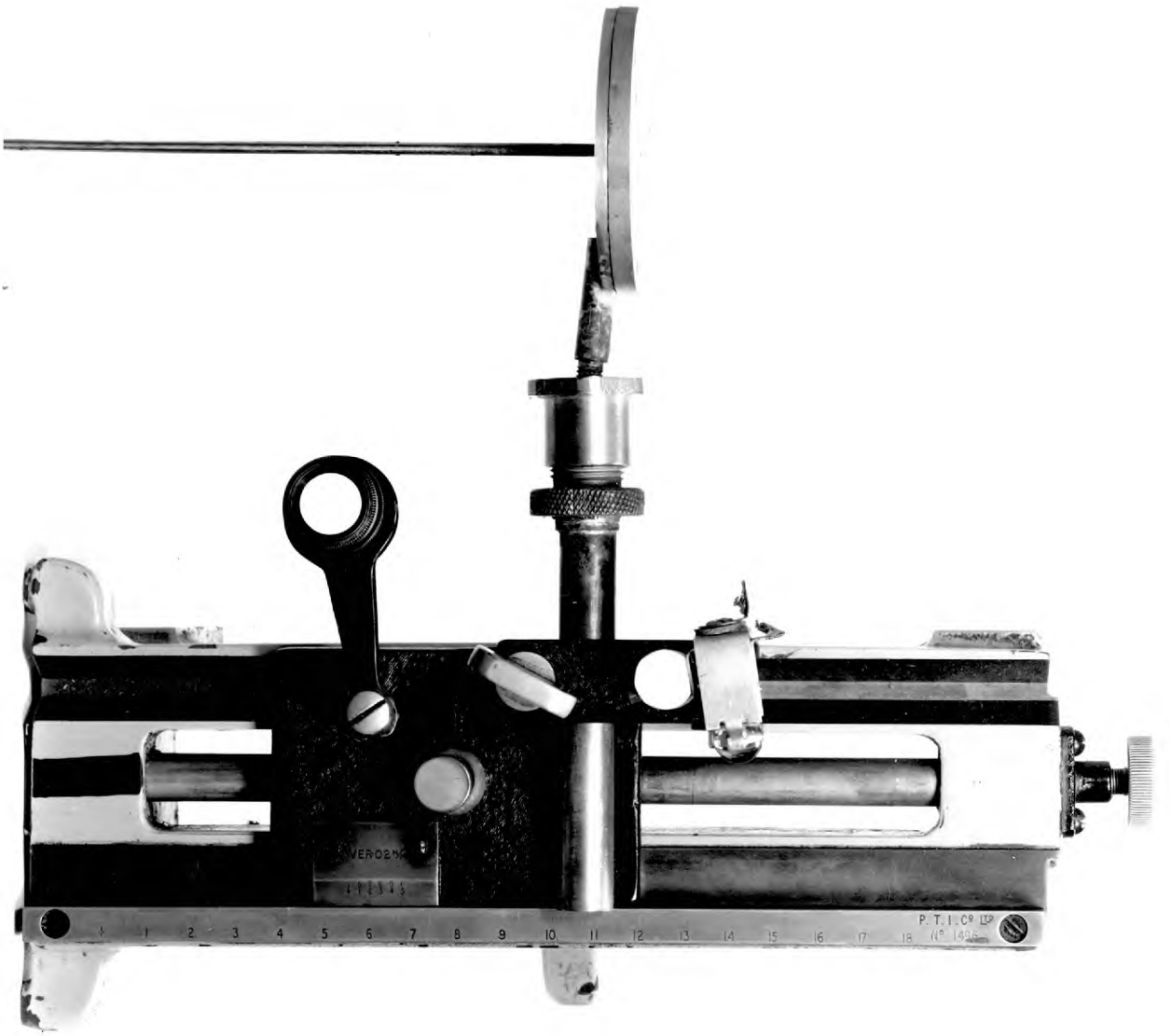
VERO2MK
1 2 3 4 5 6 7 8 9 10 11 12 13 14 15 16 17 18
P. T. I. Cº LTD

Criticism

(i) Due to an impedance mis-match between the power amplifier and the loudspeaker, there was poor power transfer to the foam tube.

(ii) The output signals of the power amplifier and the loudspeaker were distorted.

(iii) The microphone diaphragm had dents and holes in it.

(iv) Owing to its limited frequency range, the Reslo-sound pressure unit had to be replaced.

Modified electrical instrumentation

The author has re-designed the electrical instrumentation, being careful to obtain good impedance matching (see section 4.6.2).

Section 4.3.0 Measurement of foam density

Connor measured foam densities by collecting and weighing known volumes of foams.

The end of a connecting tube from the foam-generator (fig. 12a) was attached to the top of a tapered tube A of known volume, which is held with its wider end downwards and allowed to fill with foam. Then this end was closed with a plastic cap and the tube was inverted.

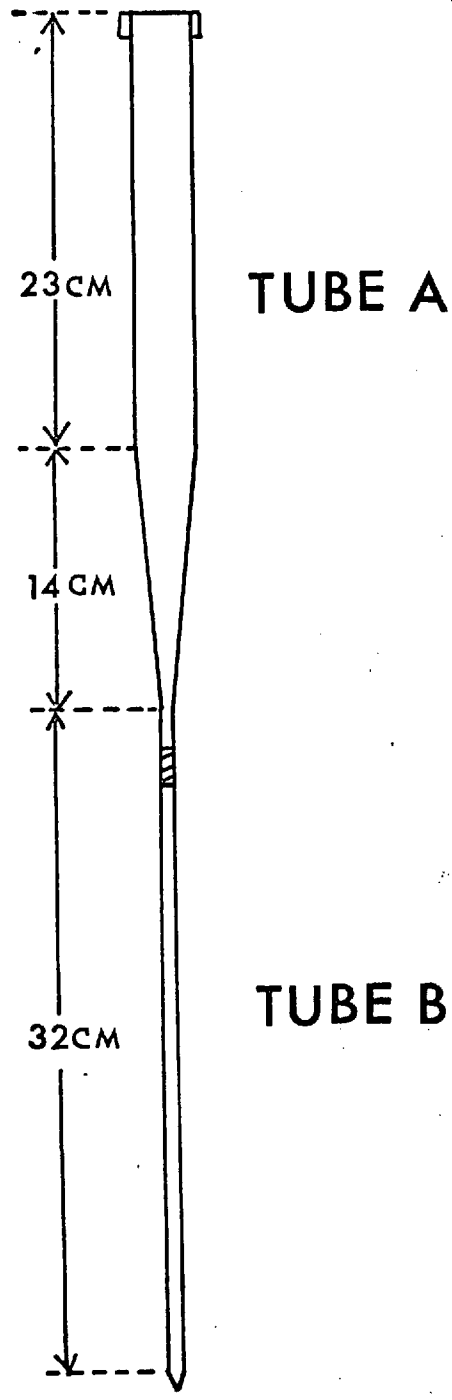

Fig. 13 A calibrated tube B of uniform cross-section attached to the lower tapered end of tube A. (Connor)

A calibrated tube B of uniform cross-section was attached to the lower tapered end (fig. 13) and the foam was left overnight to collapse and drain into B. As the system was sealed during the draining process it was assumed that there was no evaporation loss. The volume of the liquid in B was recorded, and the density of the foam was calculated as

$$\frac{\text{mass of liquid drained}}{\text{volume of foam}}$$

THE MODIFIED EXPERIMENTAL SYSTEM

The modifications of Vignaux's and Connor's apparatus will now be considered in detail.

Section 4.4.0 The modified foam generation system

The modified foam generation system is shown in fig. 14 and fig. 15.

The foam-making vessel contained the air jet and two platinum electrodes, and had a solenoid valve in the solution inlet tube to control the solution level (see fig. 16). The glass vessel surrounded by an O-ring, was held between a brass ring and tufnol base by three screws (see fig. 17a, 17b). A similar method was used to hold the four component glass tubes (see fig. 17c). This allowed them to be easily adjusted without breakages.

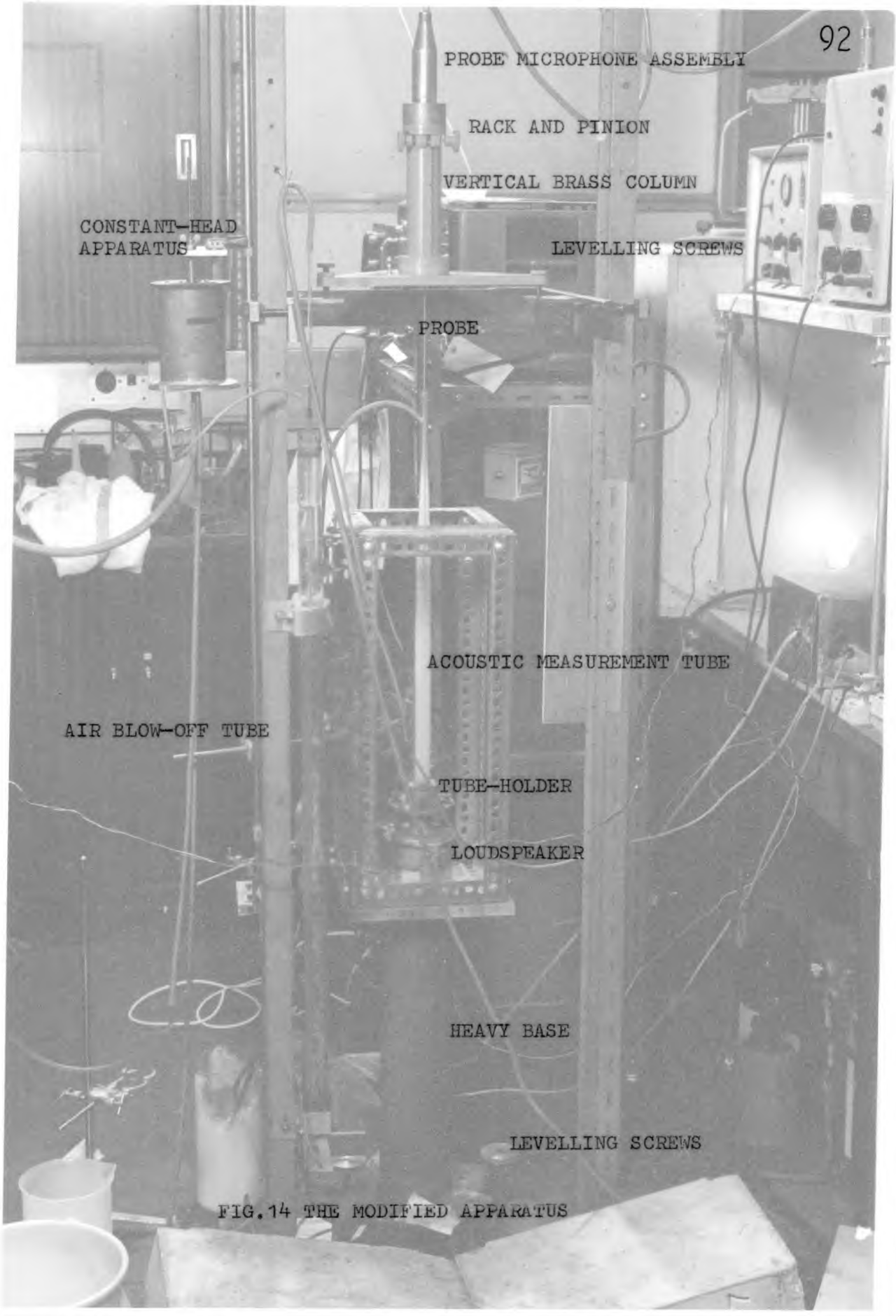

FIG.14 THE MODIFIED APPARATUS

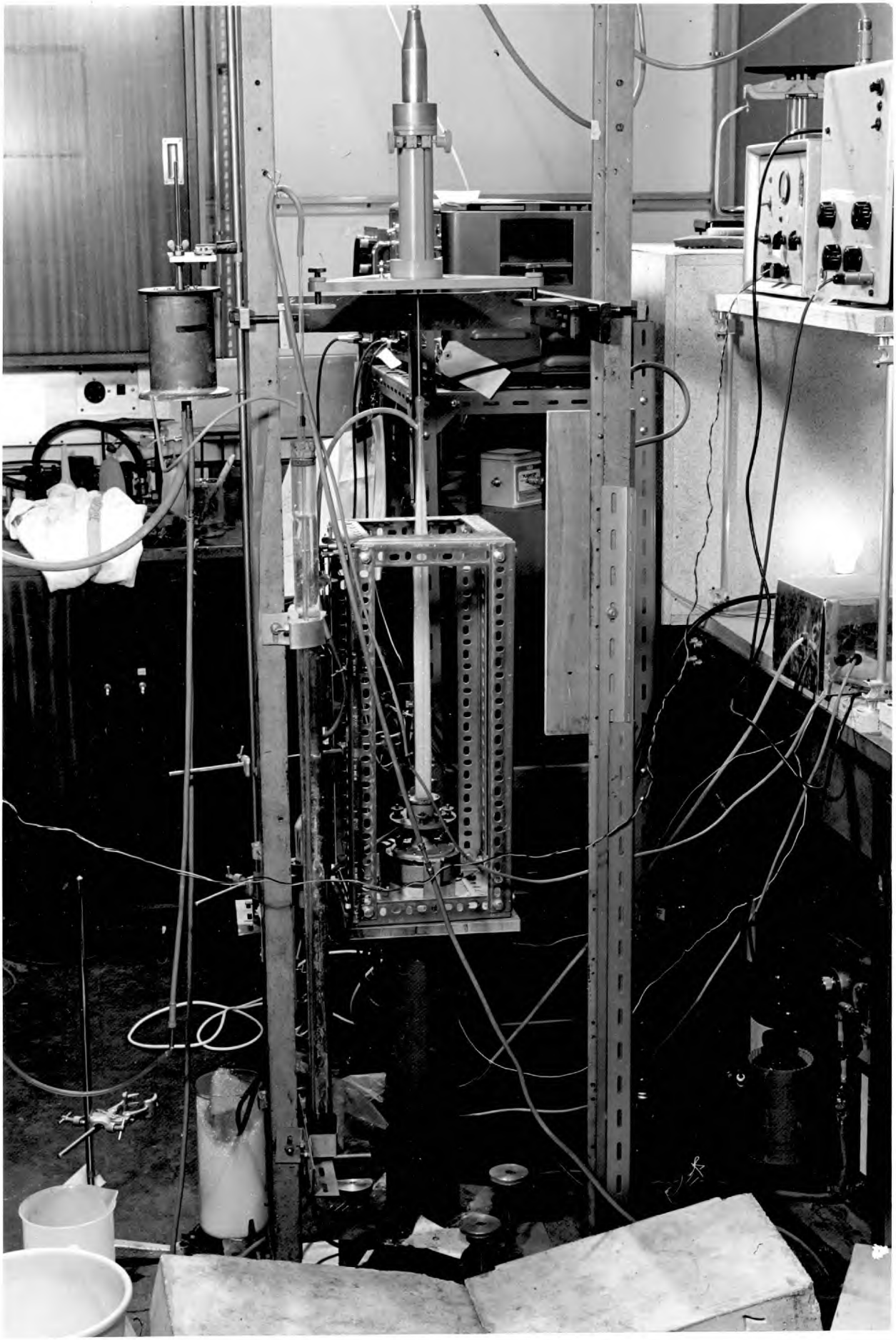

FIG. 15 FOAM GENERATING SYSTEM

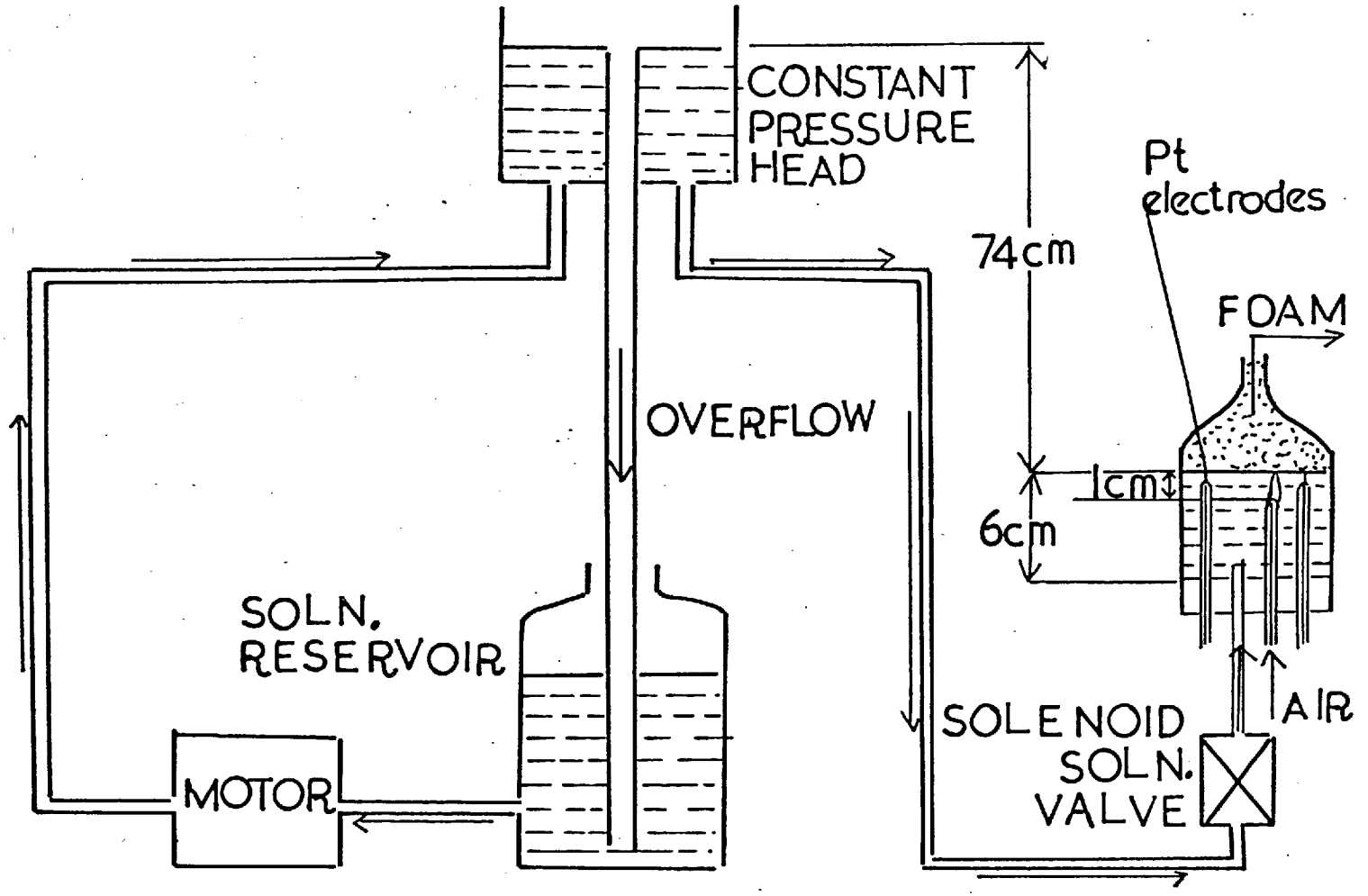

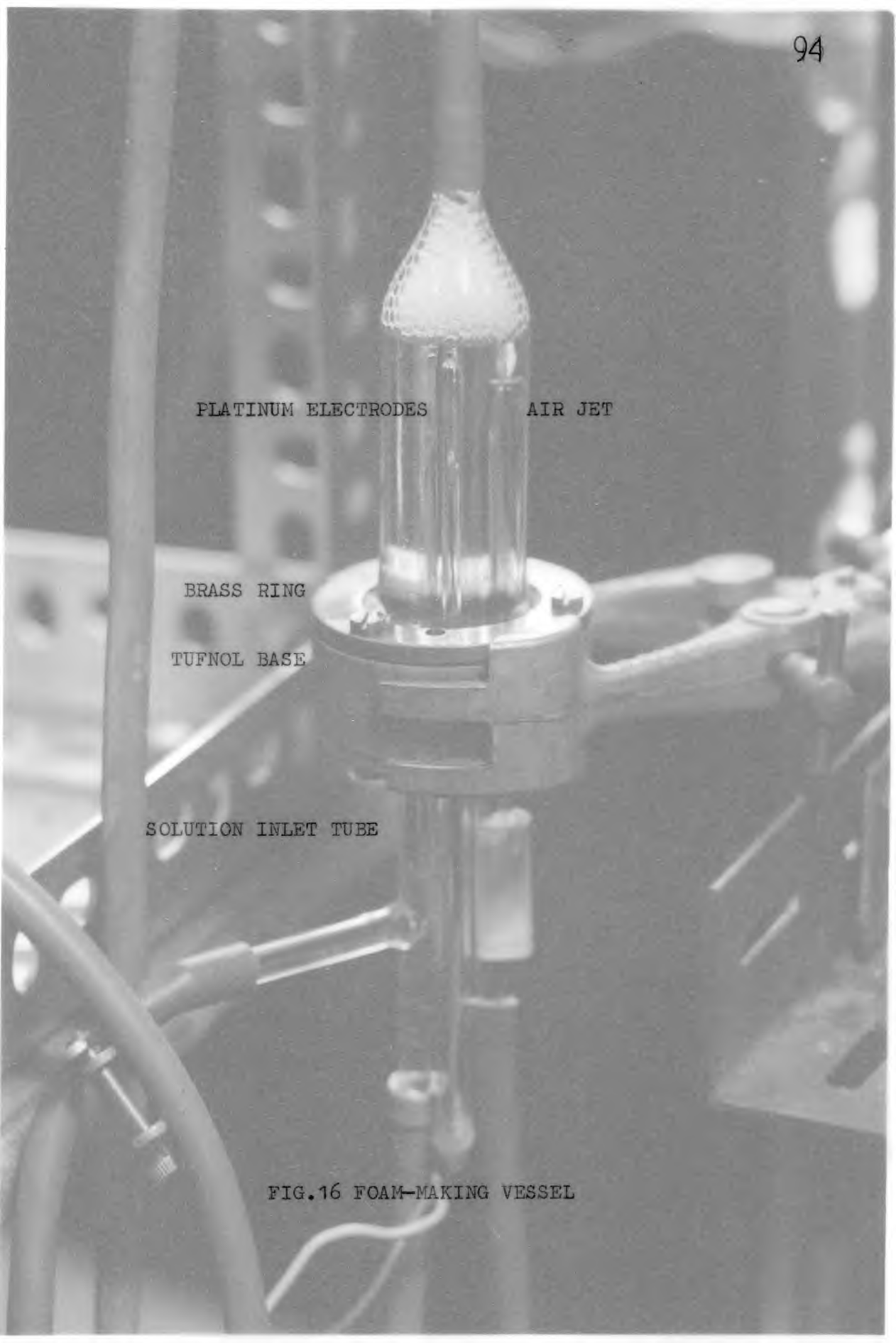

FIG.16 FOAM-MAKING VESSEL

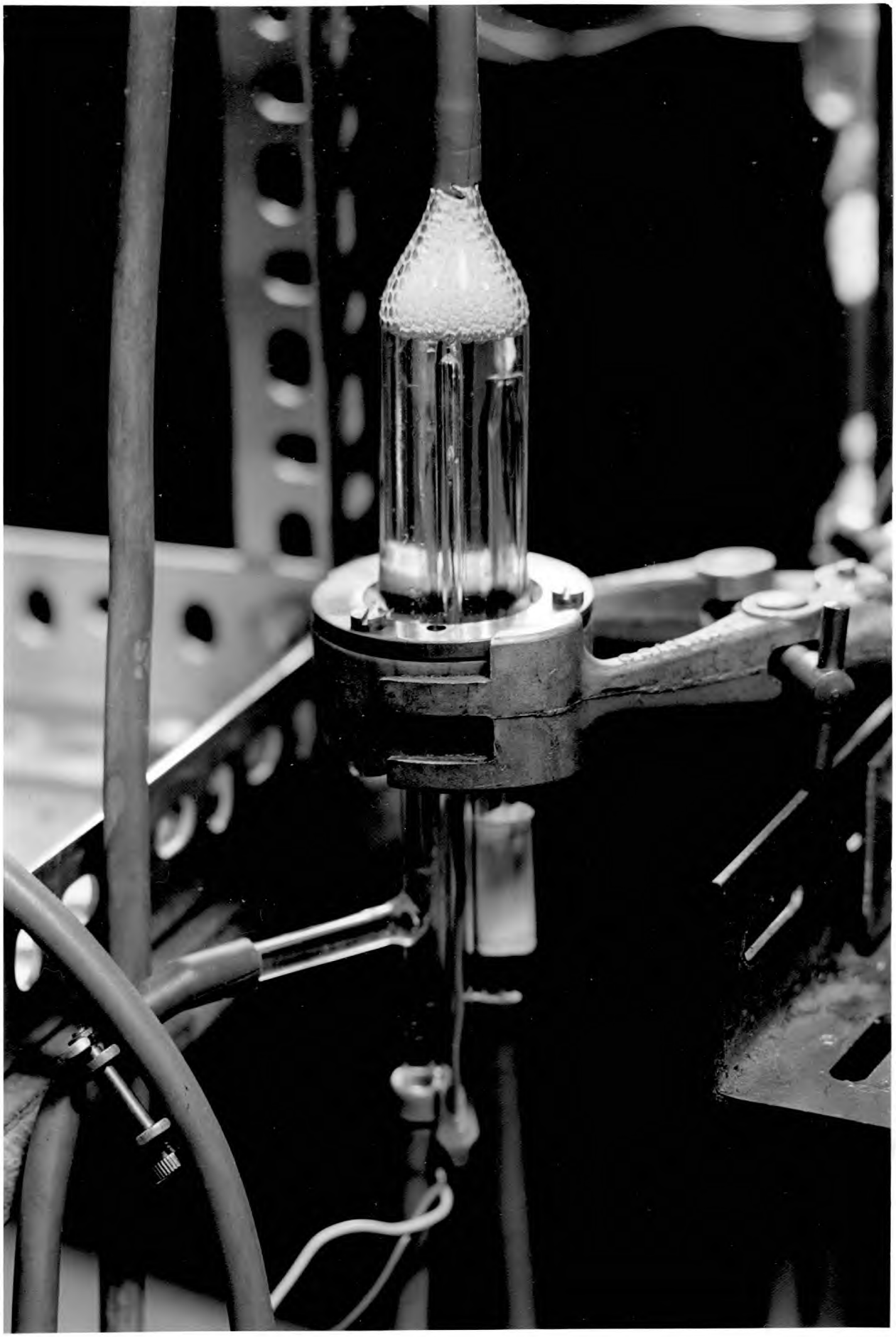

Fig. 17a Components: tufnol base, O-ring, brass ring and base plate.

Fig.17b Holder for foam-making vessel. This glass vessel surrounded by an O-ring, is held between a brass ring and tufnol base by screws.

The foam produced (approx. bubble size 1 mm) then passed down the acoustic measurement tube and was discarded at the outlet, since the foam stabilising agents may have evaporated. The dimensions of the foam-making and acoustic measurement tubes are shown in fig. 18.

4.4.1 Modified jet tube

The jet orifice was a hole in a ruby watch jewel, which was melted into the end of a pyrex tube to form an airtight seal. These holes were perfectly regular, and various sizes were used ranging from 0.07 to 0.12 mm.

4.4.2 Solution-level control circuit

Automatic control of the level of the solution to $\pm$ 1.5 mm in the foam-generator was provided by the electrical circuit shown in fig. 19. The principle of operation depended on the fact that the solution had a much higher electrical conductivity than the foam.

Operation cycle

As the solution was used in forming the foam, the level fell to the lower control position. At this

Fig.17c Method of holding jet tube.

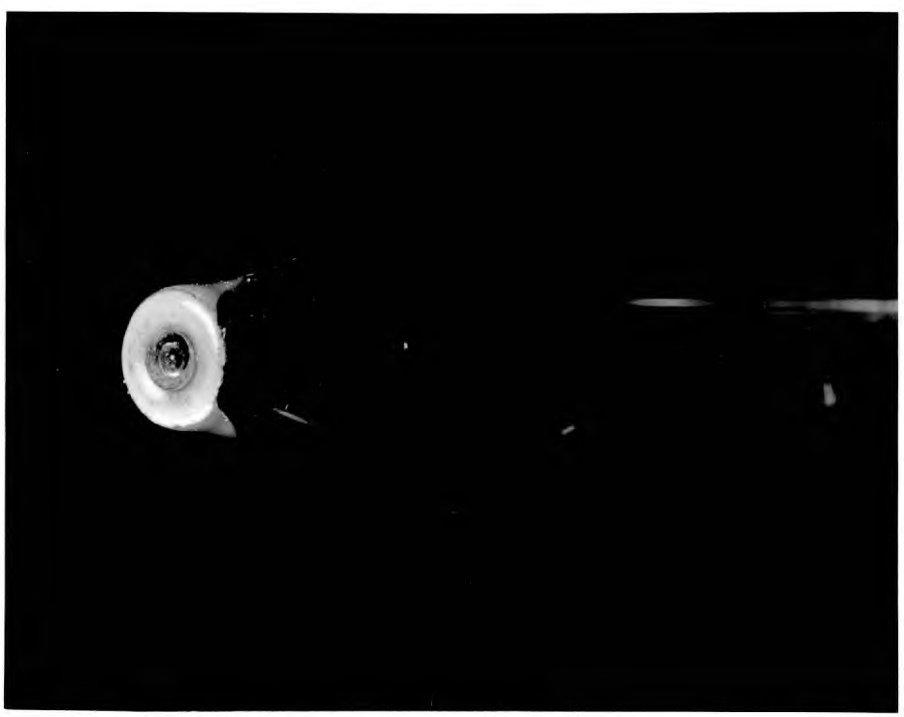

Fig.17d A jet orifice is a hole in a ruby watch jewel, which is melted into the ends of a pyrex tube to form an air-tight seal.

FIGURE 18

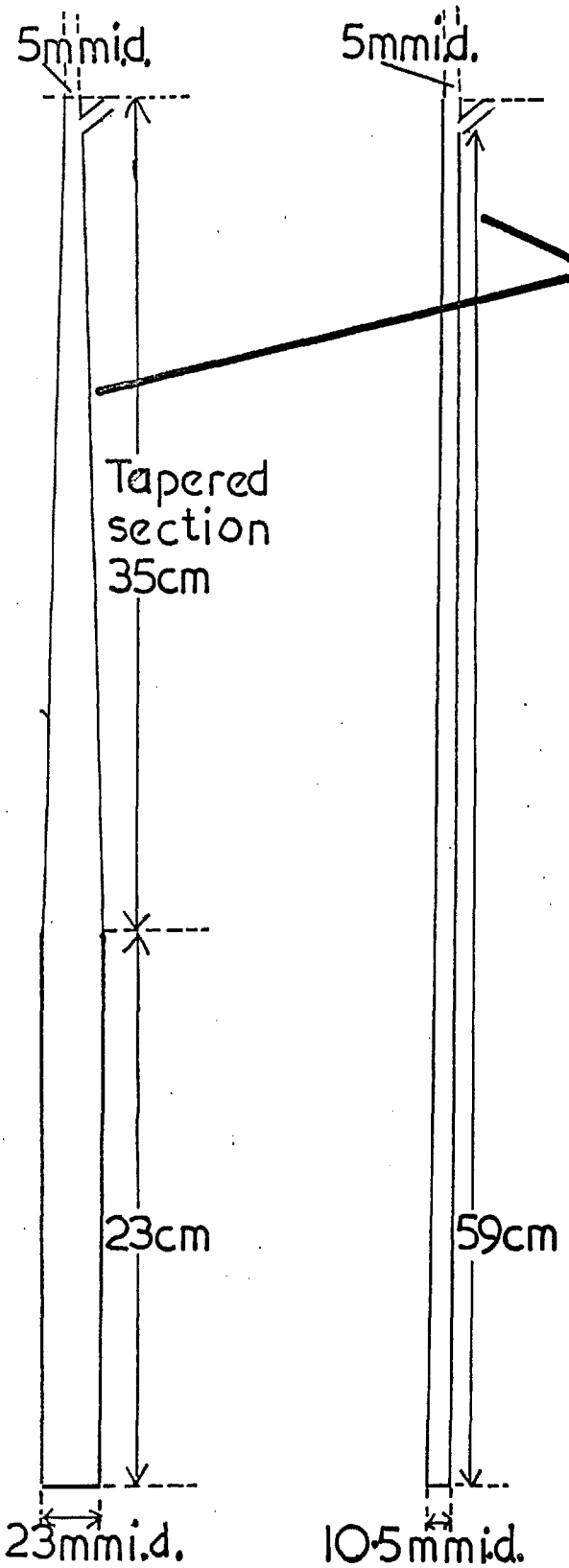

ACOUSTICAL MEASURING TUBES

Tol. i. diam. ± 0·5mm
Wall thickness 1·5mm

FOAM-MAKING TUBE

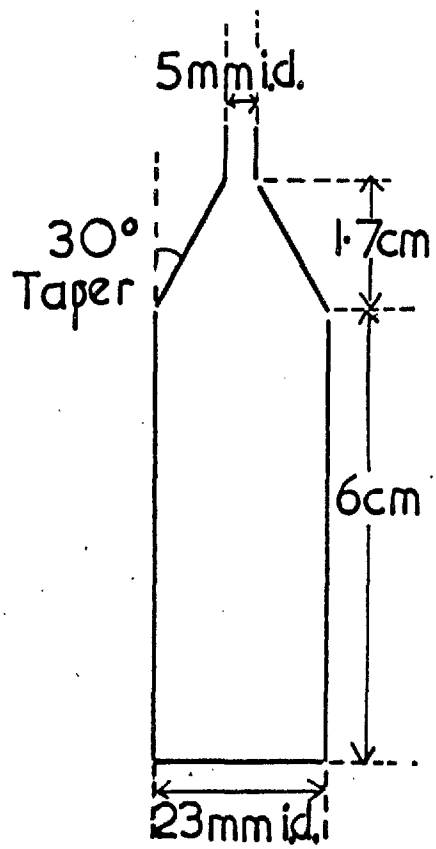

FIG.19 SOLN. LEVEL CONTROL

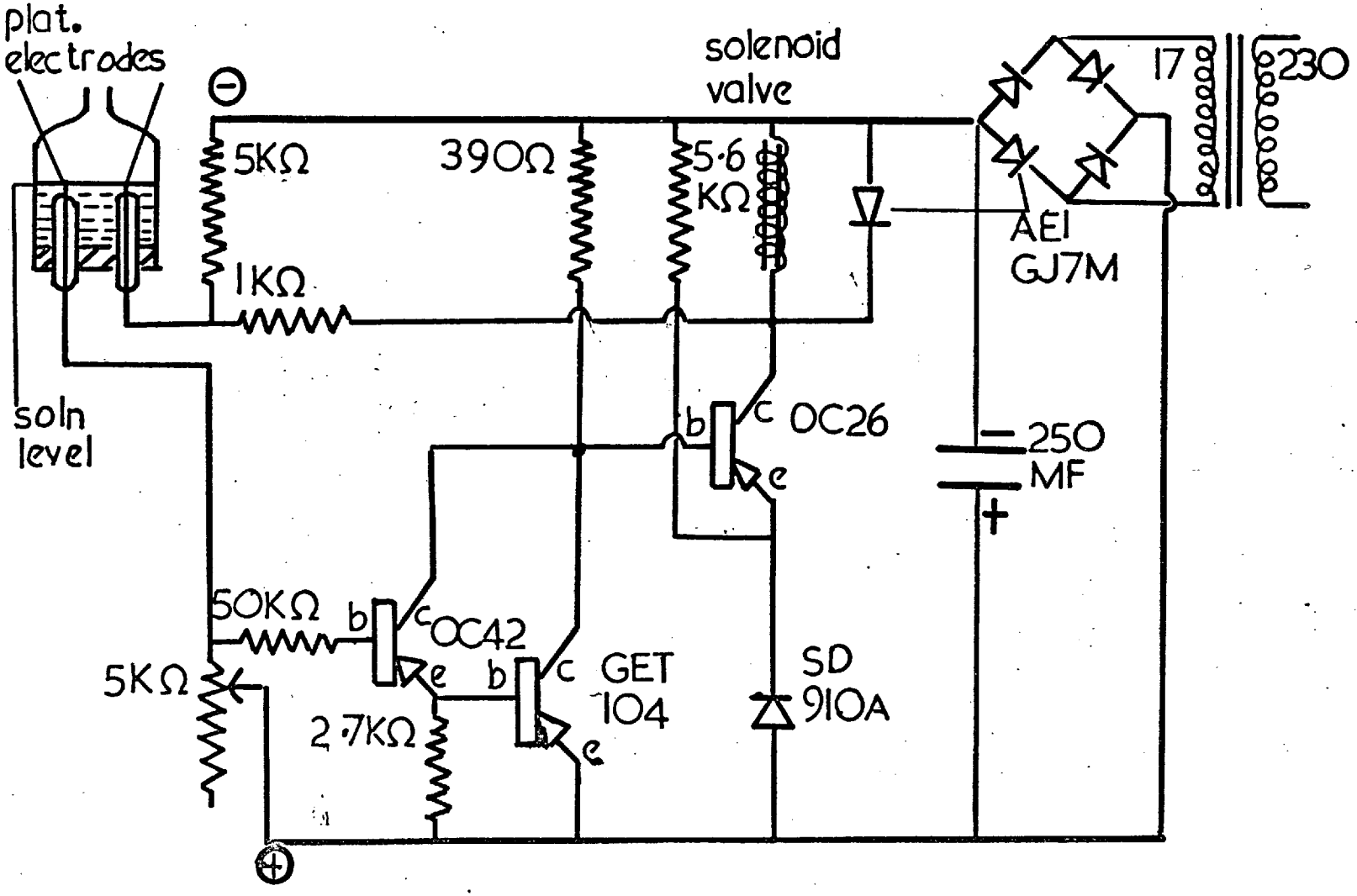

point, there was no bulk liquid connection between the platinum electrodes through the foam, and this led to the switching on of the OC26 transistor, and the consequent energising of the solenoid valve to open. The solution then rose to the higher control level. An electric current then passed between the platinum electrodes through the solution, which switched on transistors OC42 and GET 104, and switched off transistor OC26. Hence the solenoid valve was de-energised and closed. The period of the cycle was 5 mins., the valve remaining open for 10 secs.

Comments on the unconventional D.C. amplifier

(i) Transistors OC42 and GET 104 formed a Darlington connection in which the overall gain approximately equalled the product of the individual gains.

(ii) There was a 180° phase change between transitors GET 104 and OC26.

(iii) The SD 910 A diode was always forward biased. This was used to ensure that the OC26 transistor was switched off when a connection was made between the electrodes through the solution.

(iv) The diode GJ7M shunted the solenoid valve and prevented surge voltage, that otherwise would have appeared

across the inductance of the solenoid when the current was switched off.

(v) Position of 1KΩ resistor

The 1KΩ resistor was returned to the collector of the OC26 transistor. This was done to prevent any 'jitter' of the solenoid valve in the time when the connection was being made between the electrodes through the solution.

4.4.3. Air pressure control system

Automatic control of the pressure of the air entering the jet in the foam-generator is given by the system shown in fig. 20. The principle was that an RBF1 Edwards compressor pump was controlled by a micro-switch to provide a constant pressure air supply.

4.4.4 Compressor control circuit

The circuit was designed to operate on D.C. (see fig. 21) to avoid electrical interference with the acoustic instruments.

Operation cycle

(i) If the micro-switch was closed, a short circuit occurred between the 250Ω resistor and GJ7M diode.

FIG. 20 AIR PRESSURE CONTROL SYSTEM

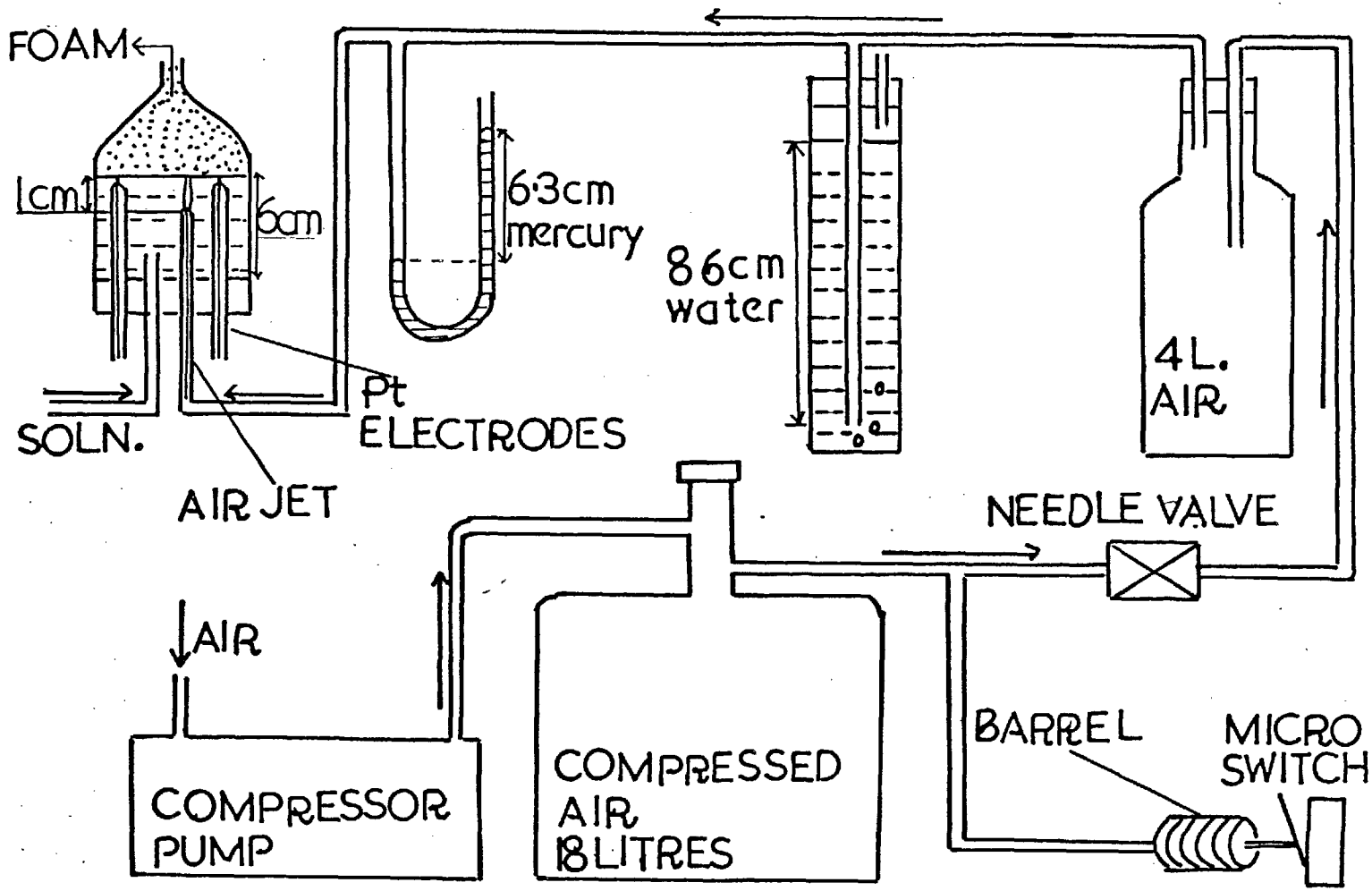

FIG. 21 COMPRESSOR CONTROL CIRCUIT

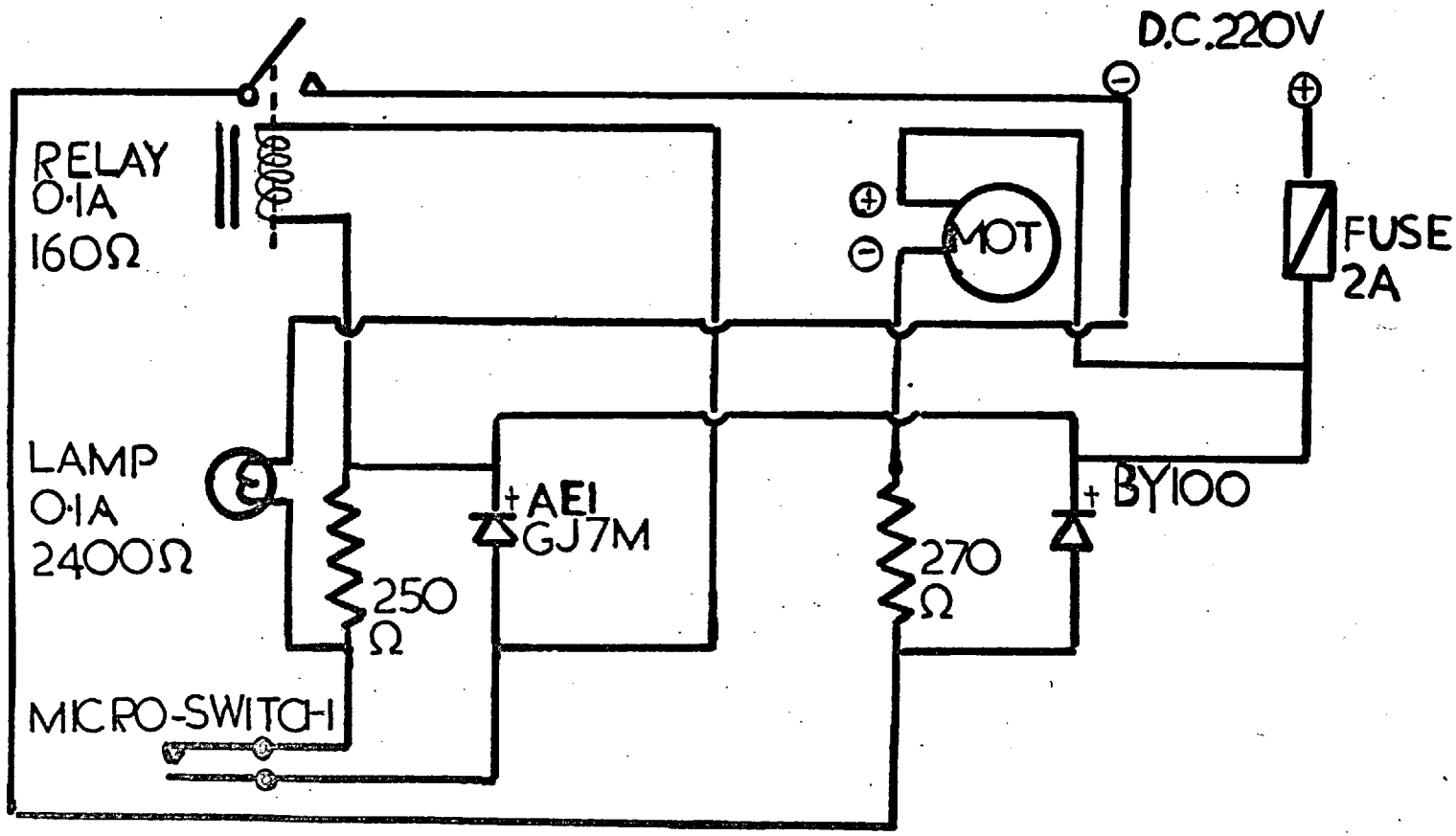

Therefore the relay coil was energised and the relay contacts closed, causing the electric motor to start.

(ii) If the micro-switch was opened, the relay coil was de-energised and the relay contact opened, causing the electric motor to stop.

The period of the complete cycle was 2 mins., the motor running for 15 secs.

Comments on the D.C. circuit

The function of the BY 100 diode (800 P.I.V.) was to prevent reverse polarity being applied to the motor. The 270Ω resistor was used to limit the motor current to approx. 1-amp. should the motor stall.

Section 4.5.0 The overall modified acoustic measurement system

The overall modified acoustic measurement system is shown in fig. 22a. The component systems ~~wa~~re considered separately.

4.5.1 Acoustic measurement tube

This tube, designed by Connor, was approx. 60 cms. long, and had a uniform taper along its upper 35 cm. (see figs. 18, 27). By making use of multiple reflections and absorption in the foam at the upper

P.I.V. = Peak Inverse Voltage

FIG. 22a

ACOUSTIC MEASUREMENT SYSTEM

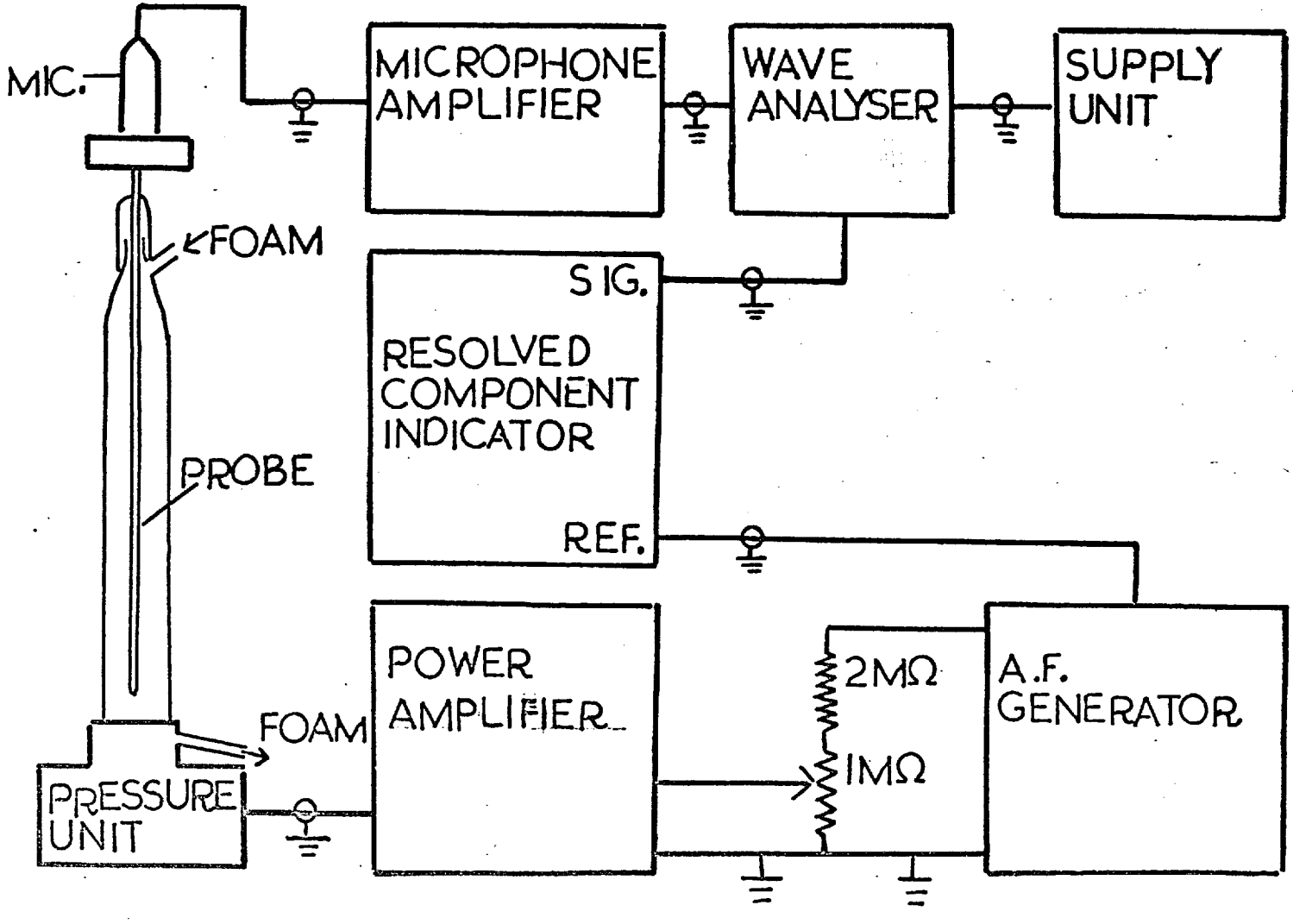

end, it was hoped to reduce the setting up of standing waves in the tube. Two such tubes of internal bores 2.3 cm. and 1.05 cm. were used.

4.5.2. Sound source

A Vitavox loudspeaker pressure unit was used as a sound source, and had a frequency response in the range 200 - 14,000 c/s. When used most efficiently with optimum loading by an exponential horn, it had a maximum power of 15 watts r.m.s.

In our application, the loudspeaker was fitted into the base of the tube holder and sealed from the foam column by a polythene diaphragm, of thickness 0.005 mm. (see fig. 23). In order to avoid excessive diaphragm displacement in its operating condition of foam loading, the power should not exceed 7.5 watts r.m.s.

The loudspeaker was fixed to a heavy base, which could be adjusted with three levelling screws (see fig. 14).

4.5.3 Probe tube

A stainless steel probe tube 90 cm. long, B.S. 11 gauge 2.95 mm. o.d.x. 2.13 mm. i.d. was used. One end

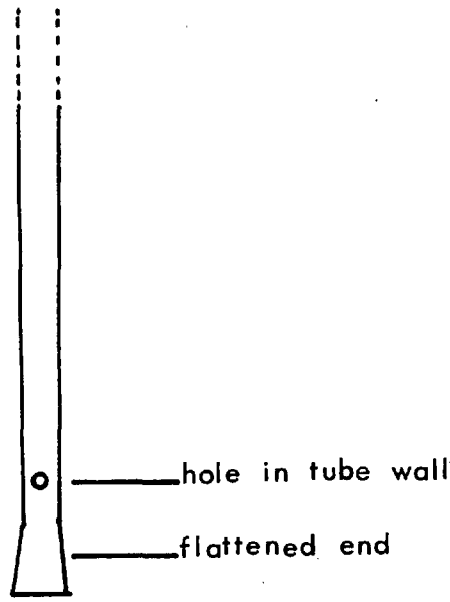

Fig. 22b Probe tube showing the flattened end, and the hole in the cylindrical wall.

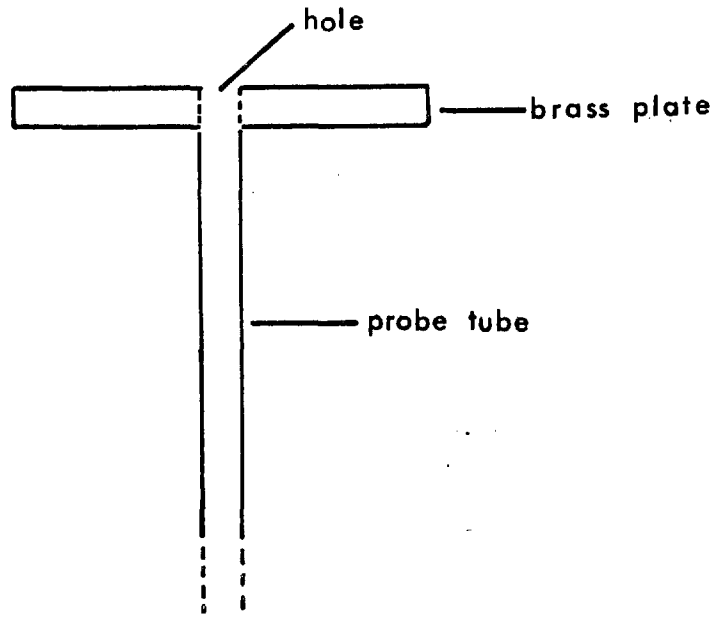

Fig. 22c Open end of probe tube brazed vertically into the hole at the centre of the brass plate.

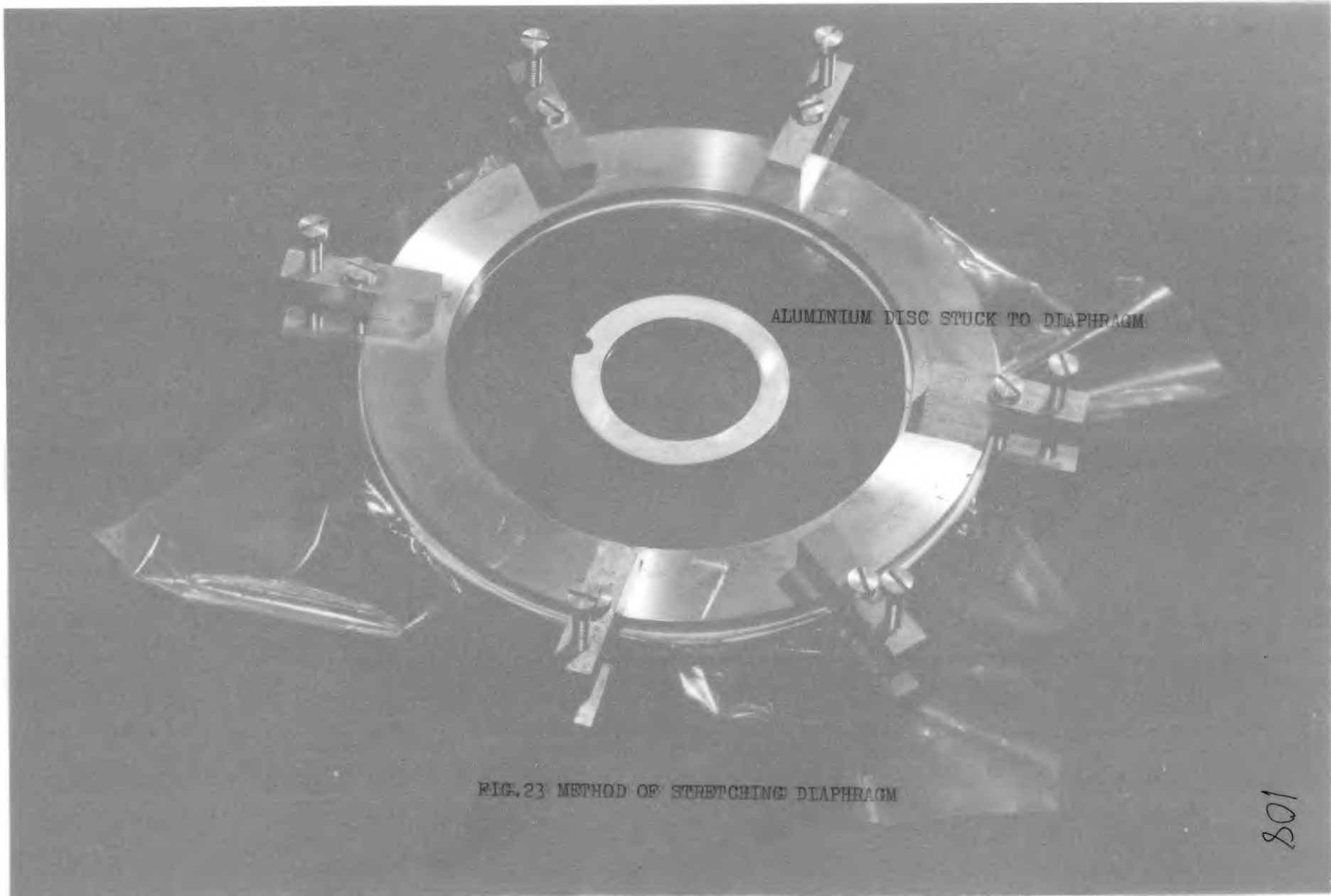

FIG.23 METHOD OF STRETCHING DIAPHRAGM

801

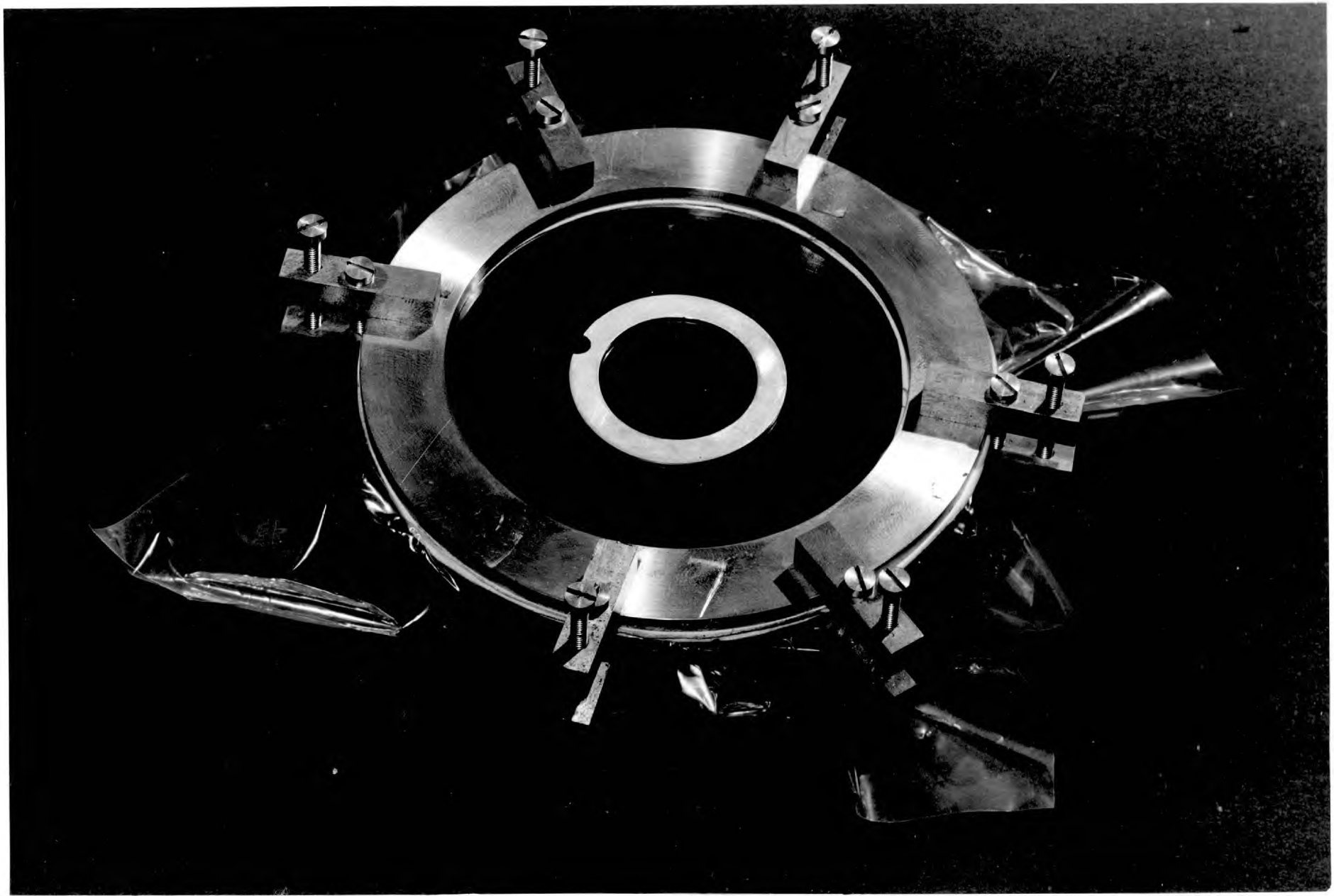

was flattened (see fig. 22b) and then a hole was drilled in the cylindrical wall near the end. This end was then closed by brazing. The hole was then covered with 0.005 mm. polythene sheet, using bostik, as adhesive, to form an "acoustic window".

The open end of the probe was then brazed vertically into the hole at the centre of the brass plate (see fig. 22c). This end of the probe terminated in a small chamber in a massive brass block, which was attached to a condenser microphone (figs. 24 and 26). The whole microphone assembly was supported from a vertical brass column, which allowed rack and pinion movement of the probe.

The closed end of the probe was inserted through the central hole of a rubber teat using a Hellerman tool. The teat was then fitted on the end of the acoustic measurement tube (fig. 27), to provide the necessary foam seal without mechanical coupling.

EXPERIMENTAL PROCEDURE

4.6.0 The modified mechanical instrumentation

A vertically traversing system is shown in side elevation (fig. 25) and vertical section (fig. 26). The system consisted of an outer vertical heavy brass

FIG.24 THE MODIFIED MECHANICAL INSTRUMENTATION

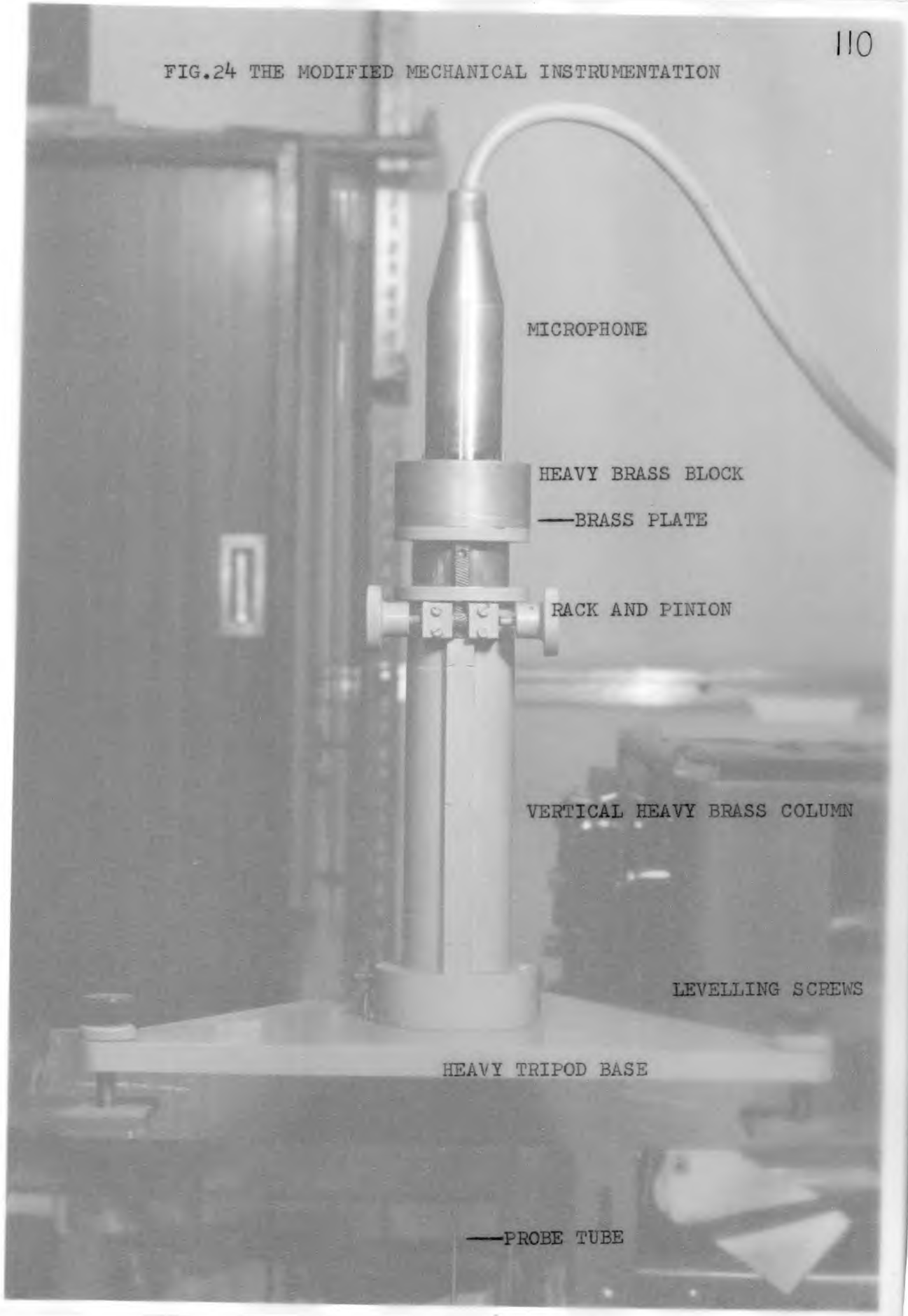

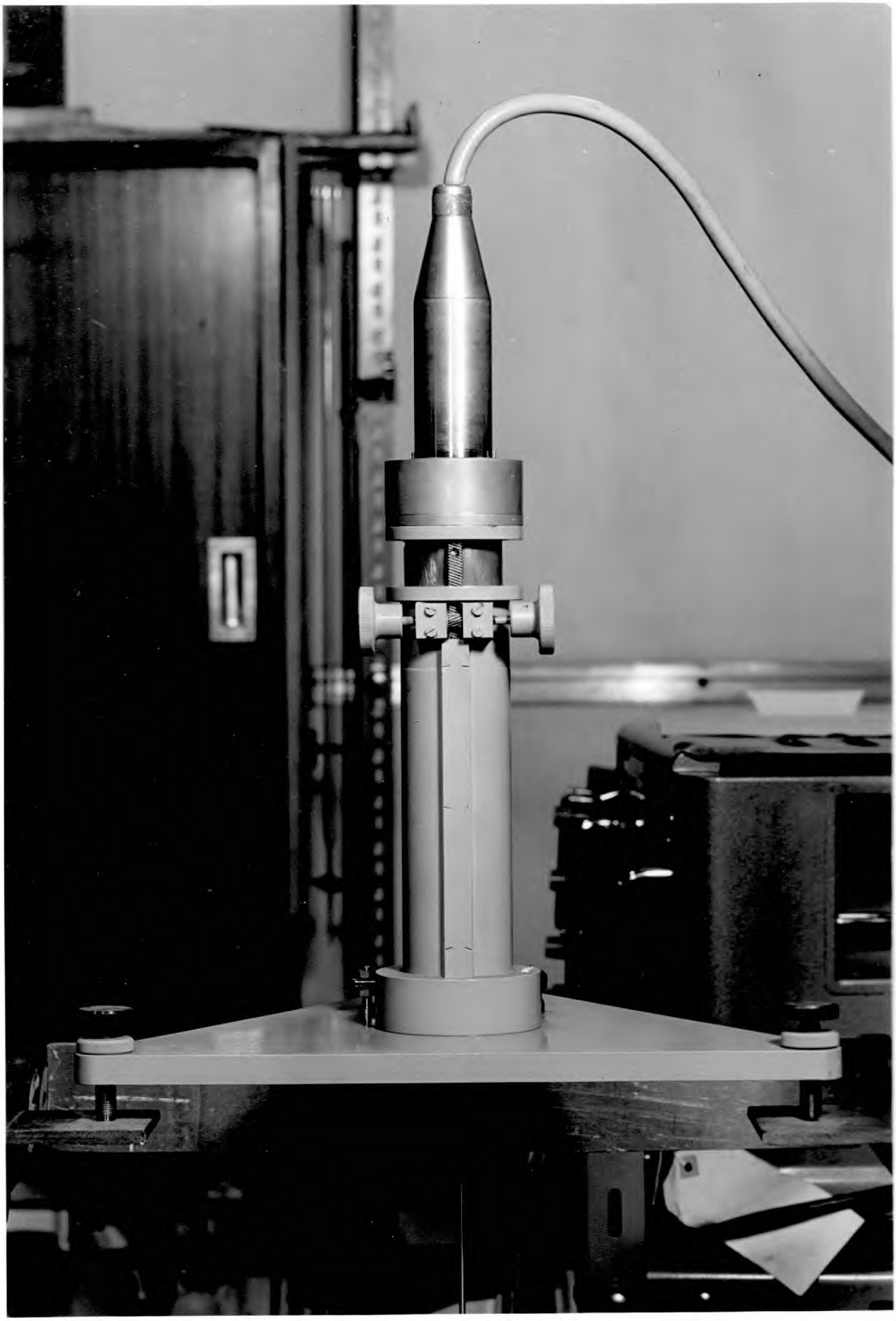

FIG.25 SIDE ELEVATION

Scale —— half full size

Axis of column passes through centre of base

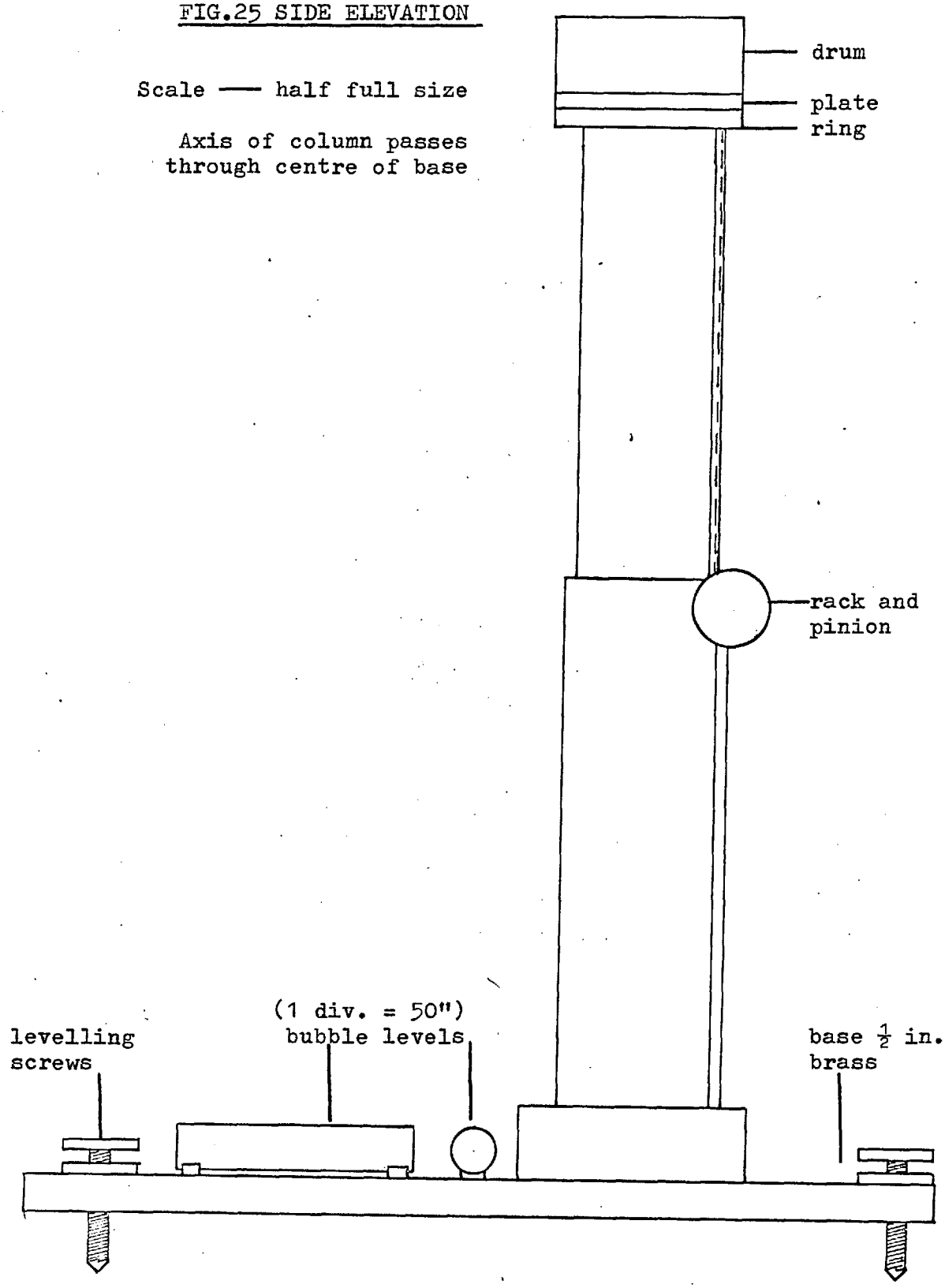

FIG.26 VERTICAL SECTION

Scale —— half full size

$1\frac{3}{4}$ in. o.d. brass tube

$\frac{1}{8}$ in. wall thickness

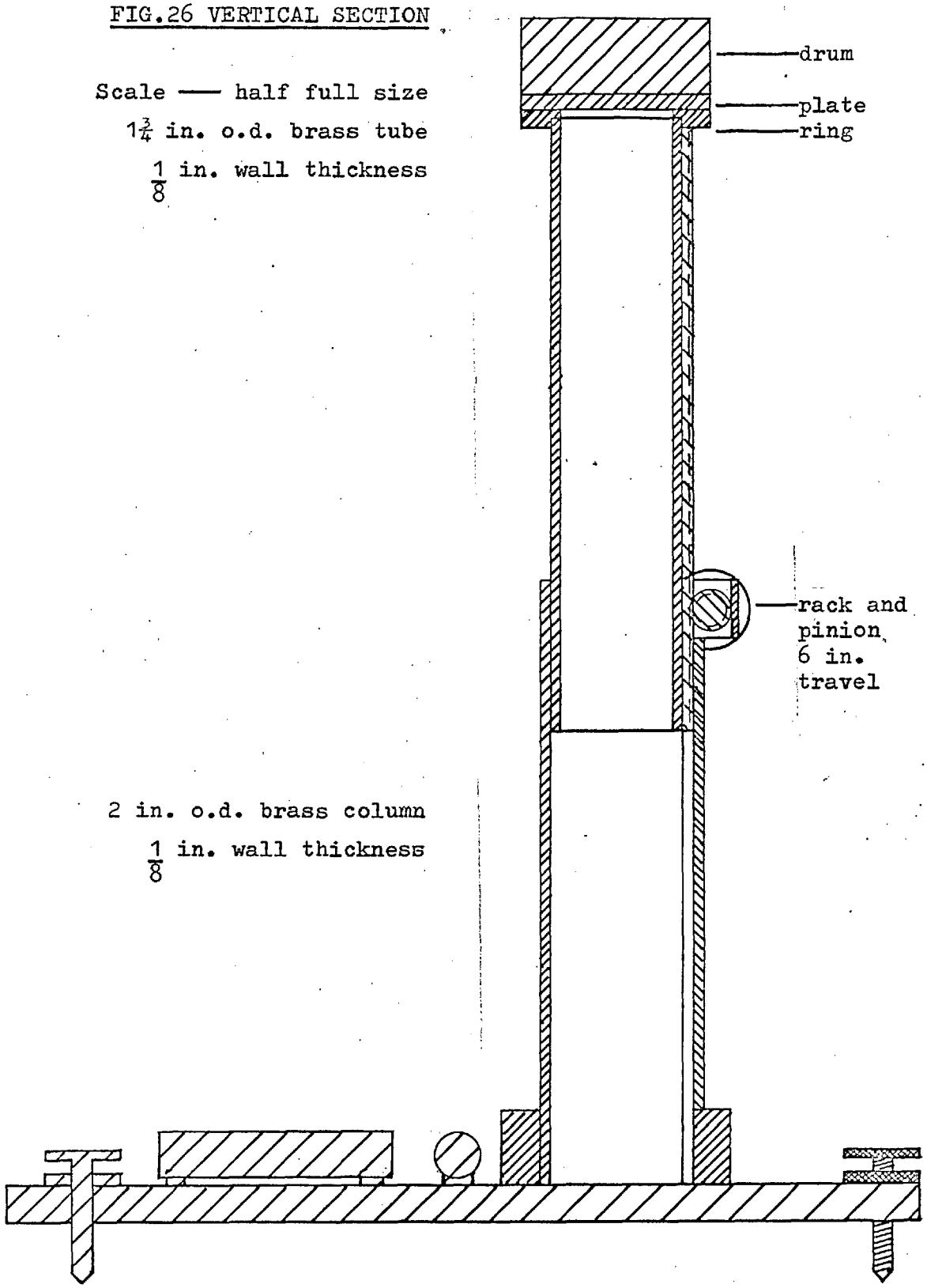

column mounted on a heavy tripod bas with three levelling screws and two sensitive divided-levels (1 DIV = 50").

The inner column travelled by a rack and pinon movement over a graduated scale, reading to 1 mm. The top of the inner column received the microphone assembly fittings (see fig. 24).

4.6.1 Axial positioning of the probe

By adjustment of six levelling screws, three on the heavy base, and three on the vertical column, the probe could be positioned axially in the acoustic measurement tube (see figs. 14, 24, 27).

4.6.2 The modified electrical instrumentation

The modified electrical instrumentation is shown by a block diagram in fig. 22. and details are given in the Appendix.

An output signal from the A.F. generator was reduced to 150 mV maximum by a 1M potentiometer. After amplification by a power amplifier, the signal was fed into the loudspeaker, situated at the base of the foam tube. The output impedance of the power amplifier was matched to that of the loudspeaker for maximum power transfer into the foam.

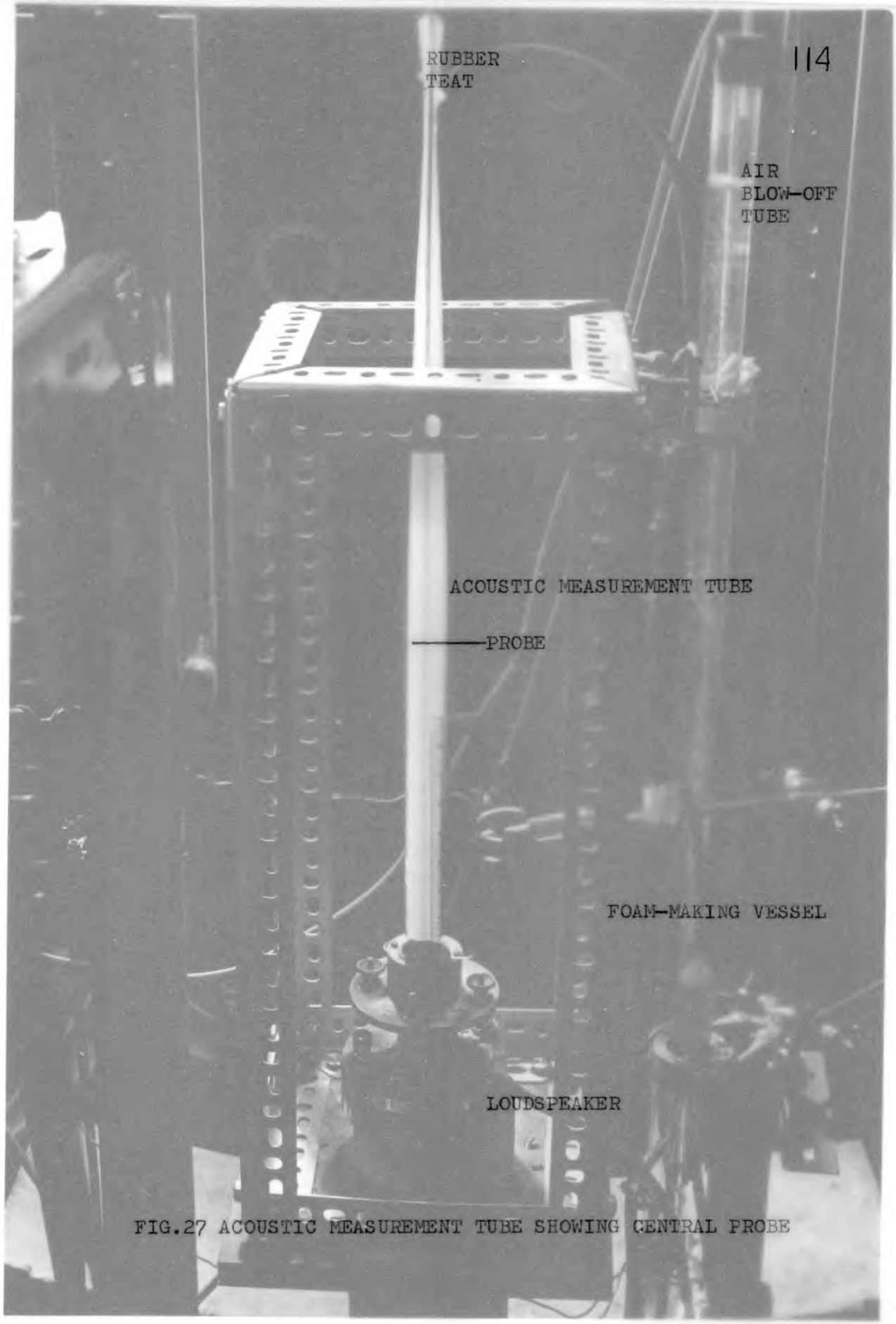

FIG.27 ACOUSTIC MEASUREMENT TUBE SHOWING CENTRAL PROBE

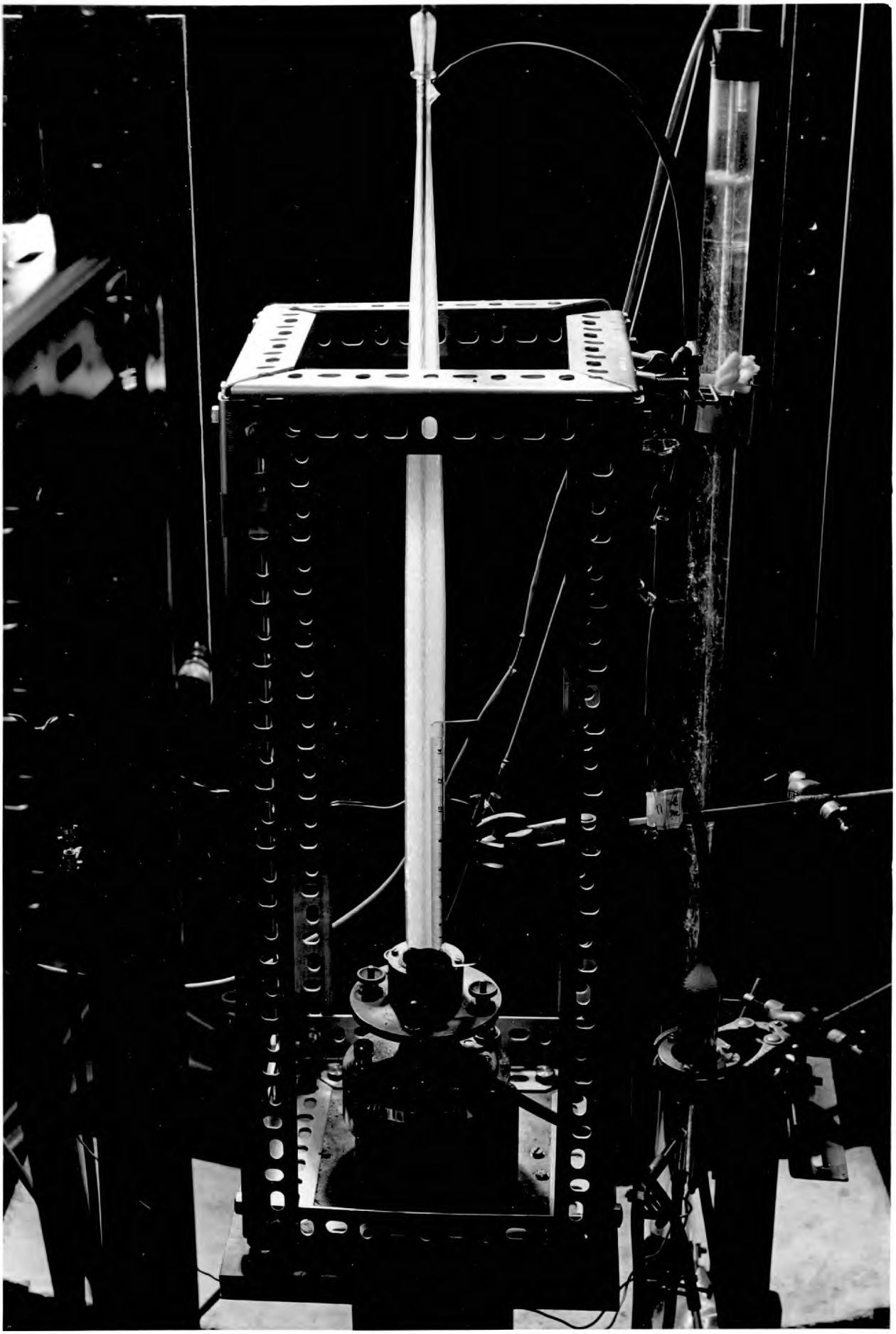

The acoustic pressure in the foam was detected by the probe microphone as it traversed the longitudinal axis of the tube. The microphone output was amplified and fed in turn to the wave-analyser, which acted as a tunable filter, and the signal channel of the Resolved Component Indicator (R.C.I.).

A signal from the A.F. generator was also applied direct to the reference channel of the R.C.I.

Let V_r and V_q be the 'reference' and 'quadratue' voltages recorded by the R.C.I. Then the phase β of the microphone output relative to the signal input was given by

$$\beta = \tan^{-1} (V_q/V_r) \quad \text{radians.} \qquad (4.1)$$

and the amplitude of V of the microphone output was given by

$$V = (V_q^2 + V_r^2)^{\frac{1}{2}} \quad \text{volts.} \qquad (4.2)$$

The relative phase β was plotted against probe microphone position. The gradient of this line, together with frequency f, (c/s) enabled the phase velocity v of the sound wave to be calculated: (see section 5.6)

$$v = f \times 2\pi/(\text{phase shift per cm}) \quad \text{cm sec}^{-1} \qquad (5.0.5)$$

Since the voltage output of the microphone was proportional to acoustic pressure, the gradient of the line $\log_{10}V$ against probe-microphone position x enabled the attenuation constant α of the sound wave to be calculated: (see section 5.2)

$$\alpha = \frac{\log_e (V_x/V_o)}{x} \quad \text{neper} \quad \text{cm}^{-1}$$

Measurement of foam parameters

The parameters of foam viscosity, and bubble size and distribution, were measured additional to that of foam density, which was the only parameter noted by previous experimenters.

The properties of the liquid in the bubble walls were also measured, viz., density, surface tension, and viscosity.

The room temperature and pressure were determined before and after each run.

4.7.0 Foam density

The volume of the acoustic measurement tube and 100 cm of connecting tubing was determined within 1% by filling with a known volume of water.

After each run, a constant pressure air stream swept out the same volume of foam from the acoustic measurement tube into a weighed flask. The flask containing the foam was re-weighed on an Otis electrical balance to 0.2 mgm.

4.7.1 Bubble size and distribution

Still photographs of foams

An Edixa-mat Reflex camera, with 40 mm f/2.8 lens in extension rings which gave a 1.1 ratio of reproduction, was used for taking photographs.

Foam in the acoustic measurement tube was illuminated with transmitted light from a Kodak Coldlight, and vertical and horizontal plastic scales were fixed to the tube. Exposure time was 1/30 sec. at aperture f/11 using FP3 35 mm film.

Focussing difficulties

(i) The axis of the tube was focussed in the centre of the field of view of the lens in order to minimise barrel distortion.

(ii) The lack of depth of field made focussing very difficult, as the front and back surfaces of a bubble could not be distinguished (wall thickness of the order of 1 micron).

Measurement of bubble size

The photographs were enlarged so that the final magnification was X10. In a section plane cut through a cylindrical tube packed with foam bubbles, the most frequent shapes occurring were hexagons. By comparison with a series of transparent circular masks of known radii, the radii r_1 of the inscribed circle and r_2 of the circumscribed circle of the hexagon were measured and the average radius $r = \frac{r_1+r_2}{2}$ calculated. (See fig. 38 in appendix A7). The mean value of r and the standard deviation of a set of results for 34 bubbles are shown in table 5.1 in chapter 5. The foam bubble radii distributions for increasing volume concentrations of glycerol in the foam-making solutions are shown graphically in fig. 40 and photographically in fig. 39, in appendix A7.

Cine-films of foams

A 16mm Bolex Reflex camera with 75mm f/1.9 lens in extension rings giving a $1\frac{1}{2}$: 1 ratio of reproduction was used for taking films.

Foam in the acoustic measurement tube was illuminated with two 500 watt photoflood lamps. Exposure time was 1/30 sec. at f/11 using Kodak Tri-X reversal film at 12 frames/sec.

The bubble size distribution along the acoustic measurement tube, at 10 cm intervals, was investigated.

4.7.2 Foam viscosity

A modified Techne viscometer[41] was used for viscosity measurements. The measurements were taken at Unilever Research Laboratory, Isleworth by courtesy of B.A. Scott and P. Hall.

The principle of this viscometer (fig. 28) was a weighed piston producing a constant air pressure which forced the foam under test through a capillary tube (2 mm internal bore) into the viscometer tube (1 cm internal bore). The tubes were calibrated with a standard mineral oil. Shell Vitrea Oil 21, of viscosity 44 centistokes and density 0.866 gm/cm^3 at 21.1°C was used for this purpose.

The end of a connecting tube from the foam-generator (fig. 16) was placed in the bottom of a weighed cup and the foam gently flowed into the cup while slowly withdrawing the tube. Care was taken to avoid the formation of air pockets. The foam slightly overfilled the cup and the excess was wiped off level with the cup mouth. The viscometer head was attached to the cup, and then connected to the pressure unit. The time from

MODIFIED TECHNE VISCOMETER

Fig. 28.

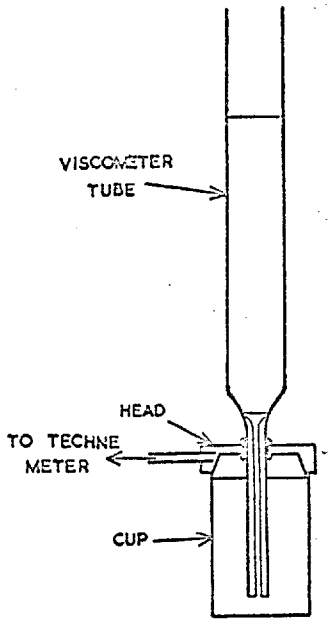

the instant at which the piston was dropped till the foam reached the upper mark was noted. The time was multiplied by the appropriate tube factor to give the foam viscosity in centistokes.

The viscometer head was then removed and the excess foam in the cup was weighed to give the density. The air temperature and foam temperature were recorded.

Three readings in all were taken. The mean and the spread were calculated. This method for viscosity was comparative and did not give absolute results.

4.7.3 Liquid density

The density of the liquids used were measured by means of a specific gravity bottle. The temperature was recorded.

4.7.4 Liquid surface tension

Jaeger's method was used for a comparative determination of the surface tension of the liquids and of pure water. The temperature was recorded.

4.7.5 Liquid viscosity

Ostwald Capillary Viscometers B.S. 188 types A and B were used for a comparative determination of the viscosities of the liquids and pure water. The temperature was also noted.

CHAPTER 5

EXPERIMENTAL RESULTS AND DISCUSSION

Section 5.1 Introduction

The acoustical properties of liquid foams of the closed-cell type have been studied experimentally, (i) to check the applicability of theoretical formulas for the sound velocity in a foam and (ii) to investigate the change of attenuation with frequency and with variation of the physical parameters of the foam.

Foam-making solutions

The standard foam-making solution was a 5 per cent solution by volume of the commercial detergent Stergene in distilled water. The life-time of these foams could be considerably extended by adding a second, non-foaming solute such as glycerol to increase the viscosity of the solution (see table 5.1), and so slow down the drainage of the liquid from the bubble walls.

Section 5.2 Computation of attenuation results

The acoustic pressure in an attenuated progressive plane wave can be described by an equation of the form

$$p_x = p_o \exp(-\alpha x) \exp j2\pi f \left(t - \frac{x}{v}\right) \qquad (5.0.1)$$

where x is the direction of wave propagation, α is the

MEASUREMENT OF FOAM PARAMETERS

[redacted]

Constant parameters

Air jet hole diameter = 0.07 mm; measurement tube radius = 1.15 cm; temperature = 23 ± 1°C; eqm. pressure of air, $P_o = 1.01 \times 10^6$ dyn. cm^{-2}; ratio of principal specific heats for air, $\gamma = 1.4$ approx; density of air $\rho_G = 1.2 \times 10^{-3}$ gm. cm^{-3}.

Vol. conc. of glycerol in soln.	Liquid density	Liquid surface tension	Liquid viscosity	Foam density	Bubble radius	Bubble wall half thickness	$\left[\frac{\text{Radius}}{\text{Wall half-thick}}\right]^2$
	ρ_L	T	η_L	ρ_F	a	$\delta = \frac{a(\rho_F - \rho_G)}{3\rho_L}$	$\frac{a^2}{\delta^2}$
per cent	gm cm^{-3}	dyn. cm^{-1}	X10^{-2} poise	X10^{-2} gm cm^{-3}	X10^{-2} cm	X10^{-4} cm	X10^4
0	0.991	27 ± 1	1.04 ± 0.02	1.01 ± 0.04	5.6 ± 0.5	1.9 ± 0.2	8.6 ± 0.7
25	1.059	29 ± 1	2.46 ± 0.04	1.08 ± 0.04	6.5 ± 0.9	2.2 ± 0.3	8.7 ± 0.7
41	1.105	30 ± 1	5.74 ± 0.12	1.25 ± 0.06	6.5 ± 0.8	2.3 ± 0.3	7.1 ± 0.6
50	1.130	30 ± 1	8.21 ± 0.16	1.57 ± 0.06	6.5 ± 0.8	3.1 ± 0.4	4.7 ± 0.4
54	1.141	31 ± 2	10.40 ± 0.20	1.98 ± 0.08	6.9 ± 0.6	4.0 ± 0.5	3.0 ± 0.2

attenuation constant, f is the frequency, and v is the phase velocity. The amplitude V_x of the microphone voltage output is proportional to the acoustic pressure p_x, and it is computed from equation (4.2) in chapter 4:

$$V_x = (V_r^2 + V_q^2)^{\frac{1}{2}} \quad \text{volts} \qquad (4.2)$$

where V_r and V_q are the "reference" and "quadrature" voltages recorded by the Resolved Component Indicator.

From equations (5.0.1) and (4.2) the attenuation constant α is given by

$$\alpha = \frac{\log_e (V_x/V_o)}{x} \quad \text{neper cm}^{-1} \qquad (5.0.2)$$

In fig. 29 the logarithm of the amplitude V_x is plotted against the probe microphone position x in cms., and the straight line that fits the set of points best is computed according to the "method of least squares" (see Appendix). The gradient of this line enables the attenuation constant α to be calculated.

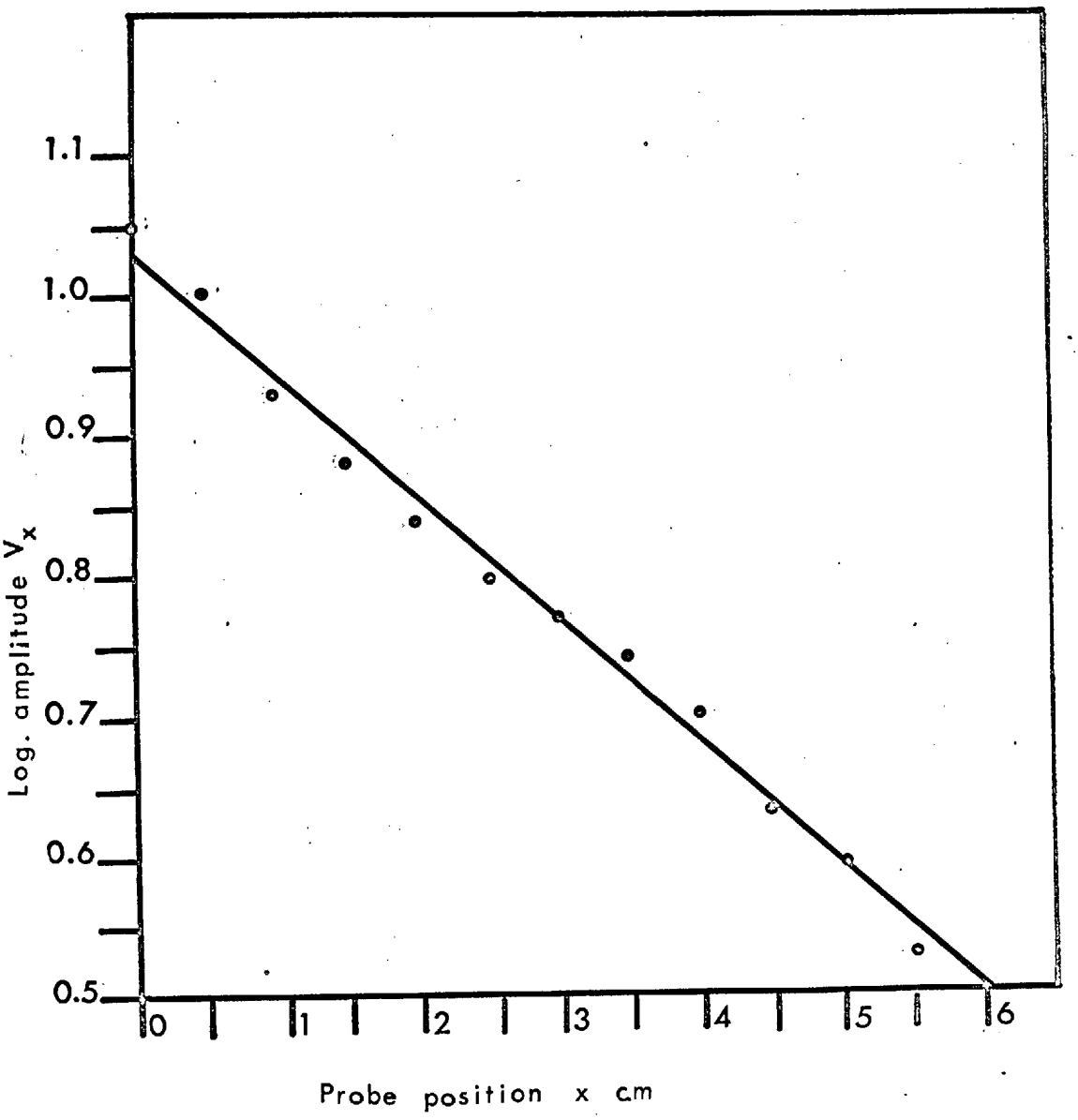

Fig. 29 Log. amplitude V_x versus probe microphone position x, for foam made from an aqueous solution of 5% stergene + 54% glycerol. (f = 1000 c/s)

Section 5.3 Attenuation in air-liquid foams of constant bubble size

The attenuation constants of air-liquid foams of constant bubble size, whose parent liquids have viscosities in the range 1-10 centipoise, at room temperature, were measured as a function of frequency and compared with computed valves according to equation (2.1.23) in chapter 2 for the viscous attenuation

$$\frac{\alpha}{f^2} = \frac{4\Pi^2}{\gamma^2 P_o^2} \cdot \eta_L \cdot \frac{a}{\delta} \cdot \rho_F c_F \qquad (2.1.23)$$

It is noted that α/f^2 is constant for a given foam.

In equation (2.1.23), γ is the ratio of the principal specific heats for air; P_o is the equilibrium pressure of the air; η_L is the measured coefficient of shear viscosity of the liquid; a is the measured bubble radius and δ is the calculated thickness of its surrounding liquid shell; ρ_F is the measured foam density and c_F is the calculated adiabatic velocity in the foam.

The following substitutions are made in equation (2.1.23). From equation (A3.7) in the Appendix, assuming spherical bubbles,

$$\frac{a}{\delta} = \frac{3\rho_L}{\rho_F - \rho_G} \qquad (A3.7)$$

where ρ_L, ρ_F, ρ_G are the measured densities of the liquid, foam and gas (air)respectively. From equation (2.4.9) in chapter 2, c_F, the adiabatic velocity in the given foam is related to the measured foam density ρ_F by

$$c_F = \left(\frac{\gamma P_o}{\rho_F}\right)^{\frac{1}{2}} \qquad (2.4.9)$$

Hence, substitution of equation (A3.7), (2.4.9) into equation (2.1.23) gives:

$$\frac{\alpha}{f^2} = \frac{12\Pi^2}{\left(\gamma P_o\right)^{\frac{3}{2}}} \eta_L \frac{\rho_L}{\left(\rho_F\right)^{\frac{1}{2}}\left(1-\rho_G/\rho_F\right)} \qquad (5.0.3)$$

Meaningfull attenuation results for four foams of different density could only be obtained in the restricted frequency range 800-1100 c/s; and for the highest density foam in the range 600-1600 c/s. This restriction is briefly discussed in section 5.4.

In table 5.2, it is shown that there is an order of magnitude agreement between the measured mean values of α/f^2 in the given frequency range and the theoretical values computed from equation (5.0.3) in air-liquid foams

TABLE 5.2

ATTENUATION OF SOUND IN AIR-LIQUID FOAMS

Constant parameters (see table 5.1)

Parent liquid viscosity η_L	Parent liquid density ρ_L	Foam density ρ_F	Measured attenuation (mean value) α/f^2	Theoretical attenuation α/f^2	Measured attenuation / Theoretical attenuation	Frequency range
$X10^{-2}$ poise	gm cm^{-3}	$X10^{-2}$ gm cm^{-3}	$X10^{-8}$ neper cm^{-1}	$X10^{-8}$ neper cm^{-1}		c sec^{-1}
1.04 ± 0.02	0.991	1.01 ± 0.04	4	0.8	5	800–1100
2.46 ± 0.04	1.059	1.08 ± 0.04	9	2.0	5	800–1100
5.74 ± 0.12	1.105	1.25 ± 0.06	16	4.4	4	800–1100
8.21 ± 0.16	1.130	1.57 ± 0.06	20	5.6	4	800–1100
10.40 ± 0.20	1.141	1.98 ± 0.08	22	6.3	3	600–1600

of constant bubble size, for increasing volume concentrations of glycerol in the parent liquids. The agreement ranges from a factor ($\alpha_{measd.}/\alpha_{theory}$) of 3 for an air-liquid foam whose parent liquid has a viscosity of 10 centipoise, to a factor of 5 for an air-water foam (where the viscosity of water equals 1 centipoise at room temperature).

This order of magnitude agreement is shown graphically in fig. 30, where log ($\alpha_{measd.}/\alpha_{theory}$) for each foam is plotted against the function $\left[\eta_L \frac{\rho_L}{\sqrt{\rho_F}(1-\rho_G/\rho_F)}\right]$

Further, in fig. 31 the measured values of α/f^2 are plotted against the frequency f, and the mean values over the frequency range considered are plotted as full-lines, for each foam. The departure of these values of α/f^2 from the horizontal straight lines is a measure of the deviation of the experimental results from the above theory (see equation 5.0.3).

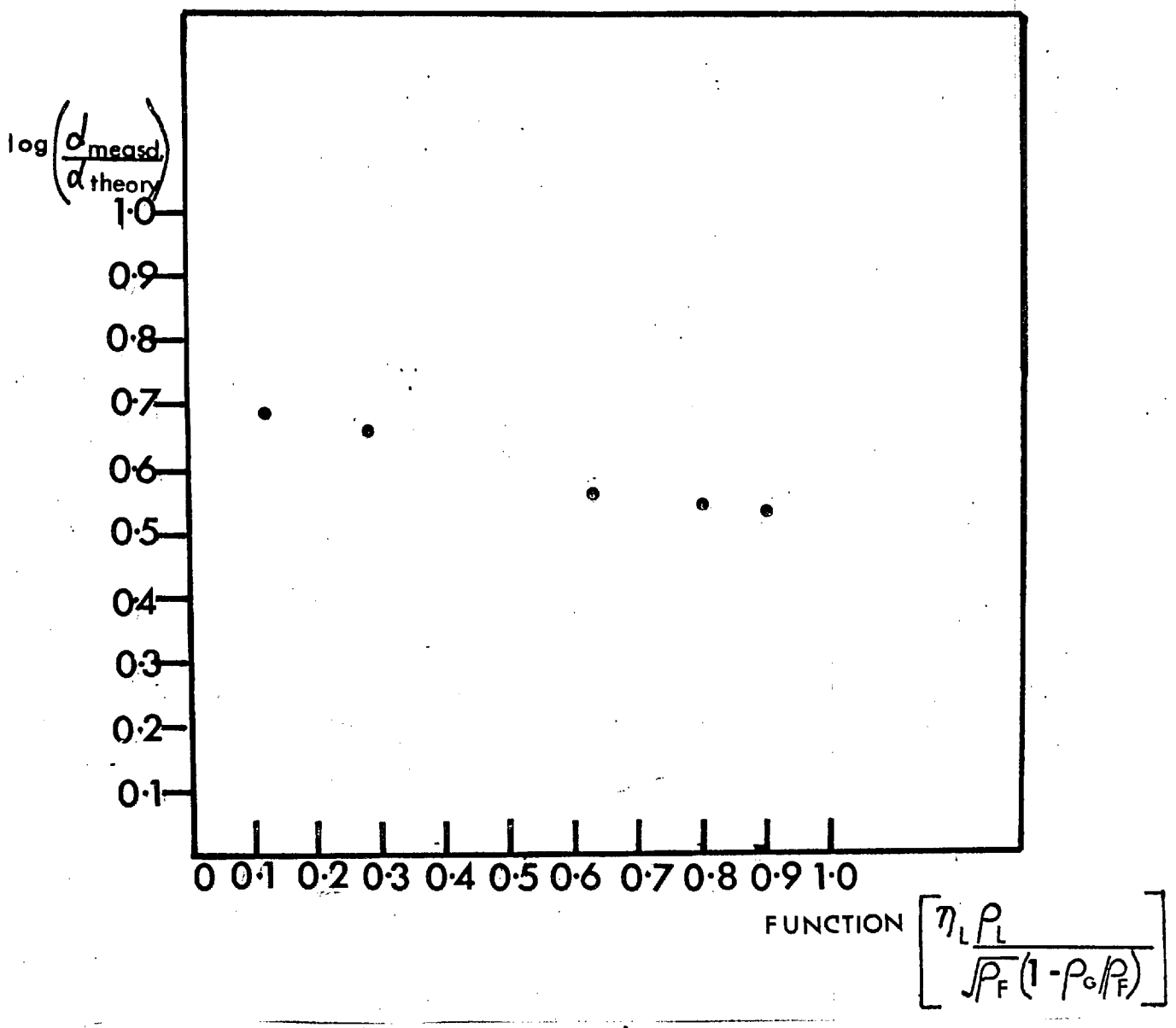

Fig. 30 The ratio $(\alpha_{measd.}/\alpha_{theory})$ for the attenuation in air – liquid foams of constant bubble size, for increasing volume concentrations of glycerol in the foam – making liquids.
Key: α = attenuation, η = viscosity, ρ = density,
L = Liquid, F = Foam, G = Gas.

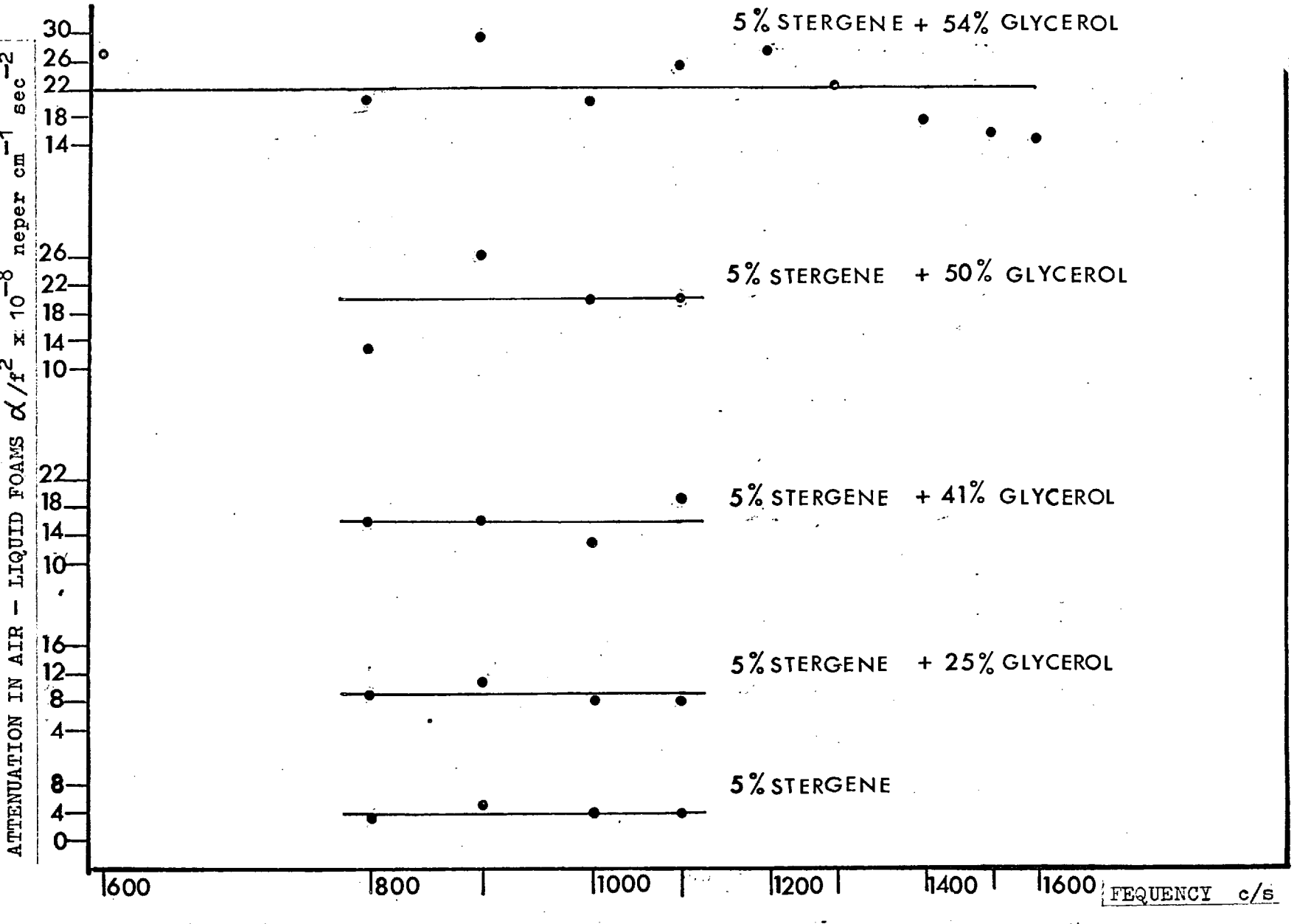

Fig.31 Measured values for α/f^2 versus f in air – liquid foams of constant bubble size, for increasing volume concentrations of glycerol in the foam – making liquids. The mean values are shown by full lines.

Section 5.4 Discussion of the limited frequency range

The lower frequency limit of repeatable observations was found to be about 800 c/s, and it suggested that at lower frequencies owing to the smaller attenuation there was appreciable interference from reflections at discontinuities in the cross-section of the tube.

Using a constant voltage drive at the loudspeaker, the signal to noise ratio was sufficiently large in the high density foam, made from an aqueous solution containing 54 per cent glycerol, for acoustic measurements to be made at frequencies up to 1600 c/s, but it was too small in the other foams to allow meaningfull measurements to be made above 1100 c/s.

Section 5.5 Computation of phase velocity

The phase constant is derived from equation (5.0.1):

$$\beta = \frac{2\Pi f x}{v} \quad \text{radians} \qquad (5.0.4)$$

where f is the frequency, v is the phase velocity and x is the direction of wave propagation. From equation (4.1) in chapter 4 the phase of the microphone output relative to the signal input is given by

$$\beta = \tan^{-1} \frac{V_q}{V_r} \quad \text{radians} \qquad (4.1)$$

where V_q and V_r are the "reference" and "quadrature" voltages recorded by the Resolved Component Indicator. In fig. 32 the relative phase β in radians is plotted against the probe microphone position x in cm., and the gradient of this line, computed according to the "method of least squares", represents the phase shift per cm in radians cm^{-1}. Thus from equation (4.1) and (5.0.4) the phase velocity of a plane sound wave in a foam is given by

$$v = \frac{2\Pi f}{(\beta/x)} \quad \text{cm sec}^{-1} \qquad (5.0.5)$$

where f is the frequency in c/s.

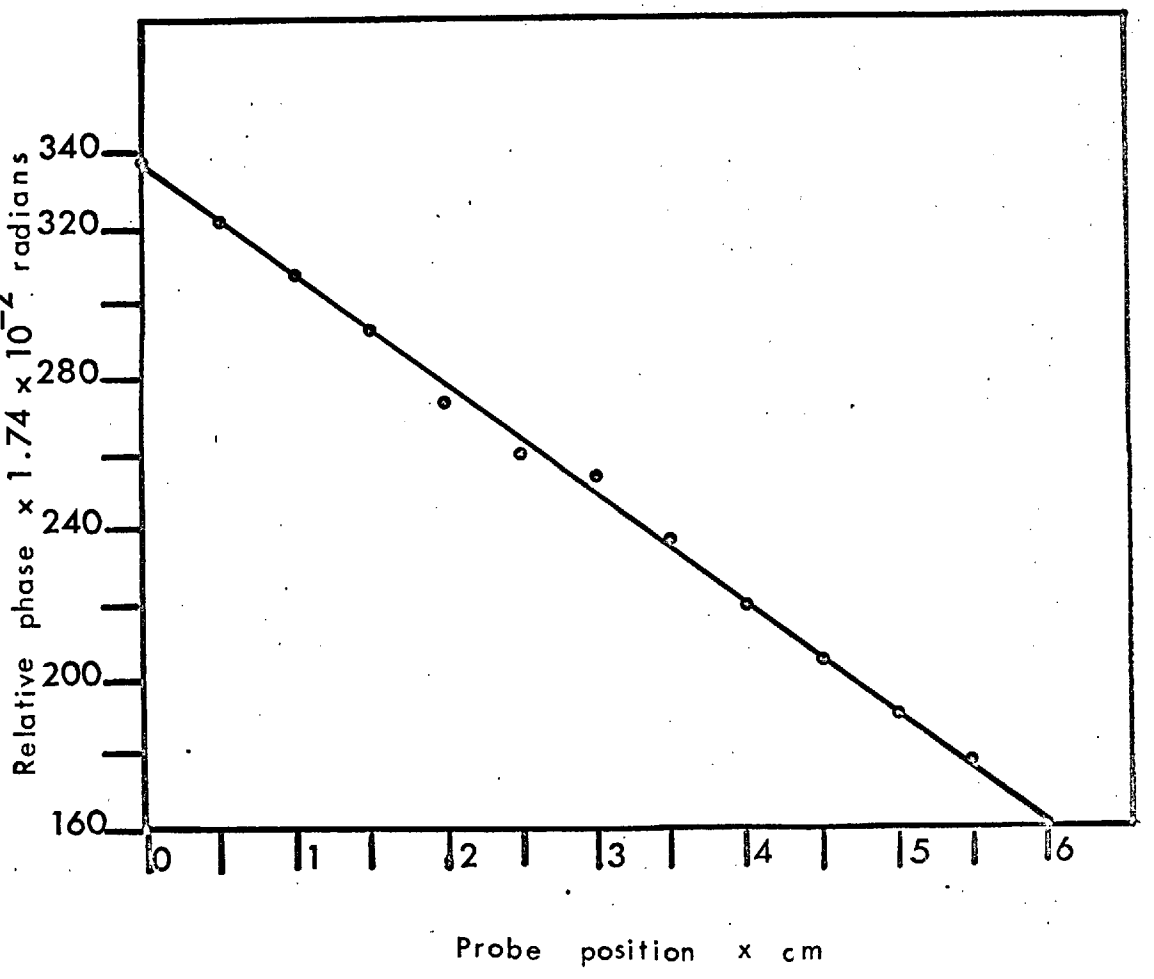

Fig. 32 Relative phase versus probe microphone position, for foam made from an aqueous solution of 5% stergene (f = 1000 c/s)

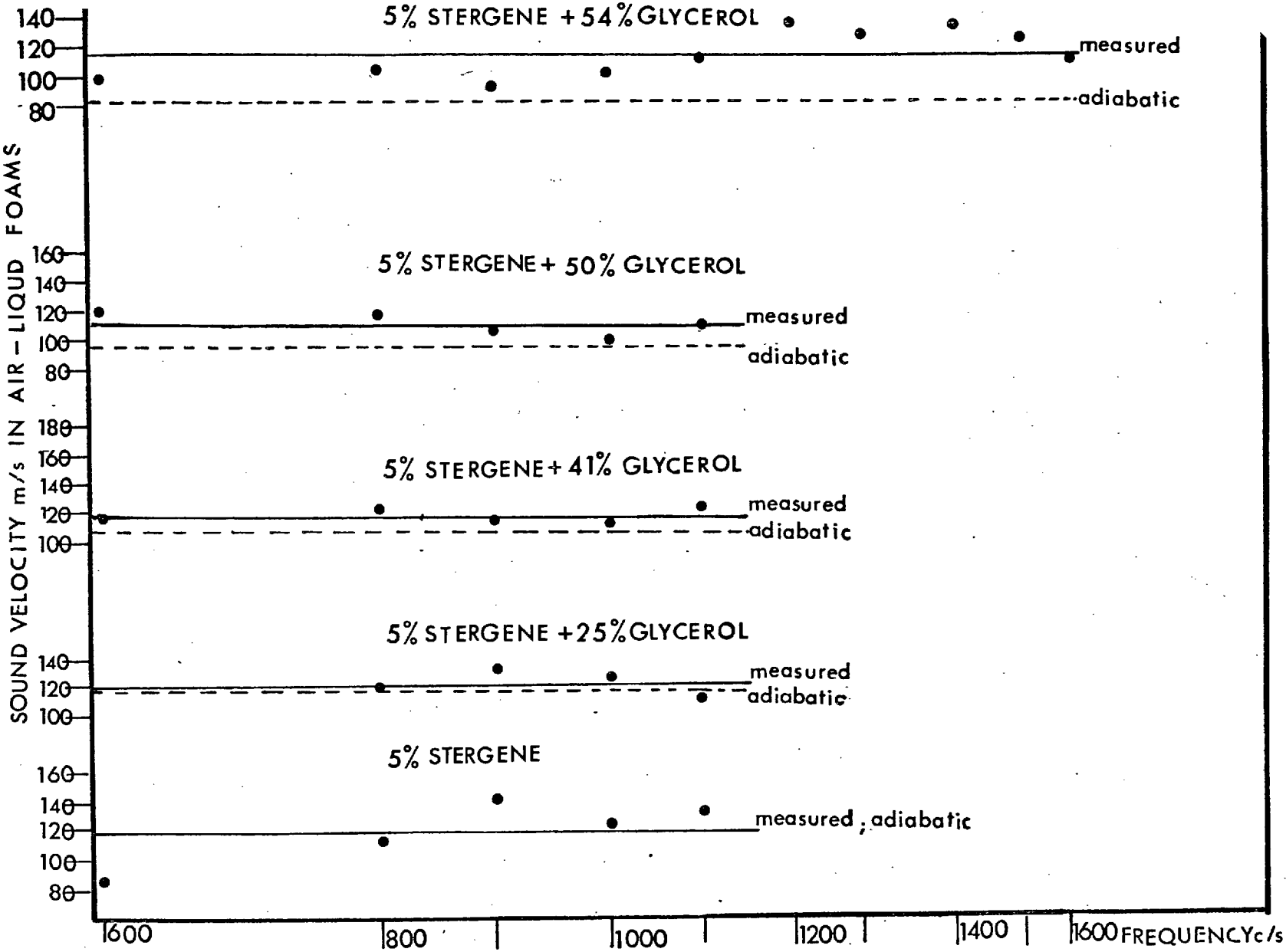

Fig.33 Measured values for phase velocity v versus frequency in foams of constant bubble size, for increasing volume concentrations of glycerol in the foam – making solutions. The mean values of v are plotted as full lines, and are compared with the computed adiabatic values c (dashed lines).

Section 5.6 Phase velocity in air-liquid foams of constant bubble size

In fig. 33, the measured values for the phase velocity v are plotted against frequency, and the mean values over the frequency range considered are plotted as full-lines, for each foam. The departure of these values of v from the adiabatic values of c_F (dashed lines) are shown in the figure, where

$$c_F = \left(\frac{\gamma P_o}{\rho_F} \right)^{\frac{1}{2}} \qquad (2.4.9)$$

In equation (2.4.9), γ is the ratio of the principal specific heats for air, P_o is the equilibrium pressure of the air, and ρ_F is the measured foam density.

Section 5.7 Conclusions from phase velocity and attenuation measurements

For air-liquid foams, such that the volume concentration of air in the mixture is in the range 0.98 - 0.99, the measured values of the velocity of sound lie in the neighbourhood of the computed adiabatic values. This contrasts with the measurements of Karplus[14] (section 1.5) in water containing air bubbles, for values of the volume concentration of air in the range 0.01 - 0.67, which agreed well with computed values for the isothermal velocity of sound.

The measurements of the attenuation of sound in air-liquid foams, whose parent liquids have viscosities in the range 1 - 10 centipoise, show an order of magnitude agreement with the theory discussed in section 2.1, which suggests that the attenuation is due to viscous dissipation in the bubble walls. Whereas the experimental value for the attenuation in an air-water foam is 10^6 times greater than the value predicted by the theory discussed in section 2.2, which suggests that the dissipation mechanism is caused by pressure relaxation due to the presence of saturated vapour.

Suggestions for further work

In order to investigate the variation of attenuation of sound with a greater range of foam densities, it is suggested that use should be made of a mechanical foam - generator, developed by Fry and French[42] for work on fire - fighting foams, in which air and foam - making solutions are metered under pressure and fed to an "improver" containing gauze discs of variable mesh where theyare "worked" together until the typical bubble structure of foam appears. (See fig. 34).

A more efficient method of picking up acoustic signals in the foam would be to mount a piezoelectric ceramic (PZT - 5A) on the end of the probe tube (see fig. 35) i.e. to act as a hydrophone. It should be covered with a thin layer of araldite to protect the ceramic transducer from moisture.

It is suggested that the correlation between the attenuation of a sound wave in foams and the surface viscosity of the detergent foam - making solutions should be investigated. Brown et al[43] have shown that for increasing concentrations of lauryl alcohol in an aqueous solution of sodium lauryl sulphate the surface viscosity passes through a sharp maximum. (See fig. 36). Whereas Pearson[44] has shown that the

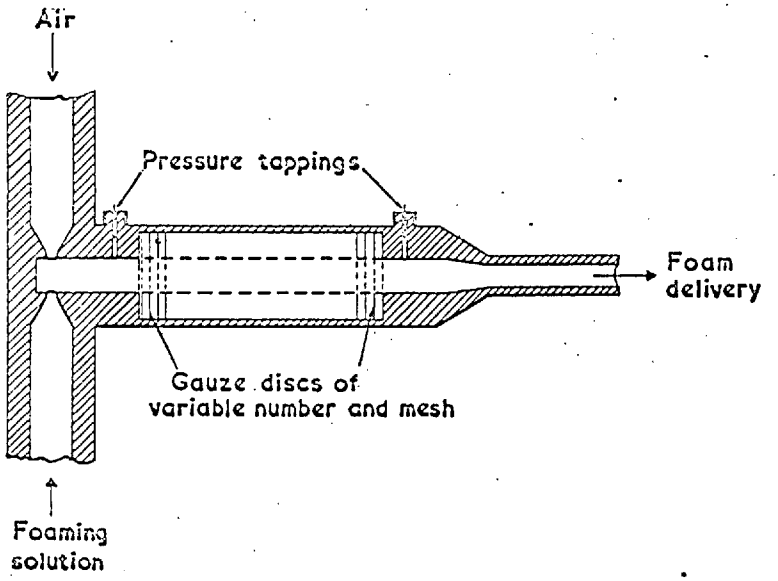

FIG. 34 *Diagram of Foam Generator showing "Improver"*

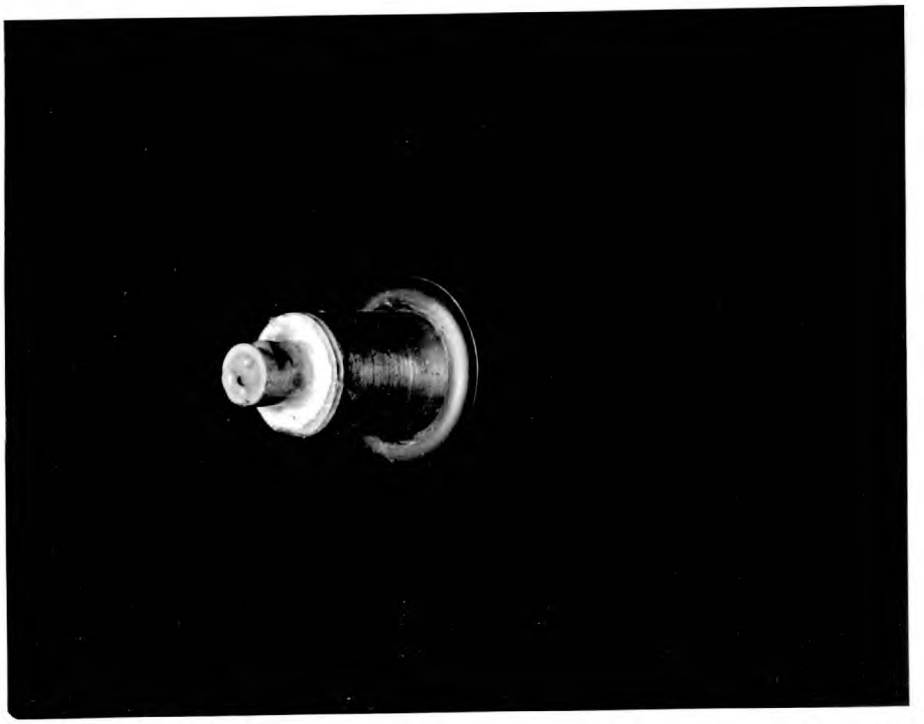

Fig.35a A piezoelectric ceramic mounted on the end of a probe tube.

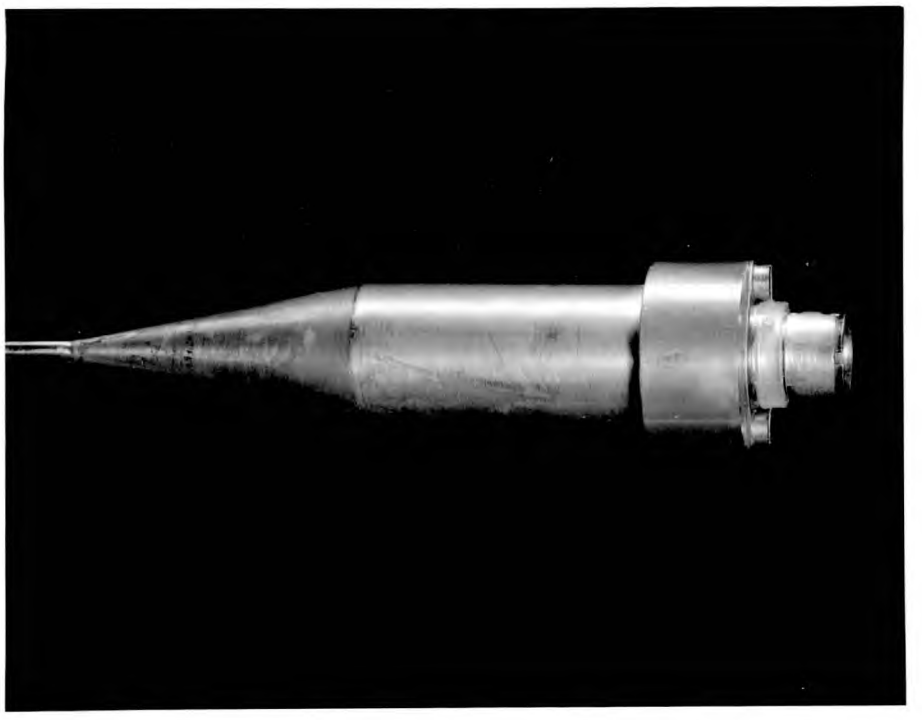

Fig.35b Microphone termination assembly.

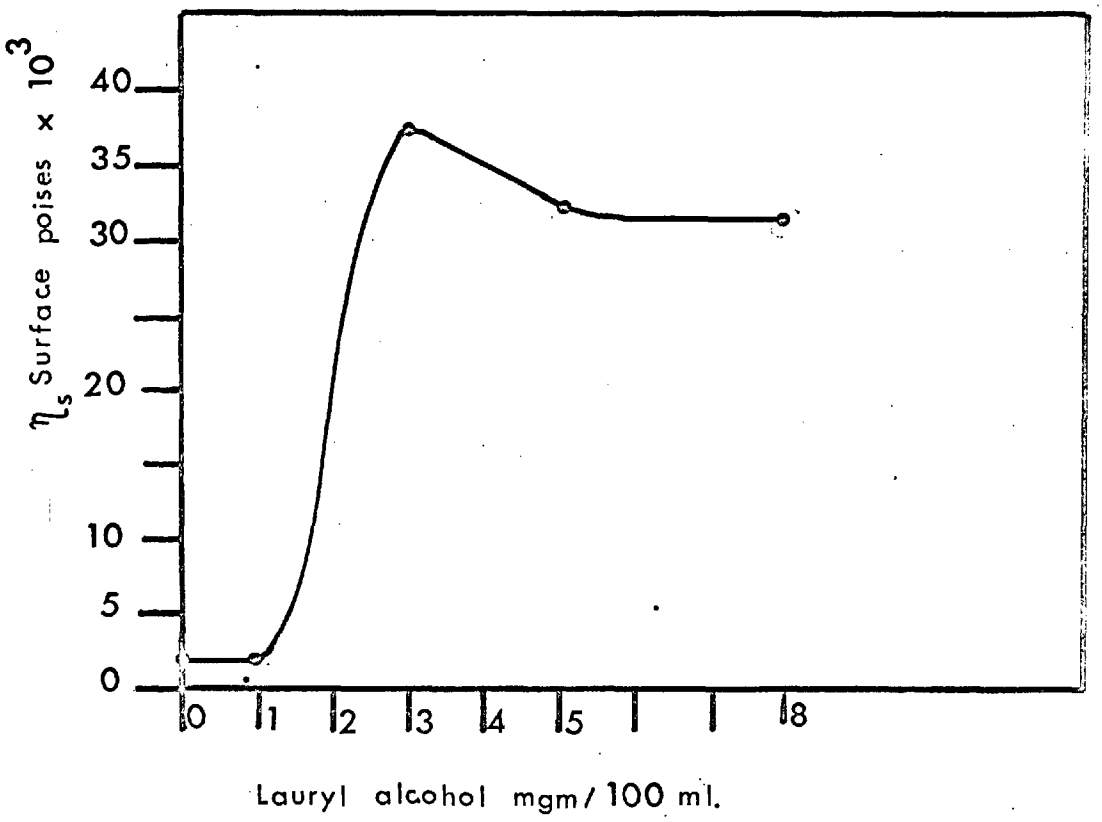

Fig 36. The surface viscosity versus the concentration of lauryl alcohol in an aqueous solution of 0.1 gm/100 ml. of sodium lauryl sulphate.

surface viscosity of an aqueous solution (less than 1 percent) of the protein bovine serum albumin decreases monotonically with increasing concentrations of the detergent sodium lauryl sulphate.

Experimental work has started on the measurement of acoustic impedance of a layer of solid gelatin - glycerol foam, employing plane waves in a rectangular wave guide. It is hoped to extend the scale of this work using polyurethane foams in an acoustic duct.

Appendix A1

(relates to section 1.5)

Resonance frequency for an isolated bubble in a liquid

The resonance frequency f_r for an isolated single bubble in a liquid was derived by Minnaert[19] and Devain[45]. For simple volume pulsations of the bubble, the condition of the bubble system is defined by the change in volume v from the equilibrium volume $4\Pi a_o^3/3$ (where a_o is the equilibrium bubble radius). The surrounding liquid acts as the inert mass m_2 which is set into vibration, while the stiffness s is due to the gas in the bubble. The equation of motion of the bubble system is

$$m_2 \ddot{v} + sv = 0 \qquad \text{(A1.1)}$$

$$\text{i.e.} \quad \frac{\rho_L}{4\Pi a_o} \ddot{v} + \frac{q\gamma P_o}{4\Pi a_o^3/3} v = 0 \qquad \text{(A1.2)}$$

where ρ_L is the density of the liquid, γ is the ratio of the principal specific heats of the gas, P_o is the equilibrium pressure, and q is a polytropic factor such that $1/\gamma \leq q \leq 1$. Hence the resonance frequency f_r is given by

$$f_r = \frac{1}{2\Pi a_o}\left(\frac{3q\gamma P_o}{\rho_L}\right)^{\frac{1}{2}} \qquad (A1.3)$$

For an air bubble in water at room temperature ($20^{\circ}C$) and atmospheric pressure, the typical parameter values used by Karplus[14] (see section 1.5) were:

$2a_o = 0.01$ cm ; $P_o = 1.01 \times 10^6$ dyn. cm^{-2}

$\gamma = 1.4$; $\rho_L = 1$ gm. cm^{-3}

If adiabatic conditions hold ($q = 1$) then

$$f_r = 65{,}000 \text{ c/s} \qquad (A1.4)$$

If isothermal conditions hold ($q = 1/\gamma$) then

$$f_r = 55{,}000 \text{ c/s} \qquad (A1.5)$$

Appendix A2

(relates to section 2.3.0)

Scattering from a single bubble

Let $p = \overset{\Lambda}{p}\, e^{-j\omega t}$ (A2.1)

where p is the excess pressure from the incident sound wave, and $\overset{\Lambda}{p}$ is a constant.

For adiabatic expansion of the air in the bubble

$$p = \frac{-\gamma P_o}{V_o}\, dV \tag{A2.2}$$

where P_o, V_o are the equilibrium pressure and volume and γ is the ratio of the principal specific heats for air.

Put $V_o = \frac{4}{3}\pi a^3$ (A2.3)

and $\gamma P_o = \rho_G\, c_G^2$ (A2.4)

where ρ_G and c_G are the density and adiabatic sound velocity in the gas (air) and a is the bubble radius. Hence, differentiation of equation (A2.1) with respect to time gives

$$\frac{\partial p}{\partial t} = -j\omega p = \left(\frac{-3\rho_G\, c_G^2}{4\pi a^3}\right)\frac{\partial V}{\partial t} \tag{A2.5}$$

Substituting for the radial velocity v_r at the surface of the bubble:

$$v_r = \frac{1}{4\pi a^2} \frac{\partial V}{\partial t} \tag{A2.6}$$

$$\text{Hence} \quad p = -j \left(\frac{3\rho_G c_G^2}{\omega a} \right) v_r \tag{A2.7}$$

The velocity potential Ψ_s of the scattered wave is given approximately by

$$\Psi_s = \frac{A}{r} e^{j(kr-\omega t)}; \quad \omega = kc_L \tag{A2.8}$$

where A is the amplitude of the velocity potential, and ρ_L, c_L are the density and sound velocity of the liquid, ρ_G, c_G the corresponding values for air.

The expressions for the excess pressure p_s and particle velocity v_s in the scattered wave, using the notation of electromagnetic scattering, are

$$p_s = -\rho_L \frac{\partial \Psi_s}{\partial t} = \frac{j\omega \rho_L A}{r} e^{j(kr-\omega t)} \tag{A2.9}$$

$$v_s = \frac{\partial \Psi_s}{\partial r} = \frac{jkA}{r} e^{j(kr-\omega t)} \frac{-A}{r^2} e^{j(kr-\omega t)} \tag{A2.10}$$

Boundary conditions (see section 2.3.0)

$$\hat{p} + \left(\frac{j\omega\rho_L}{a}\right) A = p \qquad \text{(A2.11)}$$

$$\left(\frac{j\omega}{c_L a}\right) A - \frac{A}{a^2} = v_r \qquad \text{(A2.12)}$$

where $ka \ll 1$ so that $e^{jka} \sim 1$.

Multiplication of equation (A2.12) by $-(j3\rho_G c_G^2)/\omega a$ and combining with equations (A2.7) and (A2.11) gives

$$\left(\frac{3\rho_G c_G^2}{c_L a^2}\right) A + j\left(\frac{3\rho_G c_G^2}{\omega a^3}\right) A = \hat{p} + \left(\frac{j\omega\rho_L}{a}\right) A \qquad \text{(A2.13)}$$

Thus the amplitude of the velocity potential A is given by

$$A = \frac{a\,\hat{p}/j\omega\rho_L}{(\omega_o/\omega)^2 - 1 - j(B/\omega)} \qquad \text{(A2.14)}$$

where $$\omega_o^2 = \frac{3\rho_G c_G^2}{\rho_L a^2} \qquad \text{(A2.15)}$$

and $$B = \frac{3\rho_G c_G^2}{a\rho_L c_L} \qquad \text{(A2.16)}$$

Velocity potential at the bubble surface

Velocity potential at the bubble surface is

$$\Psi_i \, e^{-j\omega t} \tag{A2.17}$$

Hence the excess pressure in the incident wave is

$$p = j\omega\rho_L \, \Psi_i \, e^{-j\omega t} \tag{2.18}$$

But $$p = \overset{\Lambda}{p} \, e^{-j\omega t} \tag{A2.1}$$

Thus $$\Psi_i = \frac{\overset{\Lambda}{p}}{j\omega\rho_L} \tag{A2.19}$$

Multiple scattering

$$A_n = \frac{a\Psi_n}{(\omega_o/\omega)^2 - 1 - j\delta(\omega)} \; ; \tag{A2.20}$$

where from equation (2.3.14) in chapter 2,

$$\Psi_n = \Psi_i \, (\underline{R})_n + \sum_{m \neq n} \frac{A_m}{R} \, e^{jkR_{mn}} \tag{A2.21}$$

where $R_{mn} = \left| \underline{r}_m - \underline{r}_n \right|$

In equation (2.3.14) in chapter 2, write

$$A_n = g_n \, \Psi_n \tag{A2.22}$$

where $$g_n = \frac{a}{[\omega_o(a)/\omega]^2 - 1 - j\delta(\omega,a)} \qquad (2.23)$$

and the scattering cross section

$$Q_{sn} = 4\Pi \left|g_n\right|^2 \qquad (A2.24)$$

The quantity $G(\underline{r})$ is the average density of the bubble scatterers at $\underline{r}$, given by

$$G(\underline{r}) = \int_o^D n(\underline{r},a)\, g(a)da \qquad (A2.25)$$

In equation (A2.21) write

$$A_m = g_m \Psi_m \qquad (A2.26)$$

and substituting for A_m from equation (A2.26) into equation (A2.21):

$$\Psi_n = \Psi_i(\underline{r}_n) + \sum_{m \neq n} \frac{g_m}{R_{mn}} \Psi_m e^{jkR_{mn}} \qquad (A2.27)$$

Appendix A3

(relates to sections 5.3 and 5.6)

Calculation of foam density

Let the suffixes G, L, F denote the gas, liquid and foam respectively. The average density ρ_F of the foam is given by

$$\rho_F = (M_L + M_G)/V_F \qquad (A3.1)$$

where M, V denote the mass and volume respectively. Assuming spherical gas bubbles of radius a and wall half-thickness δ,

$$V_F = \frac{4}{3}\pi (a+\delta)^3 \qquad (A3.2$$

$$V_L = \frac{4}{3}\pi (a+\delta)^3 - \frac{4}{3}\pi a^3 \qquad (A3.3)$$

$$V_G = \frac{4}{3}\pi a^3 \qquad (A3.4)$$

Substituting from equations (A3.2), (A3.3) and (A3.4) into equation (A3.1):

$$\rho_F = \frac{\rho_L [\ (\delta/a)^3 + 3(\delta/a)^2 + 3(\delta/a)\ ] + \rho_G}{(\delta/a)^3 + 3(\delta/a)^2 + 3(\delta/a) + 1} \qquad (A3.5)$$

At room temperature and atmospheric pressure, typical parameter values for an air-water foam are

$\rho_G = 1.2 \times 10^{-3}$ gm cm^{-3}, $\rho_L = 1$ gm cm^{-3}, $a = 6 \times 10^{-2}$ cm

Assuming $\delta/a \ll 1$, and neglecting terms $O(\delta/a)^2$, equation A3.5 becomes

$$\rho_F = 3(\delta/a)\rho_L + \rho_G \qquad \text{(A3.6)}$$

Hence the bubble wall half-thickness δ may be calculated from measurements of the foam density ρ_F and bubble radius a:

$$\delta = \frac{a(\rho_F - \rho_G)}{3\rho_L} \qquad \text{(A3.7)}$$

Appendix A 4

(relates to Chapter 3.)

Glossary of terms for surface - active agents.

Hydrophilic	water attracting
Hydrophobic	water repelling
Non-ionic surface-active agent	a single molecule which has a hydrophilic group at one end and a hydrophobic group at the other end
Ionic surface active agents	the class which includes cationic and anionic surface active agents
Cationic surface active agent	the hydrophilic part of the molecule is an acid radical
Anionic surface active agent	the hydrophilic part of the molecule is a basic radical
Micelle	an aggregate of surface active ions in sufficiently strong solutions forming a unit of colloidal dimensions
Critical micelle concentration	the concentration at which micelles begin to form

Appendix A 5

(relates to section 3.7)

Calculation of sound intensity level for foam breakdown

Using a constant voltage drive for the loudspeaker, and assuming a constant drive coil resistance of 15 Ω the electrical power supplied to the loudspeaker for foam breakdown was about 7 watts r.m.s. (at 1000 c/s). Assuming a conversion efficiency of 5 per cent, the acoustic power was about 0.35 watts.

The intensity level (IL) of a sound of intensity I with respect to a reference intensity I_o in air of 10^{-12} watt/m^2 is defined by

$$IL = 10 \log_{10} (I/I_o) \text{ dB}$$

Hence the intensity level for foam breakdown is given by

$$IL = 115 \text{ dB}$$

Appendix A6

(relates to section 4.6.2)

TABLE A6

Manufacturer	Instrument	Type	Input impedance	Output impedance
Brüel and Kjaer	Microphone amplifier	2601	2.2MΩ//15pF	20 KΩ
Muirhead Pametrada	Wave analyser	D-489-EM	100KΩ//100μF	2 KΩ
	Supply unit	D-489-DS	-	-
Solartron	Resolved Compcnent Indicator	VP 250	> 50MΩ//15pF ref. & sig. channels	-
Leak	Power amplifier	TL/12 PLUS	1MΩ	15Ω
Vitavox	Pressure unit	GP1	15Ω	
Advance Components Ltd.	A.F. generator	J Model 2	-	600Ω

Appendix A7

(relates to sections 3.1 & 4.7.1)

The most probable shape of a bubble in foam

From observations on gelatin, soap, and rosin foams Desch[50] concluded that the pentagonal dodecahedron (figure bounded by twelve equilateral pentagons) is the most frequent approximate shape of foam bubbles. This is the only figure whose repetition can fill the space and in which all faces form angles of 120 deg. with each other. (See fig. 9 in chapter 3).

If the pentagonal dodecahedron is cut through by a mirror plane, then the section is a hexagon.

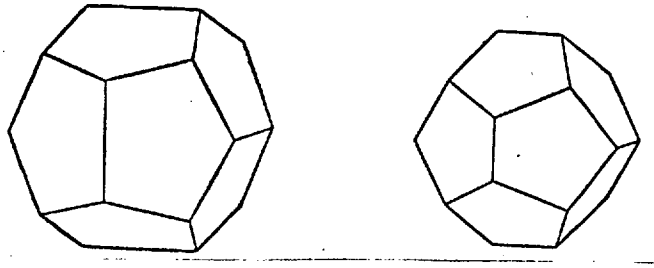

Pentagonal dodecahedra (210) (320)

Fig.37a

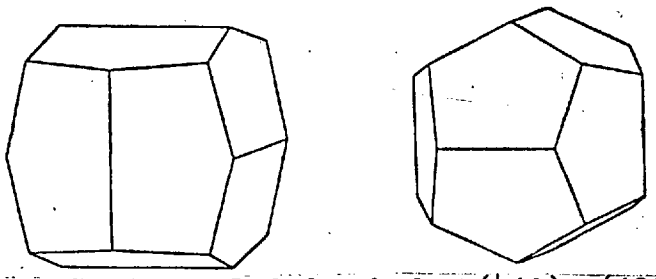

Pentagonal dodecahedra (410) (120)
The form (120) has the same shape as (210) but with a different attitude in space.

Fig.37b

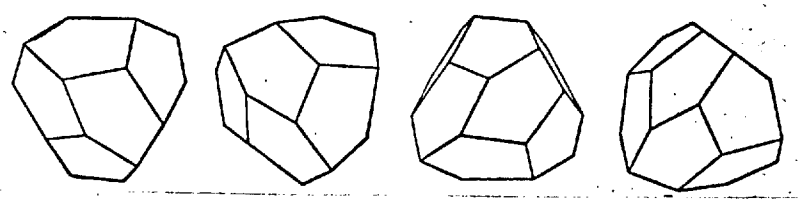

Tetrahedral pentagonal dodecahedra (321) (231) ($3\bar{2}1$) ($2\bar{3}1$)
The form (231) is the mirror image of (321).

Fig.37c

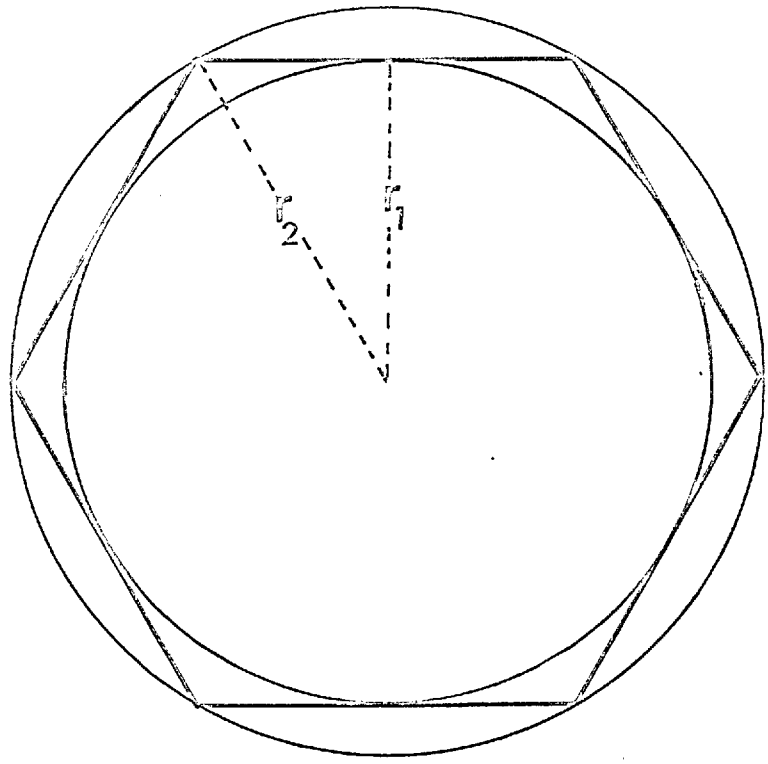

Fig.38 Hexagon

r_1 = radius of inscribed circle

r_2 = radius of circumscribed circle

$r = \frac{r_1 + r_2}{2}$ = average radius

Appendix A7

(relates to section 4.7.1)

Measurement of bubble size

The foam bubble radii distributions for increasing volume concentrations of glycerol in the foam-making solutions are shown graphically in fig. 40 and photographically in fig. 39.

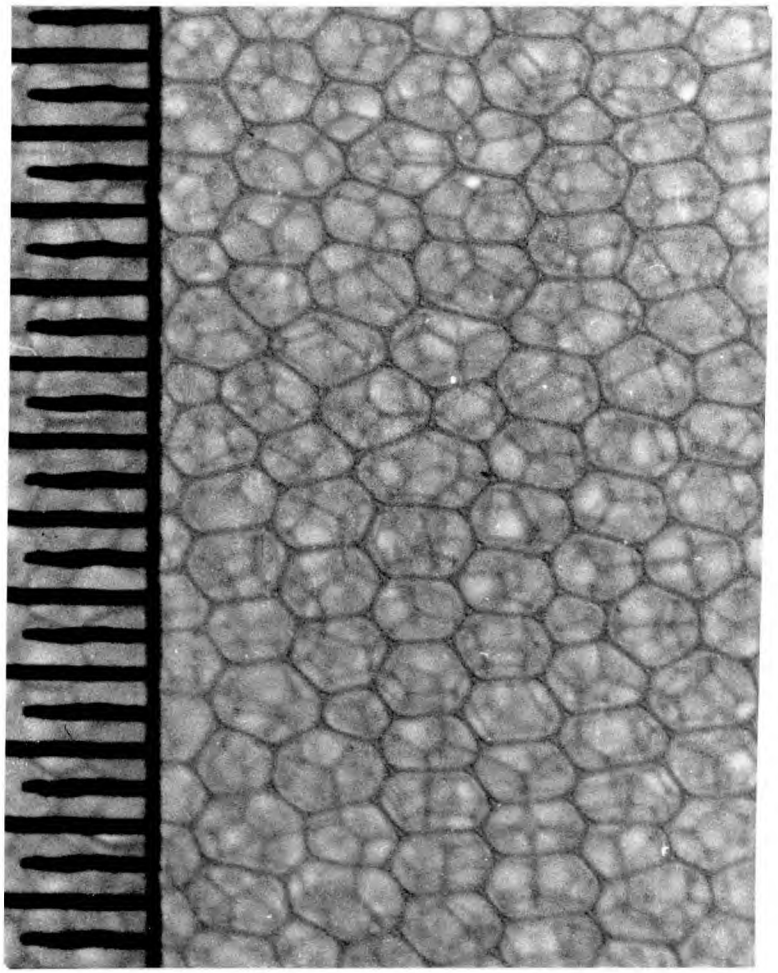

Vertical scale 0.5 mm marks.
Enlarged x 10.
Sound propagates and foam flows vertically.
Fig. 39(a)

Foam bubble equiv. radius $5.6 \pm 0.5 \times 10^{-2}$ cm.

Foam-making soln. 5% stergene.

Air jet diameter 0.7×10^{-2} cm.

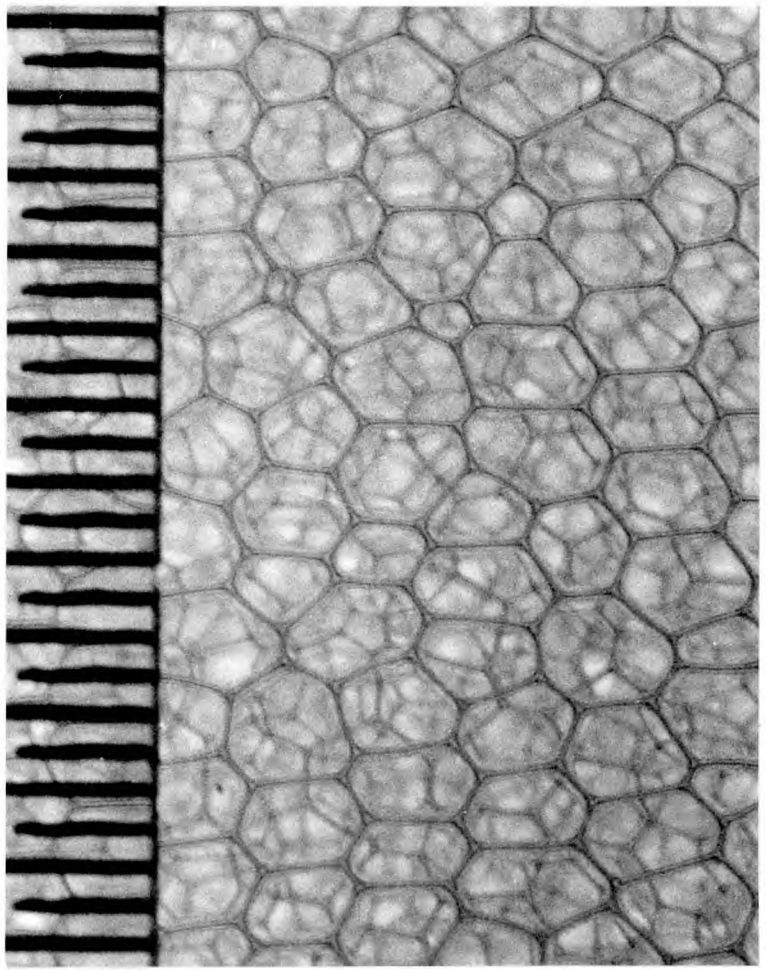

Fig.39(b)

Foam bubble equiv. radius $6.5 \pm 0.9 \times 10^{-2}$ cm.

Foam-making soln. 5% stergene + 25% glycerol.

Air jet diameter 0.7×10^{-2} cm.

(1/69)

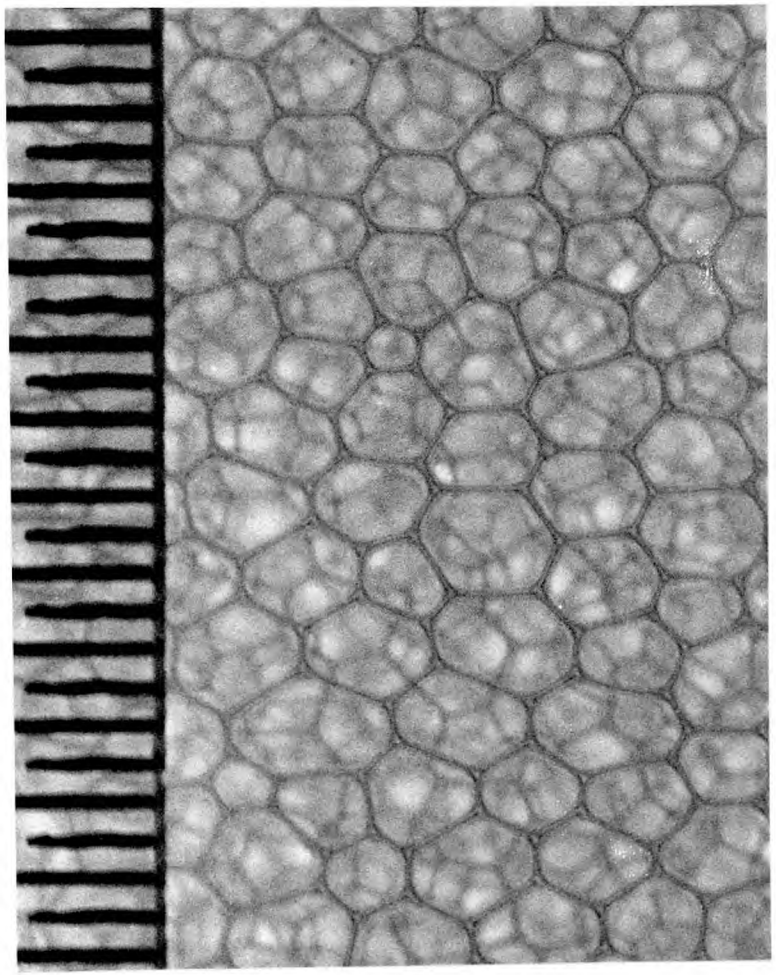

Fig. 39(c)

Foam bubble equiv. radius $6.5 \pm 0.8 \times 10^{-2}$ cm.
Foam-making soln. 5°/o stergene + 41°/o glycerol.
Air jet diameter 0.7×10^{-2} cm.

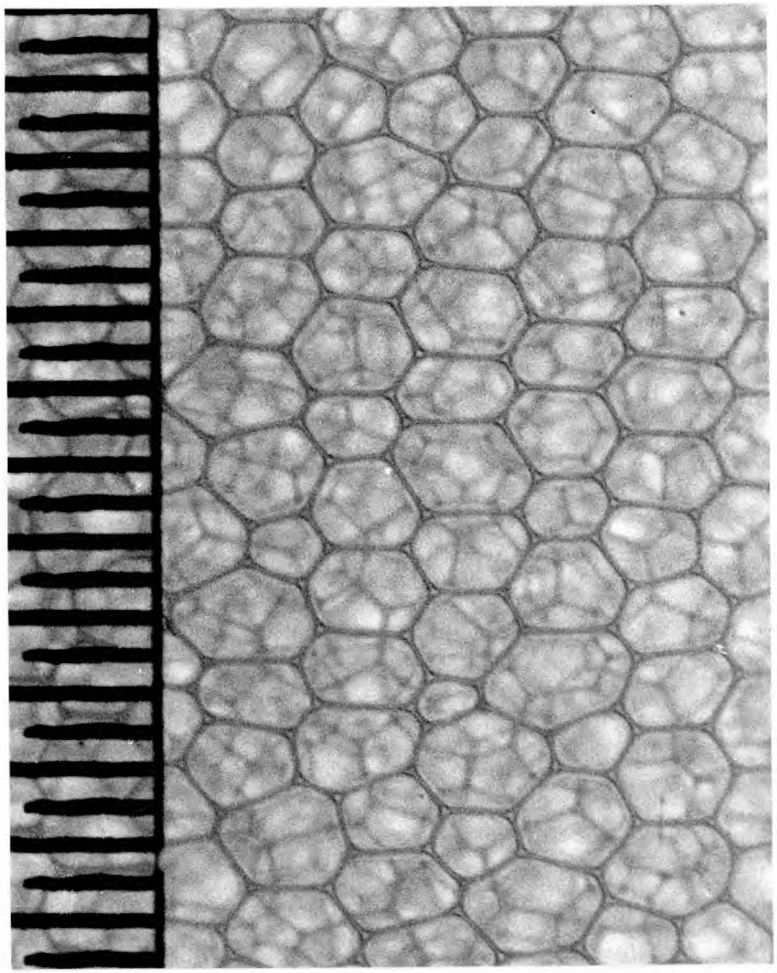

Fig.39(d)

Foam bubble equiv. radius $6.5 \pm 0.6 \times 10^{-2}$ cm.
Foam-making soln. 5°/o stergene + 50 °/o glycerol.
Air jet diameter 0.7×10^{-2} cm.

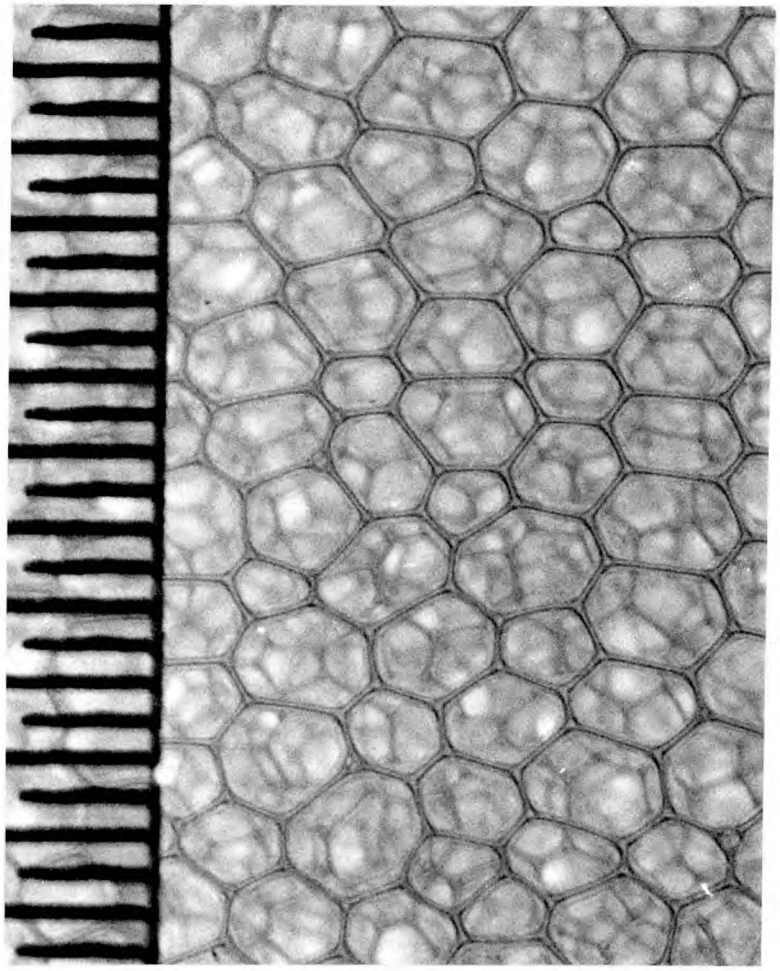

Fig. 39(e)

Foam bubble equiv. radius $6.9 \pm 0.6 \times 10^{-2}$ cm.

Foam-making soln. 5% stergene + 54% glycerol.

Air jet diameter 0.7×10^{-2} cm.

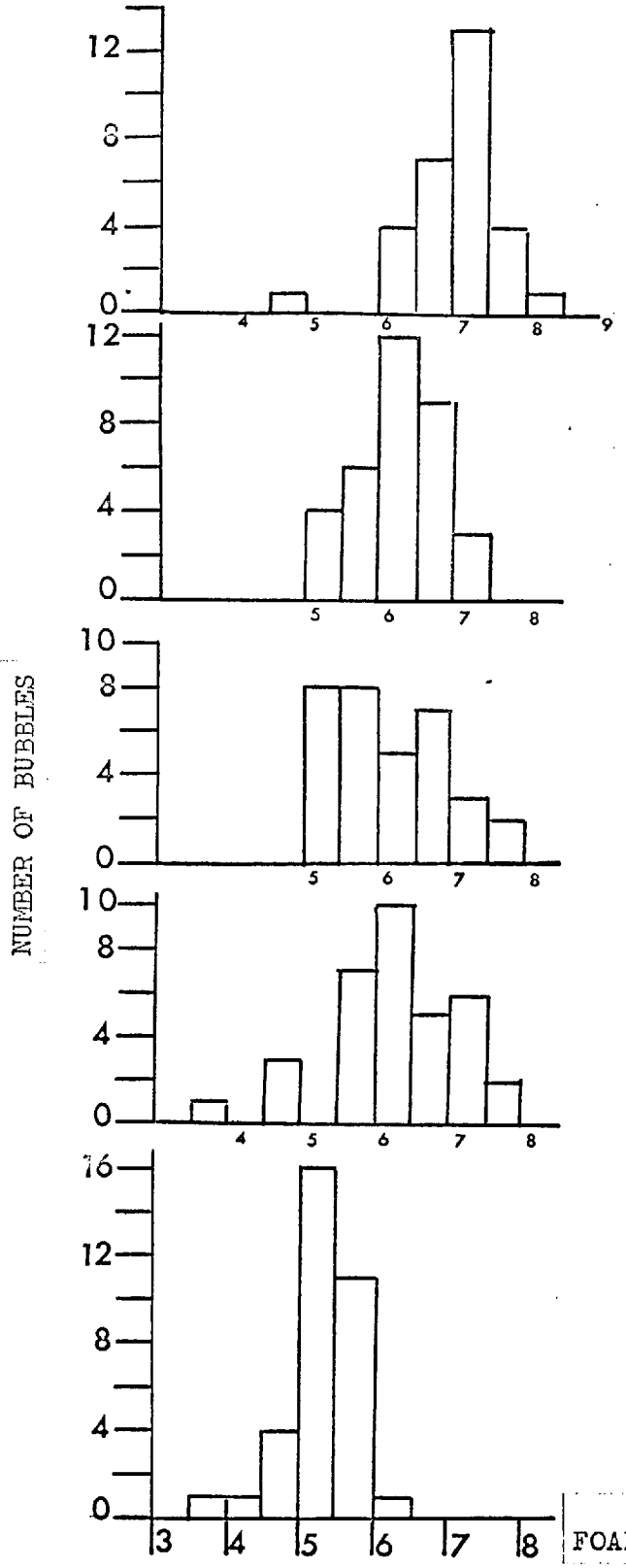

5% stergene + 54% glycerol

Foam bubble radius

$6.9 \pm 0.6 \times 10^{-2}$ cm

5% stergene + 50% glycerol

Foam bubble radius

$6.5 \pm 0.8 \times 10^{-2}$ cm

5% stergene + 41% glycerol

Foam bubble radius

$6.5 \pm 0.8 \times 10^{-2}$ cm

5% stergene + 25% glycerol

Foam bubble radius

$6.5 \pm 0.9 \times 10^{-2}$ cm

5% stergene

Foam bubble radius

$5.6 \pm 0.5 \times 10^{-2}$ cm

Fig.40 Foam bubble radii distributions for increasing volume concentrations of glycerol in the foam – making solutions. (Constant air jet hole diameter = 0.7×10^{-2} cm)

Appendix A8.

(relates to section 4.7.2)

TABLE A8

FOAM VISCOSITY MEASUREMENTS

Constant parameter air jet hole diameter = 0.07 mm

Foam - making solution (percentage by vol.)	Room temp. deg. C	FOAM VISCOSITY (measured) c. stokes	poise	Foam density gm cm^{-3}
5% stergene	25.7 ± 0.2	16 ± 2	0.28 ± 0.04	0.018 ± 0.002
5% stergene + 25% clycerol	24.2 ± 0.2	22 ± 3	0.43 ± 0.06	0.020 ± 0.001

Appendix A9

(relates to section 2.4)

Velocity of sound in terms of the volume concentration of bubbles

Sound velocity is given by

$$c = (\rho_T K_T)^{-\frac{1}{2}} \tag{A9.1}$$

where ρ_T and K_T are the average density and compressibility of the mixture. Let the suffixes G, L, T denote the gas, liquid and mixture respectively, and x the volume concentration of the gas in the mixture. The average density of the mixture is

$$\rho_T = \frac{M_G + M_L}{V_T} = \frac{V_G}{V_T}\rho_G + \frac{V_L}{V_T}\rho_L \tag{A9.2}$$

$$\rho_T = x\rho_G + (1 - x)\rho_L \tag{A9.3}$$

Compressibility is defined as strain/stress, hence

$$K_T = -(dV_G + dV_L)/(V_T\, dP) \tag{A9.4}$$

$$= -\left[\frac{dV_G}{V_G dP} \cdot \frac{V_G}{V_T} + \frac{dV_L}{V_L dP} \cdot \frac{V_L}{V_T}\right]$$

$$K_T = x\,K_G + (1-x)K_L \qquad (A9.5)$$

Substituting from equations (A9.3) and (A9.5) into equation (A9.1):

$$c = \left\{ [\, x\rho_G + (1-x)\rho_L \,]\,[\, x\,K_G + (1-x)K_L \,] \right\}^{-\frac{1}{2}} \qquad (A9.6)$$

This may be written as

$$c = [\, x^2\rho_G\,K_G + (1-x)^2\rho_L\,K_L + x(1-x)(\rho_G\,K_L + \rho_L\,K_G)\,]^{-\frac{1}{2}} \qquad (A9.7)$$

(i) Isothemal velocity

The compressibility K_{GI} of an ideal gas under isothermal conditions is given by

$$K_{GI} = 1/P_o \qquad (A9.8)$$

where P_o is the equilibrium gas pressure.

Sound propagation is known to be adiabatic in a single phase medium, so that in the gas the sound velocity c_G is given by

$$1/c_G^{\,2} = \rho_G\,K_{GA} \qquad (A9.9)$$

Substitution of equations (A9.8) and (A9.9) into equation (A9.7) gives the isothermal velocity of sound in the mixture as

$$c_I = \left[\frac{\gamma x^2}{c_G^2} + \frac{(1-x)^2}{c_L^2} + x(1-x)\left(\rho_G K_L + \frac{\rho_L}{P_o}\right) \right]^{-\frac{1}{2}} \qquad \text{(A9.10)}$$

The measurements of Karplus[14] (section 1.5) for a mixture of air bubbles in water agree well with computed values for the isothermal velocity of sound given by equation (A9.10).

Substantial simplification of equation (A9.10) is possible because of the relative sizes of the pertinent parameters of the air-water medium. At room temperature and atmospheric pressure the typical parameter values are

$c_G = 3.4 \times 10^4$ cm sec^{-1} $\qquad c_L = 1.5 \times 10^4$ cm sec^{-1}

$\rho_G = 1.2 \times 10^{-3}$ gm cm^{-3} $\qquad \rho_L = 1$ gm cm^{-3}

$P_o = 1.01 \times 10^6$ dyn cm^{-2} $\qquad \gamma = 1.4$

$K_L = 4.54 \times 10^{-11}$ cm^2 dyn^{-1}

Thus

$$\rho_G K_L \ll \rho_L / P_o$$

so that $\rho_G K_L$ in equation (A9.10) may be neglected.

In selected concentration ranges different terms dominate and the following simplified expressions may be used with a 1 percent error in c_I:

(a) At all except very low concentrations; $x > 0.0022$

$$\frac{(1-x)^2}{c_L^2} \ll \frac{x(1-x)\rho_L}{P_o}$$

Thus equation (A9.10) becomes

$$c_I = \left[\frac{\gamma x^2}{c_G^2} + \frac{x(1-x)\rho_L}{P_o} \right]^{-\frac{1}{2}} \qquad \text{(A9.10a)}$$

(b) At intermediate concentrations, $0.0022 < x < 0.94$

$$\frac{(1-x)^2}{c_L^2} \ll \frac{x(1-x)\rho_L}{P_o} \quad \text{and} \quad \frac{x^2}{c_G^2} \ll \frac{x(1-x)\rho_L}{P_o}$$

Thus equation (A9.10) becomes

$$c_I = \left[\frac{x(1-x)\rho_L}{P_o} \right]^{-\frac{1}{2}} \qquad \text{(A9.10b)}$$

If the pressure P_o is measured in atmospheres, the velocity of sound in m/sec becomes

$$c_I = 10.05\, P_o^{\frac{1}{2}} \left[x(1-x) \right]^{-\frac{1}{2}}$$

(c) At all but the very high concentrations, $x < 0.94$

$$\frac{(1-x)^2}{c_L^2} \sim \frac{1}{c_L^2} \quad \text{and} \quad \frac{x^2}{c_G^2} << \frac{x(1-x)\rho_L}{P_o}$$

Thus equation (A9.10) becomes

$$c_I = \left[\frac{1}{c_L^2} + \frac{x(1-x)\rho_L}{P_o} \right]^{-\frac{1}{2}} \qquad \text{(A9.10c)}$$

(ii) Adiabatic velocity

The compressibility K_{GA} of an ideal gas under adiabatic conditions is given by

$$K_{GA} = 1/(\gamma P_o) \qquad \text{(A9.11)}$$

Substitution of equations (A9.11) and (A9.9) into equation (A9.7) gives the adiabatic velocity of sound in the mixture as

$$c_A = \left[\frac{x^2}{c_G^2} + \frac{(1-x)^2}{c_L^2} + x(1-x) \left(\rho_G K_L + \frac{\rho_L}{\gamma P_o} \right) \right]^{-\frac{1}{2}} \qquad \text{(A9.11)}$$

At very high concentrations in the range $0.98 < x < 0.99$, such that the mixture becomes a foam, the following approximations apply

$$\rho_G K_L << \rho_L/(\gamma P_o)$$

$$(1-x)^2/c_L^2 << x(1-x)\rho_L/(\gamma P_o)$$

Thus equation (A9.11) becomes

$$c_A = \left[\frac{x^2}{c_G^2} + \frac{x(1-x)\rho_L}{\gamma P_o} \right]^{-\frac{1}{2}} \quad \text{for } 0.98 < x < 0.99 \qquad \text{(A9.12)}$$

Appendix A10

(relates to sections 5.3 and 5.6)

Sound propagation in a tube

In a "wide tube", the sound energy is diffused uniformly over the tube cross-section and the adiabatic motion approximates to that in an unbounded medium. There exists however a narrow boundary layer at the wall, where viscous processes lead to an energy loss. For a tube, such that the radius "a" satisfied the condition

$$a \gg \left[\left(\frac{1}{4\Pi f} \right) \left(\frac{\eta_F}{\rho_F} \right) \right]^{\frac{1}{2}} \qquad \text{(A10.1)}$$

the tube attenuation factor α_T is given by

$$\alpha_T = \frac{1}{a} \left[\left(\frac{\Pi f}{c^2} \right) \left(\frac{\eta_F}{\rho_F} \right) \right]^{\frac{1}{2}} \qquad \text{(A10.2)}$$

where c is the normal sound velocity, η_F is the shear viscosity of the foam, ρ_F the foam density and f the frequency.

The reduced phase velocity c' is given by

$$c' = c \left[1 - \frac{1}{2a} \sqrt{\left(\frac{\eta_F}{\rho_F} \right) \left(\frac{1}{\Pi f} \right)} \right] \qquad \text{(A10.3)}$$

At room temperature and atmospheric pressure, typical parameters for air-liquid foams are given in table (A10), computed from equation (1.0.1) for measured values of the attenuation and phase velocity.

Table (A10)

Foam-making aqueous soln.	Dynamic foam viscosity η_F (computed) $\times 10^2$ poise	Foam density ρ_F (measured) $\times 10^{-2}$ gm cm^{-3}	Kinematic foam viscosity η_F/ρ_F (computed) $\times 10^3$ stokes
5% stergene	0.3 .	1.01 $\pm$ 0.04	3 .
5% stergene + 54% glycerol	1.0 .	1.98 $\pm$ 0.08	. 5

Thus condition (A10.1) is not satisfied for the measurement tube of radius 1.2 cm in the frequency range (600 - 1600 c/s) used. Hence the sound propagation in this tube may be considered as taking place in an unbounded medium.

Appendix All

(relates to sections 5.2 and 5.5)

The method of least squares

Suppose y_1, y_2 ----, y_n are the values of a measured quantity y corresponding to the values x_1, x_2, ----, x_n of another quantity x. Assume that there are experimental errors in the values of y_s but not in the values of x_s, and there exists a linear relation between x and y, namely,

$$y = ax + b \qquad \text{(All.1)}$$

On substituting $x = x_s$, the value of y will not in general equal y_s; there will be an "error" of amount

$$ax_s + b - y_s$$

To obtain the line which best fits the data a and b are chosen such that the sum of the squares of the "errors" is least, i.e.

$$\Sigma (ax_s + b - y_s)^2 \quad \text{is least} \qquad \text{(All.2)}$$

The conditions obtained by differentiating partially with respect to a and b are

$$\Sigma x_s (ax_s + b - y_s) = 0 \qquad \text{(All.3)}$$

and

$$\Sigma(ax_s + b - y_s) = 0 \qquad \text{(A11.4)}$$

Hence

$$a\Sigma(xx) + b\Sigma x = \Sigma(xy) \qquad \text{(A11.5)}$$

$$a\Sigma x + b\,n = \Sigma y \qquad \text{(A11.6)}$$

which give

$$a = \frac{n\Sigma(xy) - \Sigma x\,\Sigma y}{n\Sigma(xx) - \Sigma x\,\Sigma x} \qquad \text{(A11.7)}$$

$$b = \frac{\Sigma y\,\Sigma(xx) - \Sigma x\,\Sigma(xy)}{n\,\Sigma(xx) - \Sigma x\,\Sigma x} \qquad \text{(A11.8)}$$

Accuracy of coefficients

The residuals d_s are given by

$$d_s = ax_s + b - y_s \qquad \text{(A11.9)}$$

Then the mean square error σ^2 in the residuals d_s is given by

$$\sigma^2 = \frac{\Sigma(dd)}{(n-2)} \qquad \text{(A11.10)}$$

Also, if σ_a and σ_b denote the standard errors in the values of a and b then, using equations (A11.5) and (A11.6)

$$\sigma_a^2 = \frac{n}{\Delta} \sigma^2 \qquad \text{(A11.11)}$$

$$\sigma_b^2 = \frac{\Sigma(xx)}{\Delta} \sigma^2 \qquad \text{(A11.12)}$$

Appendix A12

Attenuation and phase velocity in air-liquid foams of varying bubble size

(i) Attenuation

For constant values of liquid viscosity η_L and density ρ_L equation (5.0.3) in chapter 5 suggests that the attenuation α/f^2 will depend only on the foam density ρ_F and be independent of bubble radius:

$$\frac{\alpha}{f^2} = \frac{12\pi^2 \eta_L \rho_L}{(\gamma P_o)^{\frac{3}{2}}} \cdot \frac{1}{(\rho_F)^{\frac{1}{2}}(1 - \rho_G/\rho_F)} \qquad (5.0.3)$$

In this equation, P_o is the equilibrium pressure of the air, γ is the ratio of the principal specific heats of air, and ρ_G is the density of the gas (air).

The order of magnitude agreement between the measured and theoretical values for the attenuation is to within a factor of three (see table A12), for bubble radii in the range $(6.9 - 9.0) \times 10^{-2}$ cm in foams made from an aqueous solution of 5 per cent stergene + 54 per cent glycerol.

TABLE A12

Constant parameters

Foam-making solution 5% stergene + 54% glycerol; liquid viscosity, $\eta_L = 10.4 \times 10^{-2}$ poise; liquid density, $\rho_L = 1.141$ gm cm^{-3}; frequency = 1000 c /s; measurement-tube radius = 1.15 cm; temperature = 23 ± 1 deg. C; eqm. pressure of air, $P_o = 1.01 \times 10^6$ dyn. cm^{-2}; density of air, $\rho_G = 1.2 \times 10^{-3}$ gm cm^{-3}.

Air jet hole diameter	Foam bubble radius	Foam density	ATTENUATION		$\frac{\alpha_{meas.}}{\alpha_{theory}}$	VELOCITY		$\frac{c_{meas.}}{c_{adiab}}$
x10^{-2} cm	x10^{-2} cm	x10^{-2} gm cm^{-3}	x10^{-8} neper cm^{-1} sec^{-2}			m sec^{-1}		
			α_{theory}/f^2	$\alpha_{meas.}/f^2$		c_{adiab}	$c_{meas.}$	
0.7	6.9 ± 0.6	1.98 ± 0.08	6.3	20.4	3.2	85	102	1.2
0.9	7.2 ± 0.8	1.65 ± 0.07	7.0	22.2	3.2	93	107	1.2
1.0	8.0 ± 1.0	1.60 ± 0.06	7.1	20.4	2.8	94	116	1.2
1.2	9.0 ± 1.0	1.64 ± 0.07	7.0	22.6	3.2	93	125	1.3

(ii) Phase Velocity

From equation (2.4.9) in chapter 2, c_F, the adiabatic velocity in the given foam is related to the measured foam density ρ_F by

$$c_F = \left(\frac{\gamma P_o}{\rho_F} \right)^{\frac{1}{2}} \qquad (2.4.9)$$

The agreement between the measured and theoretical values for the phase velocity varies between 20 and 30 per cent (see table A12).

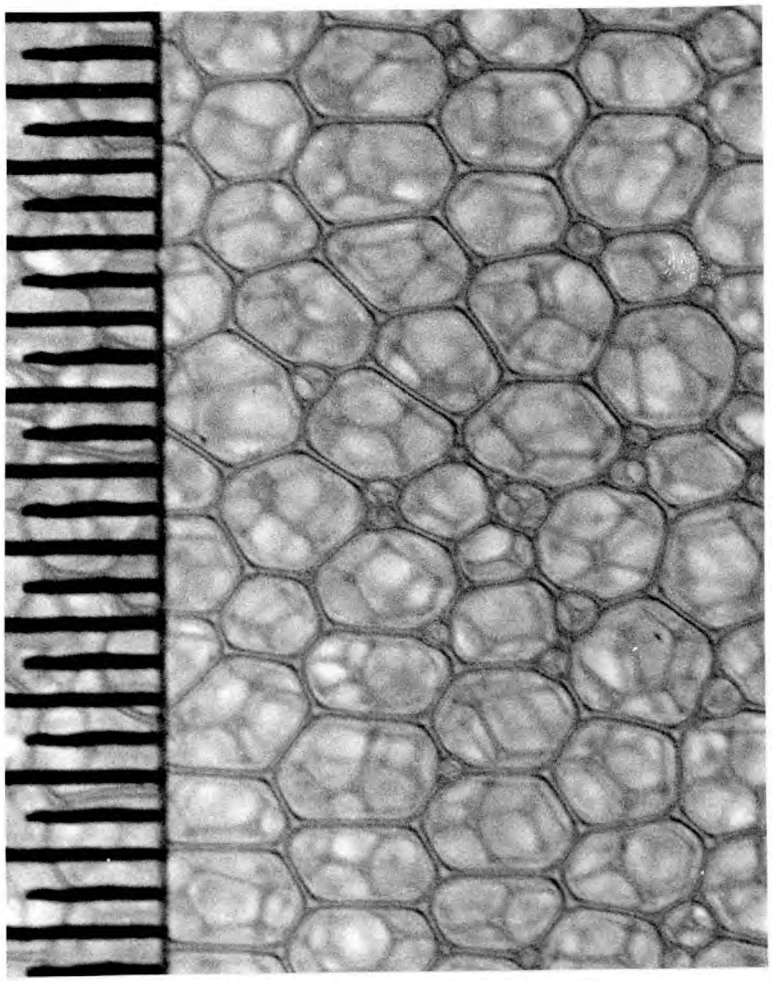

Vertical scale 0.5 mm marks.
Enlarged x 10.
Sound propagates and foam flows vertically.

Fig.41(a)

Foam bubble equiv. radius $7.2 \pm 0.8 \times 10^{-2}$ cm.

Foam-making soln. 5°/o stergene + 54°/o glycerol.

Air jet diameter 0.9×10^{-2} cm.

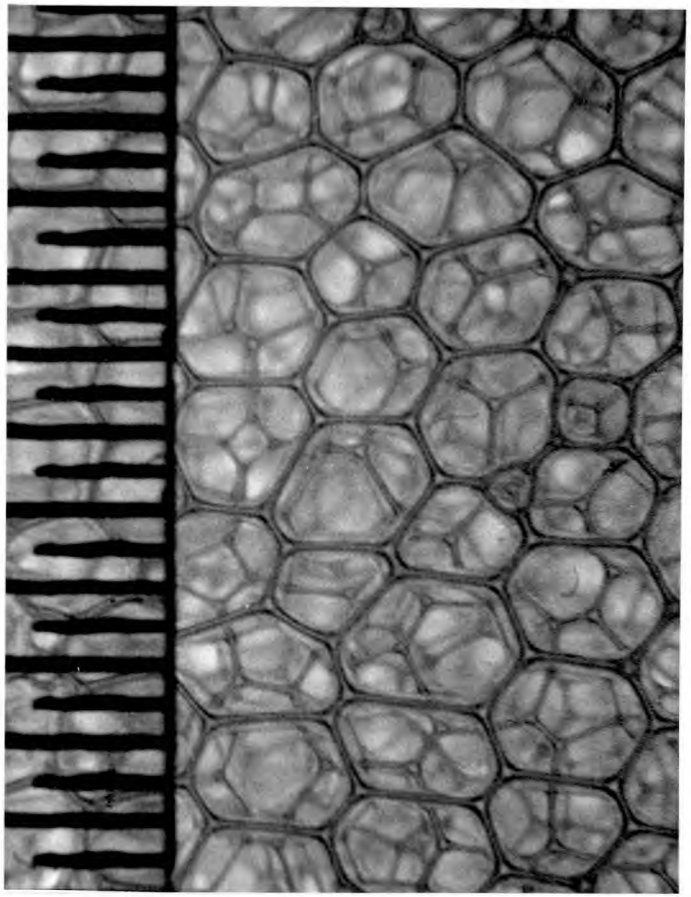

Fig.41(b)

Foam bubble equiv. radius $8 \pm 1 \times 10^{-2}$ cm.

Foam-making soln. 5°/o stergene + 54°/o glycerol.

Air jet diameter 1.0×10^{-2} cm.

176(i)

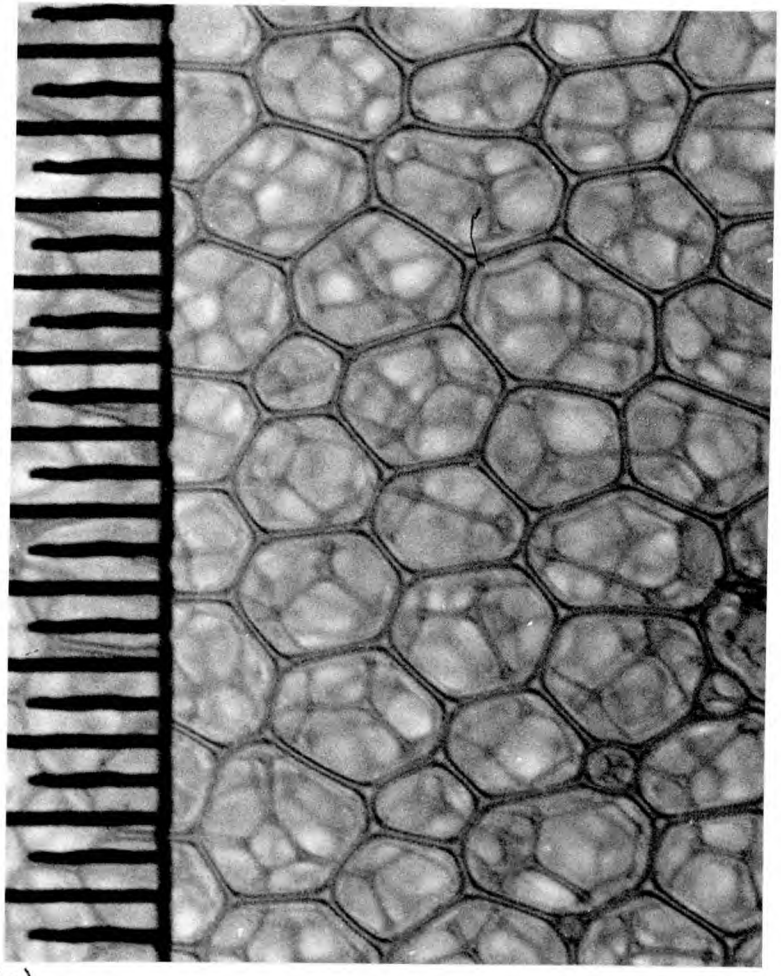

Fig.41(c)
Foam bubble equiv. radius $9 \pm 1 \times 10^{-2}$ cm.
Foam-making soln. 5°/o stergene + 54°/o glycerol.
Air jet diameter 1.2×10^{-2} cm.

176(ii)

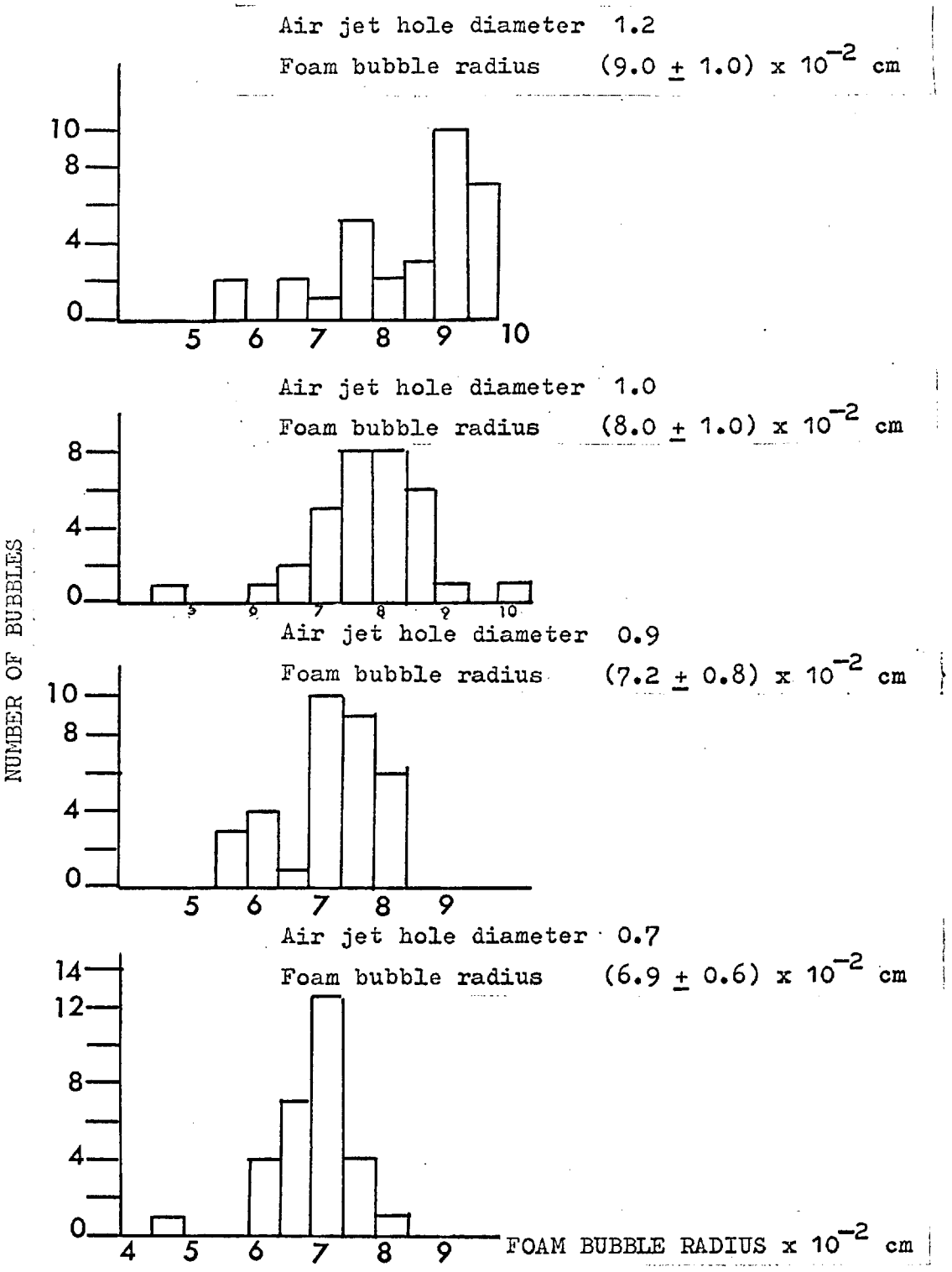

Fig.42
Foam bubble radii distributions for increasing air jet hole diameters.
(Constant foam – making solution: 5% stergene + 54% glycerol)

DEFINITIONS

Air volume concentration (x) is defined as the ratio of the volume of the air to that of the mixture.

Foam: a mixture acquires the properties of a foam as the ratio of the volume of the air to that of the mixture approaches unity.

Expansion factor (E) is defined as the ratio of the volume of foam produced to that of the solution employed. Thus $E = 1/(1 - x)$

Rheology: the study of flow deformations

(Newtonian) shear viscosity coefficient (η): if the velocity of a fluid is in the x - direction, and the fluid is flowing in layers parallel to the xy - plane, so that the velocity gradient perpendicular to the direction of motion is du/dz, then the coefficient of viscosity η is defined as the ratio of the shearing stress F_x across an area A parallel to the xy plane to the velocity gradient:

$$\eta = \left(\frac{F_x}{A}\right) \Big/ \left(\frac{du}{dz}\right) \qquad \text{(dimensions } ML^{-1}\ T^{-1}\text{)}$$

Surface shear viscosity coefficient (μ) is defined as follows: a small element dx dy of monolayer, flowing in its plane xy at the velocity u(y) in the direction of x, undergoes from the adjacent monolayer elements a resistive force equal to

$$\mu \frac{d^2u}{dy^2} \, dx \, dy \qquad \text{(dimensions } MT^{-1}\text{)}$$

Monolayer is defined as one molecule in thickness

Surface dilational viscosity coefficient represents the resistance of an interface against changes in area.

Surface compressional (bulk modulus) (B_s) in a monolayer is defined from the tangent of the surface pressure - area (F - A) curve as the reciprocal of the surface coefficient of compresibility K_s:

$$B_s = \frac{1}{K_s} = A \left(\frac{dF}{dA} \right) \qquad \text{(dimensions } L^{-1}MT^{-2}\text{)}$$

Surface shear modulus, (G_s) is defined, for small strains, as the ratio of the shearing stress to the shear strain. (dimensions $L^{-1}MT^{-2}$)

Perfectly elastic: a material is "perfectly elastic" if it recovers its original size and shape, when the forces which produce deformations are removed.

Perfectly plastic: a material is "perfectly plastic" if it retains completely its altered shape and size, when the forces which produce deformations are removed.

Visco-elastic: a material is "visco-elastic" if there is a degree of recovery from the strain when the stress is removed.

Acoustic energy density, E at a point is the sound energy per unit volume at that point.

REFERENCES

1.	Mallock, A.	Roy. Soc. (London) Proc. A	p391		1910
2.	Sewell	Phil. Trans. Roy. Soc. Sec. A	p239	210	1910
3.	Epstein, P.S.	Theodore Von Karman Anniversary Vol., Calif. Inst. Tech.	p162		1941
4.	Epstein, P.S. & Carhart, R.R.	J.A.S.A.	p553	25	1953
5.	Chow, J.C.	J.A.S.A.	p2395	36	1964
6.	Hsieh, D.Y. & Plesset, M.S.	Phys. Fluids	p970	4	1961
7.	Murray, J.D.	Appl. Sci. Res. Sec. A	p281	13	1963
8.	Taylor, G.I. & Davies, R.O.	Roy. Soc. (London)	p 34		1954
9.	Spitzer, L.	Columbia Univ. Off. Sci. Res. Dev. Rept. 1705, Sec. No. 6.1 sr. 20-918			1943
10.	Vignaux, G.A.	"The Propagation of Sound in Foams" Ph.D. Thesis Univ. Lond.			1961
11.	Connor, A.K.	"Further Experiments on the Propagation of Sound in Foams" Msc Thesis Univ. Lond.			1962
12.	Kinsler, L.E. & Frey, A.R.	"Fundamentals of Acoustics" J. Wiley & Sons, Inc. Lond. (2nd ed.)	p217	-245	1962

see also

	Stephens, R.W.B. & Bate, A.E.	"Acoustics and Vibrational Physics"	p677, 765		1966
13.	Wood, A.B.	"A Textbook of Sound" (G. Bell & Sons Ltd., Lond.)	p326		1930
14.	Karplus, H.B.	"Velocity of Sound in a Liquid containing Gas Bubbles" U.S. At. En. Com. Cont. No. AF (11-1) -528, from Off. of Tech. Serv. Dept. Commerce, Wash. 25, D.C.			1958
15.	Hartmann, G.K. & Focke, A.B.	Phys. Rev.	p221	57	1940
16.	Knudsen, V.O. et al.	J.A.S.A.	p849	20	1940
17.	Silberman, E.	J.A.S.A.	p925	29	1957
18.	Macaulay, G.A.	"Acoustic Properties of Soap Foams" Unpublished Rept., Div. Mech. Eng. Nat. Res. Council, Canada			1961
19.	Minnaert, M.	Phil. Mag.	p235	16	1933
20.	Mason, W.P.	"Electromechanical Transducers & Wave Filters" D. Van Nostrand Co.	p298		1948
21.	Kitchener, J.A. & Cooper, C.F.	Quart. Rev. Lond. Chem. Soc.	p 71	13	1959
22.	Plateau, J.	Mem. acad. roy. sci. Belgique	s.2 s.5,6 s.7 s.11	23 33 36 37	1849 1861 1867 1869
23.	Kitchener, J.A.	"Recent Progress in Surface Science" ed. Danielli (Academic Press, Lond.)	p 51-p 93	1	1964

24.	Brown, A.G. et al	J. Colloid Sci.	p491	8	1953
25.	Oldroyd, J.G.	Proc. Roy. Soc.	p567	A232	1955
	see also				
	Boussinesq, J.M.	Ann. Chim. Phys.	p349, 357, 364	29	1913
26.	Joly, M.	see ref. 23	p1-50	1	1964
27.	Miles G.D. et al	J. Phys. Chem. J. Amer. Oil Chem. Soc.	p 93	49	1945
28.	Kruglyakov, P.M. & Taube, P.R.	J. Appl. Chem. U.S.S.R.	p1514	38	1965
29.	Davies, J.T.	Proc. Sec. Int. Cong. Surf. Activity	p220	1	1957
30.	Kaertkemeyer	Proc. Sec. Int. Cong. Surf. Activity	p231	1	1957
31.	Shick, M.J. & Fowkes, F.W.	J. Phys. Chem.	p1062	61	1957
32.	Spitzer, E.L.T.M.	Third Int. Cong. Surf. Activity	p556	2	1960
33.	Pilpel, N.	Discovery	p 40		1964
34.	Eisner, H.S. & Smith, P.B.	Safety in Mines Res. Establ. Sheffield, Res. Rept. No. 130			1956
	see also				
	Linacre, E.T. & Jones, D.H.	Ibid., No. 179			1959
35.	Penney, W.G. & Blackmann, M.	"The Mechanical Properties of Foam" Home Office, R.E.N. 282			1943

see also

	Blackmann, M.	"Properties of Foam", Home Office, R.E.N. 420			1944
	Clark, N.O.	D.S.I.R. Chem. Res. Spec. Rep. No. 6			1947
	Clark, N.O. & Blackmann, M.	Trans. Farad. Soc.	p 7	44	1948
36.	Bikermann, J.J.	"Foams, Theory & Industrial Practice" Reinhold Pub. Corp. N. York	p 3,10, 22.		1953
37.	De Vries, A.J.	Rec. Trav. Chim.	p 81, 209, 283, 383	77	1958
38.	Boucher, R.M.G. & Weiner, A.L.	Brit. Chem. Eng.	p808	8	1963
39.	Morse, P.M.	"Vibration & Sound" McGraw Hill	p187, 305		1948
40.	Redwood, M.	"Mechanical Wave-guides" Pergamon	Chap.3		1960
	see also				
	Connor, A.K.	See ref. 11	p 47		1962
41.	New, G.E.	J. Soc. Cosmetic Chem.	p390	11	1960
		Fourth Int. Cong. Surf. Act.	B/VI	13	1964
	see also				
	Mawbey, P.A.	Unilever Res. Lab. Rept. S/TP/451 U01/7 S/TP/451 B01/1			1964
42.	Fry, J.F. & French, R.J.	J. Appl. Chem.	p425	1	1951

43.	Brown, Thuman & McBain	J. Colloid Science	p491	8	1953
44.	Pearson, J.T.	Unilever Res. Lab. Private Communication			1966
45.	Devin, C.	J.A.S.A.	p1654	31	1959
46.	Lamb, H.	"Hydrodynamics" Dover Public. N.Y.	Sec. 56		1945
47.	Lamb, H.	Ibid.	Sec. 294		
48.	Goldstein, R.F.	"The Petroleum Chemicals Industry" J. Wiley (2nd ed.)	p396		1949
49.	Jenkins, F.A. & White, H.E.	"Fundamentals of Physical Optics" McGraw Hill			1937
50.	Desch, C.H.	Rec. trav. chim.	p823	42	1923
51.	Phillips, F.C.	"An Introduction to Crystallography" Longmans 3rd edit.	p60, 142,145, 307		1963
52.	Landau, L.D. & Lifshitz, E.M.	"Fluid Mechanics"	p51,298		1959
53.	Meksyn, D.	"New Methods in Laminar Boundary Layer Theory", Pergamon Press, Lond.	p6		1961
54.	Newman, F.H. & Searle, V.H.L.	"The General Properties of Matter"	p260		1957
55.	Morse, P.M. & Feshbach, H.	"Methods of Theoretical Physics", McGraw Hill, N.York	p1489, 1498		1953

56.	Twersky, V.	J. Math. Phys.	p700	3	1962
		J. Math. Phys.	p724	3	1962
		J. Appl. Phys.	p1118	27	1956
	Twersky, V.	"Proc. Int. Conf. Electromagnetic Scattering" ed. M. Kerker, Pergamon Press.	p523	5	1963
57.	Strutt, J.W., Baron Rayleigh.	Scientific Papers, Cambridge.	p351	3	1899 - 1920